Examination and Validation of the Fundamental Lower Extremity Mobile Testing System, and Identification of Best Practice to Mount Synthetic Turf to a Force Platform

A Dissertation Presented for the

Doctor of Philosophy

Degree

The University of Tennessee, Knoxville

Sean Eric Quisenberry

August 2020

Copyright © by Sean Eric Quisenberry
All rights reserved

Dedication

This dissertation is dedicated to my family, and the friends I have gained throughout my graduate career. I would not have been able to complete this degree without their support during the personal and professional difficult times during these past years. That support aided in my ability to face my struggles head-on while allowing my creative spirit to flourish. Allowing me to keep my inner childish curiosity, which has always driven me to find new ways to answer the questions I desire to understand.

Acknowledgment

There are many people who deserve acknowledgment for helping me throughout this process. I would like to thank those who motivated me to not quit throughout my graduate process. My fellow students, both at the University of Tennessee and the University of Southern Mississippi, have provided vital support through this long process. The conversations I have had with Derek Yocum, Eric Hummer, Edward Kelley, and Alisha Sink have aided in the education I received. Additionally, I would like to thank Dr. Robert Doan, Elizabeth Edwards, Dr. Trenton Gould, and Dr. Mark Jesunathadas for the time and work they put into my education prior to my time at the University of Tennessee. Without their dedication, I would not have had the experience necessary to complete this project.

Further, this doctoral degree would not have been possible without my committee members: Drs. Songning Zhang, John C. Sorochan, Joshua T. Weinhandl, Jeffrey Reinbolt, and Kyley Dickson. All committee members played a vital role in my development as a researcher and teacher. A special thank you to my advisor Dr. Zhang, who was willing to take in a student at the last minute and educate him on a range of topics. Thank you for your understanding, kindness, and guidance throughout my time at Tennessee.

Author Acknowledgment

As of March 18th, 2020, the University of Tennessee, Knoxville all Human Subjects Research, was halted in response to the global pandemic. Due to health concerns related to severe acute respiratory syndrome coronavirus 2 (or COVID-19), this dissertation was modified from the initially proposed studies with the removal of studies related to human subject data collection.

Abstract

Annually, over 4 million high school and college athletes participate in competitive sports played on turf surfaces. Since the introduction of synthetic turf in the 1970s, it has become a common alternative to natural grass playing surfaces. However, athletes playing on synthetic turf has been found to have an increased incidence of lower extremity injury compared to natural grass.

Mechanical surface testing has found that synthetic turf exhibits significantly higher rotational and translational tractions compared to natural grass. The cleat-turf interface is often examined using a force platform, an instrument commonly used in a biomechanical laboratory. Mobile surface testing instruments have been developed to examine traction characteristics and have rarely examined measurement agreement with the measurements taken by the force platform. The one system that attempted to establish this relationship was found to overestimate horizontal forces and underestimate vertical forces significantly, and no system has examined free moment agreement. Aim one of this study was to compare agreement levels between a force platform, and a customized novel mobile surface testing instrument (fLEX). Additionally, within the laboratory setting, there has been no clear method for mounting synthetic turf to a force platform in order to acquire force platform data during human subject testing. Therefore, the aim two was to examine agreement between the force platform and fLEX to identify the best synthetic turf mounting method for high (cleatform) and low (court shoe) traction interfaces during static and dynamic movements. The method for producing a high level of agreement may be suitable for future human testing in the laboratory setting.

For Aim one, fLEX rotational and translational measurements were not found to be significantly different from measurements obtained by the force platform. Torque measurements by fLEX were found to have a mean system bias of less than 1% of free moment measurement by the force platform. Translational measurements were found to have high vertical and shear force agreement with the force platform yielding a relative bias of less than 1 and 3.8 %, respectively.

For Aim two, it was found an independent piece of synthetic turf with the backing glued to an aluminum mounting plate and bolted into a force platform (mounting method two) yielded agreement levels most similar to aim 1. fLEX torque and vertical force system biases were less than 4%, and shear bias was less than 11%. Only low static traction and high dynamic traction shear force measurements were found to be statistically different between systems. Mounting method two used double-sided tape on the backing of an independent piece of synthetic turf in lieu of glue. This condition was found to have a similar measurement agreement to aim one during low traction conditions. However, during high traction trials, the bonding of tapes failed, and synthetic turf detached from the mounting plate. Mounting condition three used the same adhesive method as the mounting method two, but the turf was not independent of the surrounding turf and yielded the lowest level of agreement. The poor agreement of mounting method three could have been linked to the surrounding wood surface interacting with the mounting plate. This interaction may have resulted in applied forces not being experienced by the force platform.

Table of Contents

Chapter I 1
Introduction 1
Background 1
Statement of the Problem 7
Research Hypotheses 8
Limitations 9
Delimitations 9
Chapter II 10
Literature Review 10
Introduction 10
Traction Testing Instrumentation 18
Tractions Influences on Lower Extremity Biomechanics 27
Cheat/Stud Influence on Foot Plantar Pressure 27
Tractional Influence on Ground Reaction Forces 31
Tractions Influence during Cutting Movements 34
Chapter III 41
Literature Review Examination and Validation of the Fundamental Lower Extremity Mobile Testing System, and Identification of Best Practice to Mount Synthetic Turf to a Force Platform 41
Methods 44
Surface Conditions 44
Footform Conditions 46
Instrumentation 48
Experimental Testing Protocols 50
Static Translational Tests 51
Static Rotational Tests 51
Dynamic Translation Tests 52
Data Processing (Data Acquisition Validation) 52
Statistical Analysis (Data Acquisition Validation) 53
Results 55
Discussion 59
Conclusion 66

CHAPTER IV 69
PRACTICAL APPLICATIONS 69
fLEX Practical Applications 70
Mounting Methods Applications 70
List of References 72
Appendices 84
VITA 171

List of Tables

Table 1. Interface Conditions 50
Table 2. Static Peak Torque (Nm). 96
Table 3. Dynamic Peak Torque (Nm). 97
Table 4. Static Shear Force (N) 98
Table 5. Dynamic Shear Force (N) 99
Table 6. Dynamic Vertical Force (N) 100
Table 7. Filtering Table Lowpass Cutoff Frequency (Hz) 162

List of Figures

Figure 1.Court Shoe Footform 47
Figure 2.The cleatform with threaded holes for detachable studs. 47
Figure 3. The fLEX translational test schematic diagram. 86
Figure 4. The fLEX rotational test schematic diagram. 87
Figure 5. Impact Normalized Vertical Force. 88
Figure 6. BASP Control Condition 89
Figure 7. Interface Condition 2 (Tape-Court Shoe) 90
Figure 8. Interface Condition 3 (Tape -Cleatform) 91
Figure 9. Interface Condition 4 (Decoupled Glued - Court) 92
Figure 10. Interface Condition 5 (Decoupled Glued - Cleatform) 93
Figure 11. Interface Condition 6 (Uniform Glued - Court) 94
Figure 12. Interface Condition 7 (Uniform Glued – Cleatform) 95
Figure 13. Peak Torque Agreement during Static Tests, Interface Condition 1 (Control) 102
Figure 14. Peak Torque Agreement during Dynamic Tests, Interface Condition 1 (Control) ... 103
Figure 15. Resultant Force Agreement during Dynamic Test, Interface Condition 1 (Control) 104
Figure 16. Vertical Force Agreement during Dynamic Test, Interface Condition 1 (Control) .. 105
Figure 17. Peak Torque Agreement during Dynamic Tests, Interface Condition 2 (Taped-Court) 106
Figure 18. Resultant Force Agreement during Dynamic Test, Interface Condition 2 (Taped-Court) 107
Figure 19. Vertical Force Agreement during Dynamic Test, Interface Condition 2 (Taped-Court) 108
Figure 20. Peak Torque Agreement during Dynamic Tests, Interface Condition 3 (Taped-Cleat) 109
Figure 21. Resultant Force Agreement during Dynamic Test, Interface Condition 3 (Taped-Cleat) 110
Figure 22. Vertical Force Agreement during Dynamic Test, Interface Condition 3 (Taped-Cleat) 111
Figure 23. Peak Torque Agreement during Dynamic Tests, Interface Condition 4 (Independent Glue-Court) 112
Figure 24. Peak Torque Agreement during Static Tests, Interface Condition 4 (Independent Glue-Court) 113
Figure 25. Resultant Force Agreement during Dynamic Test, Interface Condition 4 (Independent Glue-Court) 114
Figure 26. Vertical Force Agreement during Dynamic Test, Interface Condition 4 (Independent Glue-Court) 115
Figure 27. Peak Torque Agreement during Static Tests, Interface Condition 5 (Independent Glue-Cleat) 116
Figure 28. Peak Torque Agreement during Dynamic Tests, Interface Condition 5 (Independent Glue-Cleat) 117
Figure 29. Resultant Force Agreement during Dynamic Test, Interface Condition 5 (Independent Glue-Cleat) 118

Figure 30. Vertical Force Agreement during Dynamic Test, Interface Condition 5 (Independent Glue-Cleat) 119
Figure 31.Peak Torque Agreement during Dynamic Tests, Interface Condition 6 (Uniform Glue-Court) 120
Figure 32. Resultant Force Agreement during Dynamic Test, Interface Condition 6 (Uniform Glue-Court) 121
Figure 33. Vertical Force Agreement during Dynamic Test, Interface Condition 6 (Uniform Glue-Court) 122
Figure 34. Peak Torque Agreement during Dynamic Tests, Interface Condition 7 (Uniform Glue-Cleat) 123
Figure 35. Resultant Force Agreement during Dynamic Test, Interface Condition 7 (Uniform Glue-Cleat) 124
Figure 36. Vertical Force Agreement during Dynamic Test, Interface Condition 7 (Uniform Glue-Cleat) 125
Figure 37. Peak Torque Agreement during Static Tests, Interface Condition 1 (Control) 127
Figure 38. Peak Torque Agreement during Dynamic Tests, Interface Condition 1 (Control) ... 128
Figure 39. Resultant Force Agreement during Dynamic Test, Interface Condition 1 (Control) 129
Figure 40. Vertical Force Agreement during Dynamic Test, Interface Condition 1 (Control) .. 130
Figure 41.Peak Torque Agreement during Dynamic Tests, Interface Condition 2 (Tape-Court) 131
Figure 42. Resultant Force Agreement during Dynamic Test, Interface Condition 2 (Tape-Court) 132
Figure 43. Vertical Force Agreement during Dynamic Test, Interface Condition 2 (Tape-Court) 133
Figure 44. Peak Torque Agreement during Dynamic Tests, Interface Condition 3 (Tape-Cleat) 134
Figure 45. Resultant Force Agreement during Dynamic Test, Interface Condition 3 (Tape-Cleat) 135
Figure 46. Vertical Force Agreement during Dynamic Test, Interface Condition 3 (Tape-Cleat) 136
Figure 47. Peak Torque Agreement during Dynamic Tests, Interface Condition 4 (Independent Glue-Court) 137
Figure 48. Peak Torque Agreement during Static Tests, Interface Condition 4 (Independent Glue-Court) 138
Figure 49. Resultant Force Agreement during Dynamic Test, Interface Condition 4 (Independent Glue-Court) 139
Figure 50. Vertical Force Agreement during Dynamic Test, Interface Condition 4 (Independent Glue-Court) 140
Figure 51. Peak Torque Agreement during Static Tests, Interface Condition 5 (Independent Glue-Cleat) 141
Figure 52. Peak Torque Agreement during Dynamic Tests, Interface Condition 5 (Independent Glue-Cleat) 142

Figure 53. Resultant Force Agreement during Dynamic Test, Interface Condition 5 (Independent Glue-Cleat) 143
Figure 54. Vertical Force Agreement during Dynamic Test, Interface Condition 5 (Independent Glue-Cleat) 144
Figure 55. Peak Torque Agreement during Dynamic Tests, Interface Condition 6 (Uniform Glue-Court) 145
Figure 56. Resultant Force Agreement during Dynamic Test, Interface Condition 6 (Uniform Glue-Court) 146
Figure 57. Vertical Force Agreement during Dynamic Test, Interface Condition 6 (Uniform Glue-Court) 147
Figure 58. Peak Torque Agreement during Dynamic Tests, Interface Condition 7 (Uniform Glue-Cleat) 148
Figure 59. Resultant Force Agreement during Dynamic Test, Interface Condition 7 (Uniform Glue-Cleat) 149
Figure 60. Vertical Force Agreement during Dynamic Test, Interface Condition 7 (Uniform Glue-Cleat) 150
Figure 61. Filtering and Event Picking Loop 155
Figure 62. Mean Bias Filtering Matrix 156
Figure 63. Mean Bias Ranked Matrix 157
Figure 64. Standard Deviation Filtering Matrix 158
Figure 65. Stand Deviation Ranking Matrix 159
Figure 66. Mean Ranked Matrix 160
Figure 67. Reranked Matrix for Control Dynamic Peak 161
Figure 68. PCB X Free Weight Calibration 164
Figure 69. PCB Y Free Weight Calibration 165
Figure 70. Reaction Torque Sensor Calibration 166
Figure 71. Rotary Actuator Pressure Calibration Linearity 167
Figure 72. Vertical System Pressure 168
Figure 73. Horizontal Velocity 169
Figure 74. Vertical Velocity 170

Chapter I

Introduction

Background

The 2018 United States (US) Census Bureau reported that 16.2 million people (ages 10-19) were enrolled in US high schools (School Enrollment in the United States, 2018). During the 2018-19 academic year, the National Federation of State High School Associations (NFHS) reported that 7.9 million high school students participated in school-organized sports programs, with approximately 43% being deemed female (NFSHSA, 2019). The NFHS found 3.26 million (41.1%) of all high school athletes participated in turf-sports, and of that, 31.3% were females. During that same academic year, the National High School Sports-Related Injury Surveillance Study 2018-2019 reported an estimated 1.3 million high school sports-related injuries (Comstock and Pierpointm, 2019). Turf-sports contributed 75.4% (986,964) of all reported high school injuries reported. The top three sports contributing to injury were American football (455,449), boys' soccer (184,656), and girls' soccer (227,951). Over half (654,684/1,306,753 = 50.1%) of reported injuries were associated with the lower extremity, and of those lower extremity injuries the most common locations for injury were the ankle making up 18.3% (ranked #2 overall), knee 13.8% (#3), and hip/thigh/upper leg 9.9% (#4).

During the late 17th century, Guillaume Amontons established Amonton's law of friction (Otsuki and Matsukawa, 2013). This law is comprised of three aspects: 1) friction force is

directly proportional to the applied load, 2) friction force is independent of the apparent area of contact, and 3) kinetic friction is independent of sliding velocity. Court-sports utilize a more traditional interface yielding actively to frictional laws (shoe and surface). However, turf-sports are influenced by a variety of factors associated with environmental conditions producing greater interface variability (Heidt et al., 1996). This variability has led to the modification and addition of cleated studs to athletic shoes. A cleat stud is a protruding structure located at the base of the outer sole of the shoe designed to improve the production of tractional forces via penetration of the adjacent surface. Tractional forces can be defined as "a physical process in which a tangential force is transmitted across an interface between two bodies through frictions resulting in motion, stoppage, or the transmission of power." (Raymond, 2004). Although friction is a component of tractional force, the addition of the penetrating structure increases the complexity of the interface. This increased complexity can best be illustrated by the frictional force opposing or producing motion being more significant than the normal force, resulting in a coefficient of friction (CoF) being greater than one (Cooper, 2009; Torg et al., 1974).

Since the early 1970s, the examination of tractional forces related to turf-sports injury has sparsely been examined in the literature. An early study found cleats with a less aggressive cleat pattern, commonly seen on soccer cleats, showed a reduced severity of knee injury compared to the more aggressive 7-stud configuration (Torg and Quedenfeld, 1971). This assumption was mechanically supported three years later when Torg et al. (1974) found molded soccer cleats

produced significantly lower rotational release coefficients (CoR = torque/normal force), compared to the more aggressive 7-stud configuration. Since then, stud geometry has been found to play a significant role in both CoF and CoR (Heidt et al., 1996; Serensits and McNitt, 2014; Wannop et al., 2012a), but the traditional cone shape stud has been found to produce the highest degree of traction concerning number and shoe outer sole distribution of studs (Heidt et al., 1996; Kuhlman et al., 2010). Lambson et al. (2007) collected the cleat-surface interface characteristics of 3119 high school football player cleats during the 1989-1991 high school football seasons. The study found players wearing cleats with an elevated forefoot CoR value (0.117 = 52 Nm/ 441.30N) were significantly more likely to sustain a documented anterior cruciate ligament (ACL) rupture (injury rate of 0.017%) compared to cleats with CoR values less than 0.1 (injury rate of 0.005%). This study was limited by the fact that the cleat-surface interface was quantified on a standard synthetic turf and not the turf where the injury occurred. This limitation was addressed by Mack et al. (2019), which tracked all lower extremity injuries reported during the 2012-2016 National Football League (NFL) regular season. The authors performed a cleat-surface interface analysis on experimental surfaces designed to replicate the turf conditions at the instance of injury. Elevated rotational traction levels, commonly observed on synthetic turf, resulted in a 16% increase in lower extremity injury per play (incidence rate ratios 1.16, 95% confidence interval of 1.1-1.23) compared to lower traction levels observed on natural grass (incidence rate ratio 1).

Historically, biomechanical researchers have aimed to replicate common settings where injuries occur to understand the mechanisms behind the injuries. However, laboratory studies examining turf-based athletes and movements have primarily been performed under non-turf conditions. The lack of clear laboratory studies could be due to the logistical complexity of appropriately preparing experimental surfaces for data collection within the laboratory setting, as well as limited methodological literature examining how to acquire laboratory data appropriately. Sports movements composing American football, soccer, and rugby have primarily been examined under common court-based laboratory conditions (Hanson et al., 2008; S. Sigward and Powers, 2006; S. M. Sigward and Powers, 2006). Thus, neglecting the playing surface component of turf-sports. Turf-sports have been found to have significantly greater numbers of lower extremity injuries compared to court-sports (Comstock et al., 2019); this lack of experimental surface replication can be a limitation in the literature. In recent years, studies examining CoF and traction modification have begun to be presented in the literature (Luo and Stefanyshyn, 2011; Müller et al., 2010a, 2009; Schrier et al., 2014a; Stefanyshyn et al., 2010; Wannop et al., 2019). These studies have predominately focused on examining the influence the sports surface interface has on physically active male populations. Thus, creating a void in the understanding of how the sport turf-interface influences the lower extremity biomechanics during plant and cut movements of different biological sexes.

Since the introduction of synthetic turf, researchers have been comparing the safety of synthetic playing surface alternatives to natural grass. The cleat-surface interface has been found to be a contributor to lower extremity injuries (Lambson et al., 2007; Mack et al., 2019), and as a result, a variety of instruments have been developed to quantify this interface, adding valuable information to the literature. Heidt et al. (1996) examined fifteen different cleats and their behavior on natural and synthetic turf under a normal force of 111N. The study found that synthetic turf produced significantly higher peak rotational traction, cleats produced greater rotational traction compared to turf or court shoes (non-studded shoes), and surface moisture decreased peak rotational traction. However, Kuhlman et al. (2010) found that normal forces less than 666 N had a difficult time differentiating peak rotational traction of various cleats sampling at 250 Hz, indicating normal force contributing to rotational traction. Additionally, Wannop et al. (2009) examined 106 used high school football cleats and found that stud geometry plays a significant role in cleat traction characteristics, and this influence degraded throughout a season.

In recent years studies examining various degrees of traction have been found to influence male mechanics during various cutting movements significantly. A series of studies by Müller et al. (2009, 2010a, 2010b) examining various cutting movements on synthetic turf with uncontrolled interface modification found studs composed of more rigid materials and producing greater surface penetration produced significantly higher anterior-posterior ground reaction force (GRF), foot inversion, and knee flexion angles, ankle eversion and abduction moments, and knee

flexion and internal rotation moments. Wannop et al. (2019) examined two surfaces that produced two different peak rotational traction values (62.4 Nm and 77.5 Nm, normal force 650 N) on a single cleat found the high CoR significantly increased peak ankle external and eversion moments, and knee adduction moment during a 90º cutting movement. However, other studies adopting sampling frequencies under 240 Hz for optical data, and 2,000 Hz force platform data have produced limited differences between traction conditions (Gehring et al., 2007; Kaila, 2007; R. Gdovin et al., 2018). One such study collected force platform data at 1000 Hz was unable to detect a change in braking or propulsive forces between two studded cleats and non-studded running shoes (R. Gdovin et al., 2018). These findings are not supported in the biomechanical (Brock et al., 2014; Morag and Johnson, 2001; Müller et al., 2009; Wannop et al., 2019) or mechanical testing literature (Heidt et al., 1996).

Female athletes have been found to be 3-5 times more likely to sustain a non-contact ACL injury compared to their male counterparts (Arendt and Dick, 1995; Griffin et al., 2000; Gwinn et al., 2000; Messina et al., 1999; Myklebust et al., 2003; Uhorchak et al., 2003). The mechanism most commonly responsible for those injuries is related to a single leg plant and cutting movement (Faunø and Jakobsen, 2006; Koga et al., 2010; Olson et al., 2011), with upwards of 70% of all non-contact injuries resulting from cutting movements (Boden et al., 2000). Laboratory studies replicating cutting movements have provided valuable information examining differences between sexes. Kinematically, females have been observed to have

significantly greater peak rearfoot pronation (Ford et al., 2005; Landry et al., 2007), reduced peak knee flexion angle (McLean et al., 2004), greater knee adduction angle (McLean et al., 2004; Pollard et al., 2004), and decreased peak internal knee rotation (McLean et al., 2004; Pollard et al., 2004) compared to males. Kinetically, females have been observed to have significantly greater knee flexion, adduction, and external rotation moments compared to male counterparts (McLean et al., 2005; Pollard et al., 2004; Sigward et al., 2015, 2012; S. M. Sigward and Powers, 2006). Neuromuscularly, females, have presented significantly greater knee extensor muscle activation, reduced knee flexor, and delayed activation of tibialis anterior and biceps femoris during cutting movements. These mechanical and neuromuscular differences have the potential to be exacerbated by the modification of rotation traction (Beaulieu et al., 2008; Hanson et al., 2008).

Statement of the Problem

Searching the peer reviewed literature, there are no methodological studies examining the means of collecting GRF data with surfaces mounted on a force platform producing a coefficient of friction greater than or approaching 1. Empirical evidence has built an active link between traction and incidence of lower extremity injuries. Thus, an understanding of how to adequately acquire force platform data during laboratory studies examining the shoe-surface interface is vital to understanding its influence on sports movement-related injuries, specifically turf-sports

movements. Therefore, the purposes of this dissertation are presented below. The primary aim of this study was identifying the static and dynamic levels of agreement between an in-ground force platform, and a novel designed mobile sports surface testing instrument. The secondary aim was to identify the best method to mount synthetic turf to an in-ground force platform to adequately force measurement in future laboratory biomechanics studies looking to examine the influence of the cleat-turf interface on human mechanics.

Research Hypotheses

1. It is hypothesized that the currently proposed novel designed mobile sports surface testing instrument would possess high levels of torque and force agreement with an in-ground force platform.
2. It is hypothesized that as synthetic turf mounting rigidity increases, a subsequent increase in the degree of agreement in anterior-posterior, medial-lateral, and vertical GRF between a novel designed mobile sports surface testing instrument and an in-ground force platform would been seen.
3. It is hypothesized that as synthetic turf mounting rigidity increases, a subsequent increase in the degree of agreement between in-ground force platform free moment about the Z-axis and torque sensor measurements of novel designed mobile sports surface testing instrument would be seen.

4. It is hypothesized that rigidly mounting synthetic turf to an in-ground force platform would remove the need to modify the synthetic turf system in order to collect force and moment data adequately without the introduction of residual environmental forces.

Limitations

- fLEX and the force platform did not share a rigid structure.
- The court shoe deterioration throughout trials
- Movements were performed at the same location and not randomized.
- Trigger Signal – 50-foot BNC wire resulted in an average 96 ms (≈480 samples) delay in TTL trigger signal reaching the Vicon System (corrected for during processing).

Delimitations

- The fLEX system was designed and constructed in minimally environmentally controlled workspace (fLEX was built on a farm).
- PCB triaxial force sensors have a load capacity of Z = 44,482 N and X-Y = 17,792 N.

Chapter II

Literature Review

Introduction

The purpose of the study was the identify the levels of agreement between a novel mobile turf testing instrument, an in-ground force platform, and to identify the best method for surfaces to be mounted to a force platform to acquire static and dynamic GRF and free moment.

The purpose of this chapter was to summarize: 1) brief history of the introduction of synthetic turf, 2) epidemiology injury prevalence on synthetic turf during sport, 3) history of instruments quantifying the cleat-turf interface, 4) influences the cleat-turf interface has on kinematics, kinetics, and foot pressure during various cutting movements and 5) examining lower extremity biological sex differences during cutting movements in recreationally active and competitive populations.

Synthetic Turf History

In the late 1950s following the Korean War, the US military noticed that rural youths were significantly more fit than their inner-city counterparts. This difference was believed to be linked to inner-city youths lacking a suitable recreational environment. To improve the physical fitness of inner-city youth, the Ford Foundation created the Education Facilities Laboratory (EFL) with the goal to develop more suitable recreational areas for the inner-city (I. M. Levy et al., 1990). At the same time, the Chemstrand Corporation (Decatur, AL) was in the process of

developing a new synthetic carpet fiber to improve carpet durability. The Chemstrand Corporation was awarded $200,000 by the EFL to modify their new synthetic carpet "ChemGrass" for installation in new inner-city recreation areas. The association between the two grouped set off to make an urban sports surface for the schools within the ford foundation. The two groups examined cushioning, drainage, flammability, and carpet wear of the newly developed outdoor carpet.

In 1964, ChemGrass was installed at the Moses Brown School in Providence, Rhode Island (I. M. Levy et al., 1990), marking the first instance of synthetic turf in a school setting. The following year in Houston, Texas, the construction of the Astrodome was completed. At the time, the grandiose magnitude of the structure resulted in it being referred to as the "Eighth Wonder of the World." During its tenure, the Astrodome would be home to two professional sports organizations the Houston Astros (1965-1996) and Houston Oilers (1968-1996). Both baseball and football traditionally had been played outdoors on natural grass playing surfaces, but the domed structure limited natural light preventing natural grass photosynthesis. This logistical challenge resulted in the installation of ChemGrass in the astrodome and renamed "Astroturf" (Whitehurst, 1968). Minnesota Mining & Manufacturing (3M; St. Paul, MN) also developed a synthetic surface that was originally designed for horse racing then modified and marketed as an all-weather playing surface. Tartan Turf was a modification of the Tartan Track (first used in the 1968 Olympic games in Mexico City) and was installed as the playing field for

the University of Tennessee and Wisconsin in 1968 (Mattingly, 2018). The first generation of synthetic turf was constructed of nylon and polypropylene structural fibers, and a high-density nylon thermoplastic turf backing. The tightly packed fibers were knitted into the backing similar to any other carpet. Unlike normal carpets, the nylon fibers were highly resistant to being pulled out ("Turf Lock") (Hawkins, 1984). The synthetic turf was installed on a concrete surface with a porous rubber backing and irrigation under the synthetic structure (Whitehurst, 1968).

In 1976, the first synthetic turf evolution occurred with the addition of longer synthetic fibers/blades (leading to the name "shag turf"), sand, and shockpad. The sand was used to weigh the surface down and fill gaps between fibers, and shockpad was introduced as a sub-turf liner system designed to increase surface compliance and dampen impact forces (I. M. Levy et al., 1990). The first shock pads were composed of porous open-cell foam produced from plastics and rubbers. Additionally, Bowers and Martin (1976) observed a high incidence of sprains of the plantar capsule ligament of the metatarsophalangeal joint on synthetic turf and coined the term "turf toe." Turf toe was defined as acute traumatic bursitis of the first MTP joint associated with tendinitis of the extensor and flexor hullicus longus (Doller and Strother, 1978).

The 3rd and current generation of synthetic turf was introduced in the 1990s. Composed a polyethylene yarn, which created a softer synthetic turf blade, decreased fiber density with longer fibers, supported by a synthetic thatch layer and infill (I. M. Levy et al., 1990). The thatch

layer was designed as structural support for the improved polyethylene material blades. The infill was added to be an extra comfort layer to the playing surface. The improvement in material, reduction of fiber density, and the addition of rubber infill made the 3rd generation of synthetic turf the closest to mimic natural grass to date. As of 2019, the Synthetic Turf Council reports there are between 12,000 and 13,000 active synthetic sports field in the United States, with approximately 1,200 to 1,500 new systems installed each year (Synthetic Turf Council, 2019).

Synthetic Turf vs. Natural Grass Injury

Since the introduction of synthetic turf, researchers have sought to examine differences between natural and synthetic turf and their effects on athlete safety. The first and second generations of synthetic turf were quickly clinically observed to have an increased incidence of lower extremity injury compared to natural grass. Skovron et al. (1990) found the turf sports athletes of the National Collegiate Athletic Association (NCAA) on the first-generation synthetic turf from 1975-1977 were 20 percent more likely to sustain a knee injury (meniscus/sprains). A knee injury resulted in missed ≥7 consecutive days of activity compared to the same activity on natural grass (injury ratio of 1.2, the injury rate of 1.0 per 1000 athlete exposures on synthetic turf compared to 0.8 per 1000 on natural surfaces). The same study also found ankle sprains were 13 percent greater on synthetic turf compared to natural grass (injury ratio of 1.4, 0.45 per 1000 on synthetic turf compared to 0.32 per 1000 on natural grass) during American football

competition. Additionally, the study found during game activity athletes were observed to be 50% more likely to sustain an injury on synthetic turf compared to natural grass (injury ratio of 1.5, 39.6 per 1000 injuries vs. 4.4 per 1000). During the same time, Powell (1992) reported players in the National Football League (NFL) had an 8.2% increase risk for all lower extremity injuries on synthetic turf during games compared to natural grass (relative risk ratio of 1.14, 1.94 per 1000 team game on artificial vs. 1.78 per 1000 team game on natural grass). Major knee injuries had a relative risk ratio of 1.33 (0.2 on synthetic turf vs. 0.15 on natural grass), and ankle and foot injuries were observed to have a relative risk ratio of 1.8.

In 1971, a study conducted at the University of Michigan randomly sampled Sixty-four teams from a pool of 140 teams participating in student intramural touch football (Stevenson and Anderson, 1981). Thirty-two of the sixty-four were assigned to play on Tartan synthetic turf and the other thirty-two on natural grass. Touch football games were comprised of two fifteen-minute halves with a five-minute intermission and played on a reduced dimension football field 91.44m x 36.576m (standard field 109.728m x 45.72m). During the experimental season, 107 total injuries occurred during match play, with 64.5% of those injuries sustained by the lower extremity (69/107), and an injury rate of 15.9 per 100 player injuries occurred on Tartan turf compared to 9.5 per 100 player injuries on natural grass. 50.4% of all injuries were to the lower extremity (54/107), and the ankle and knee made up 96.3% (52/54) of these injuries. 54.2% of all ankle injuries and 67.9% of all knee injuries occurred on Tartan turf. Marking this study as one

of the first large-sample experimentally designed studies comparing synthetic to natural grass playing surfaces.

During the 2003-2004 European soccer season, Ekstrand et al. (2006) followed 290 elite European soccer players playing on synthetic turf and 202 elite Swedish players on natural grass. The study found no evidence that synthetic turf placed elite soccer players at an increased incidence of lower extremity injury compared to natural grass. However, the study did find that ankle sprains had a higher incidence injury rate ratio of 1.81 for synthetic turf during match play (4.83 per 1000 match play hours on synthetic turf vs. 2.66 per 1000 match play hours on natural grass). Additionally, in 2007, an NCAA surveillance study of 242 soccer teams (106 men and 136 women) from 2005 to 2006 examined the incidence of injuries during match play (Fuller et al., 2007). The study found biological sex to not influence incidence of injury for men (25.43 per 1000 synthetic vs. 23.92 per 1000 natural, a ratio of 1.06) or women (19.15 per 1000 synthetic vs. 21.79 per 1000 natural, a ratio of 0.88) on synthetic turf compared to natural grass with the majority of injuries occurring due to player to player contact.

In more recent years, more rigorous longitudinal studies have been performed - an NCAA American football surveillance study from 2004 to 2009 tracked the incidence of injuries to the ACL (Dragoo et al., 2013). Throughout the period, athletes were 1.39 times more likely to sustain an ACL injury on synthetic turf compared to natural grass (1.73 per 1000 vs. 1.24 per

1000). In a follow-up to Dragoo et al. (2012), an NCAA surveillance study by Loughran et al. (2019) examined data from 2004 to 2014 tracking 3,009,205 NCAA athletes across all three divisions. Over the ten years, 2,460 knee injuries were sustained (1,389 MCL, 522 ACL, 269 lateral menisci, 164 medial menisci, and 116 PCL). Division I athletes were 2.94 times more likely to sustain a posterior cruciate ligament (PCL) on synthetic turf, and athletes in Division II and III experienced ACL injuries at 1.63 times and PCL injuries at 3.13 times on synthetic turf compared to natural grass. Similar to previous studies, athletes were significantly more likely to sustain injuries during match play compared to practice.

The previous epidemiological studies primarily tracked injuries, but minimally addressed the potential mechanisms of those injuries. Mack et al. (2019) performed a more in-depth study tracking NFL players from 2012-2016 of all 32 teams. The study found NFL players were 16 percent more likely per play to sustain a lower extremity injury on synthetic turf compared to natural turf. The incidence rate was calculated using all lower extremity injuries per play and resulted in an in IRR 1.16 (95^{th} % CI = 1.10-1.23) when play was on synthetic turf compared to natural grass. Non-contact injuries on synthetic turf resulted in 1.27 (1.15-1.41) for a lower extremity injury, 1.46 (1.20-1.77) for a knee injury, and 1.68 (1.36-2.08) for an ankle/foot injury, respectively. Players were 2.03 times more likely to sustain a non-contact foot or ankle injuries resulting in greater than eight days of missed field time on synthetic turf compared to natural grass. The study used a “crude” approach to assess the mechanism of injury, injured athlete cleat

information and surface information associated with cleat turf interaction characteristics obtained from the BioCore Elite Athlete Shoe-Surface Tester (BEAST). The study found that injured athlete's cleat-surface interface on the synthetic turf systems had significantly higher traction characteristics linking those injuries to the cleats' inability to release/disentangle from the playing surface. Thus, the cleats rotational interface characteristics can be linked to the mechanism of lower extremity injury in turf-based sports.

A five-year prospective study comparing injuries on natural grass to FieldTurf's synthetic turf (Fieldturf USA, Inc., Calhoun, GA) of eight high school American football teams in West Texas(Meyers and Barnhill, 2004). The study found natural grass had a higher number of anterior cruciate ligament (ACL) injuries, but injuries occurring without contact with another athlete, muscle sprains, and skin abrasion injuries were higher on synthetic turf. A subsequent study published in 2010 following twenty-four collegiate American football teams across three years and 465 games (230 FieldTurf synthetic and 235 natural grass) found lower extremity injury differences between FieldTurf synthetic turf systems and natural grass playing surfaces (Meyers, 2010). This study concluded that "FieldTurf is in many cases safer than natural grass." In 2017, Meyers (2017) followed eleven male collegiate soccer teams across six seasons (380 matches on FieldTurf and 385 on natural grass). Throughout the six seasons, 722 injuries were observed. Of those 722 injuries, 268 occurred when playing on FieldTurf (37.1 percent), and 454 occurred on natural grass (62.9 percent). Knee injuries were more prevalent when playing on

natural grass compared to FieldTurf, but the article did not address injuries related to foot, ankle, and hip.

Traction Testing Instrumentation

The notion of elevated levels of shoe-surface interaction (traction) and lower extremity injury has been around since the late 1960s. Since that time, numerous instruments have been developed to test the shoe-surface interface. Torg et al. (1974) developed an instrument presented in the journal of sports medicine. The instrument was designed to quantify rotational traction of the outer sole of a cleat. Similar to a person standing in the anatomical position, the normal force was applied perpendicular to the heel and transferred anteriorly via a rigid structure within the shoe. Normal forces varied from 25 to 150 lbs., and a torque wrench was positioned superior to the applied normal force. A test consisted of an applied normal force and a foot with experimental shoe rotating 60-90 degrees. The study was designed to test various shoes and cleat configurations and the interaction with both natural and first-generation synthetic turf and presented a recommendation for each cleat configuration on the various playing surfaces. A release coefficient greater than 0.5 (computed as a ratio of normal force and rotational force) was termed “Not Safe” on the specified playing surface.

Andreasson et al. (1986) presented the next instrument in 1986, but unlike Torg’s instrument applying torque via the foot, a motion was applied to the surface and resulting forces

were computed. The aim was not to replicate rotation induced by the foot but examine forces created by the surface on foot via the shoe surface interface. Similar to previous instruments, the normal force was applied to the heel, but normal force was generated using a pneumatic cylinder compared to the system used by Torg et al. (1974) utilizing free weight. The experimental surface was mounted to a motorized structure that rotated the surface about a central axis. Within the rigid foot structure, strain gauges were positioned within the instrument to compute force and torque exerted on foot as a result of the shoe-surface interface. The study found that with a normal force of 241N, the coefficient of frictions ranged from 0.1 to values greater than 1.7, and reaction torque ranged from 37.4 to 74.5 Nm.

Heidt et al. (1996) studied the interaction between 15 different cleats and second-generation synthetic turf and natural grass under various environmental conditions. This instrument was the first to implement an anterior-posterior translational traction test to the cleat-turf interface literature. The instrument utilized a six-degrees-of-freedom AMTI load cell (Advanced Manufacturing Technology, Inc.) positioned at the talocrural joint superior to the shoe collar with a normal force of 25 lb applied during each trial and pneumatic actuator generating both translational force and rotational torque. The study found that the four categories of shoes (turf, modeled cleat, traditional cleats, and court shoes) produced significantly different translational and rotational values. Molded cleats produced 39.01-51.45% greater translational reaction force and 49.4-67.5% greater rotational torque compared to the next

closest configurations on the dry and wet synthetic turf condition. However, traditional cleat configuration produced 70.1% greater translational reaction force and 37.6% reaction torque on natural grass compared to the next closest cleat configuration. Additionally, the study found the additional tape to the bottom of the shoe (shoes with spat) decreased both translational reaction force and reaction torques. Wet synthetic turfs produced significantly less translational forces and rotational reaction and reaction torque compared both natural and dry synthetic turf.

McNitt et al. (1997) introduced the PENNFOOT system composed of a single pneumatic cylinder producing translational force and attached a moment arm to compute rotational traction. The system utilized free weights to apply normal force during experimental trials. PENNFOOT utilized an aluminum block foot that requires shoe modification. The shoe tongue needed to be removed in order to be inserted, and a rectangular block is used (representing a foot) in the shoe to apply force to the mid and forefoot. The study examined natural turf types, mowing height, and normal forces and their influence on peak reaction torques. McNitt et al. (1997) found significant differences between turf type, mowing height, or normal force influenced peak reaction torque. However, as normal force increased, a subsequent increase in reaction torque was observed for all testing conditions. Unlike previous traction testing instruments, PENNFOOT is still in use as of 2019 producing yearly cleat traction reports.

In 2006, Livesay et al. (2006) introduced a simple manual test examining just cleats under the mid and forefoot and rotational reaction torque comparing the second generation to the third generation of synthetic turf. The manual test used free weights to modify normal force ranging from 67 to 511N, and manual rotation was applied. This test was the first to introduce an encoder and torque sensor, both sampling at 500 Hz and using a national instrument data acquisition board. The study illustrated that independent of testing surface, lower magnitude normal forces are curved linearly related to peak reaction torque.

The first European contribution to the traction literature was introduced in 2007, and one of the most innovative. The TrakTester was primarily developed as an indoor Adidas shoe testing instrument (Grund et al., 2007). Similar to automotive anthropomorphic test devices (ATD), the TrakTester has an independent foot and shank with instrumented proximal and distal shank. A 99-sensor plantar pressure insole system was positioned between the plantar surface of the ATD footform and the experimental cleat condition. Superior to the calcaneal region of the ATD footform, a six-component load cell was positioned at a theoretical ankle location. Additionally, a triaxial force sensor was positioned superior to the actuator representing the shank at a theoretical knee location. A pneumatic system was used to generate linear motion via a pneumatic cylinder, and additional motion with pneumatic bladders stimulating muscle motion. The instrument can move translationally in the vertical, horizontal, and rotationally in pitch, roll, and yaw planes. Two studies have been published with this instrument. The first study was a

technical note introducing and detailing the instrument. The second study examined four cleat-turf interfaces and no significant differences were observed at the insole, six-component load cell, or triaxial force sensor (Grund and Senner, 2010). However, Lehner et al., (2013) compared the foot strike pressure patterns produced by the TrakTester and experimental human plantar pressure data and found the TrakTester was able to replicate the foot strike pressure pattern during a cutting movement, however, experimental human data were not presented in the study.

In 2009, two new instruments were introduced to the literature from Michigan State University (East Lansing, MI) and the University of Calgary (Calgary, AB). Villwock et al. (2009) were the first to introduce a traction instrument, producing normal forces referenced to anthropomorphic data. The instrument used free weights to apply the normal force of the 95th percentile male, or 1000N, and a pulley system to generate rotation (Robbins et al., 1983). Force, torque, and encoder data were collected for 5 seconds at 1000 Hz, and a torque threshold of 3 Nm was used to process data. The study found 1000N of normal force produced reaction torque greater than 120 Nm and presented a safety threshold of 95 Nm referencing cadaver ankle fracture threshold (Hirsch and Lewis, 1965). That same year the group published a study examining nine different cleats on various playing surfaces (FieldTurf, AstroPlay, Grass-Sand, grass-natural), the study found the seven-year-old FieldTurf surface produced significantly greater peak reaction torque (118.3 Nm), followed by AstroPlay (111.8 Nm), Sand-based natural grass (95.9 Nm), and finally native soil natural grass (83.1 Nm). However, significant differences

between shoe models were only observed between the turf shoe (Non-rigid studs) and the eight cleated shoes.

Wannop et al. (2009), affiliated with Adidas International, collected data using a portable traction testing instrument, examined cleat traction characteristics of 106 high school football players in the Calgary area on Poa pratensis L. (Kentucky bluegrass) sports fields. A normal force of 580 N was implemented to minimize damage to the playing surface during both translation and rotation tests. The footform was oriented to simulate 20º plantarflexion at the ankle joint during traction testing. This angle was selected, so only the forefoot cleats were in contact with the playing surface. A Horizontal motion was produced by a hydrologic ram wire pulley system attached to a carriage mounted to a low friction linear bearing system and produced a horizontal velocity of 0.25 m/s. A horizontal load cell was positioned between the carriage and wire pully system to compute horizontal resistance force exerted on the system as a result of the cleat-surface interface. The horizontal carriage was locked into place, allowing the pully wire to create torque by pulling on a rotational metal dowel resulting in a rotational velocity of 90 degrees per second. A force transducer mounted to a moment arm was utilized to estimate torque. Data was collected at 2000 Hz, and the vertical force was validated on a force platform and found to have “very good agreement” with the vertical ground reaction force of the force platform. Day to day instrument reliability produced a high agreement.

Wannop et al. (2009) tested shoes ranging from US 8.5-15 with a mean and mode of 11 and categorized as edge, stud, and fin stud configuration. Edge cleats were characterized by long cleats on the peripheral margin of the forefoot, stud cleats possessed a large number of small rubber cone-shaped structures distributed across the outer sole surface, and fin cleats possessed a large number of rubber fin (hallow triangle shape) placed on the shoe. The study found fin cleats produced significantly less rotational traction compared to the other categories and no differences were observed in translational coefficients between the cleat designs. Additionally, when previously used cleats were compared to new cleats of the same model, the cleats used during the course of the 2008 season exhibited a higher degree of variability for both translational and rotational traction compared to new cleats. This variability within used cleats illustrates stud degradation at different rates inferring an athlete-specific stud degradation.

In 2009, the National Football League (NFL) funded the production of the Turfblaster traction testing instrument developed at Boise State University (Kuhlman et al., 2010), the first of two traction testing instruments funded by the NFL. The study examined four different cleats rotational and translational traction characteristics under normal forces ranging from 222-1780 N. The Turfblaster utilized two pneumatic cylinders with one horizontal and one vertical. The vertical force was applied perpendicular to the surface, and horizontal force was produced parallel to the playing surface. Unlike other instruments, the cleat required no modification to be secured to the instrument, maintaining shoe integrity, with plantarflexion being manipulated up

to 15º. The instrument utilized an adjustable flat rigid footform and could simulate foot strike for the entire outer sole of the cleat system, or plantarflexion angle could be modified so that only forefoot studs would interact with the testing surface. However, this study only examined the forefoot stud interface of four cleats on a FieldTurf field. Horizontal and vertical force sensors and torque sensor data were collected at 250 Hz. The study found normal forces less than 666 N resulted in cleat systems behaving similarly for translational and rotational variables. It was found that a minimum of 888 N of normal force began producing a "distinct separation" in peak translational and rotational forces between all four cleat models.

The second of the two NFL funded traction testing instruments were developed by the head of the NFL's Foot & Ankle subcommittee at BioCore labs and named BioCore Elite Athlete Shoe-Surface Tester (BEAST). Kent et al. (2011) presented three mechanical tests designed to emulate force produced during human movements which were comprised of a performance test, a foot twisting, and a cut/stop test. The performance test applies a vertical pre-load of three times a 95 kg athlete (2800 N), then a translational force of 4200 N and collected the displacement of the cleat pattern (greater displacement would result in decreased player performance). A pre-loaded rotational test applies a normal force on the instrument than a 190 Nm of rotational torque on the foot (similar to all previous traction testing instruments just increased data acquisition frequencies and literature referenced normal forces). The cut/stop test horizontally pulls a carriage down linear rails at a velocity of 1.5 m/s then drops from a 67 mm

height. The test examined hardness and horizontal braking forces acting on the body as a result of the forefoot cleat pattern. Kent et al. (2015) found that rotational traction on synthetic turfs could reach peak reaction moments approaching 225 Nm compared to natural grass peak reaction moments of 175 Nm. The drop test horizontal reaction forces on synthetic turf reached highs of 3,250 N compared to 2,650 N on natural grass. These results illustrate significantly larger differences existed between natural turf and synthetic turf then previously reported by other traction testing instruments.

In summary, since the early 1970s, multiple traction testing instruments have been developed to quantify the cleat-turf interface. Early systems utilized mechanical means of measuring normal forces and reaction torque during data collection. Thus, resulting in limitations such as standardization of data collection and repeatability (Andreasson et al., 1986a; Heidt et al., 1996; Livesay et al., 2006; McNitt et al., 1997; Torg et al., 1974). As technology has evolved, so have the instruments utilized to collect data as well as data acquisition techniques. New instruments all had some form of rotational test (Kent et al., 2011; Kuhlman et al., 2010; Villwock et al., 2009; Wannop et al., 2009a), and the addition of a translational test has been presented (Kent et al., 2011; Kuhlman et al., 2010; Wannop et al., 2009a). However, only Kent et al. (2011) collected data attempting to replicate athlete translational velocities and normal force as well as utilized standardized impact data acquisition and processing techniques. This

methodological approach has revealed significantly more substantial tractional differences between natural grass and synthetic turf.

Tractions Influences on Lower Extremity Biomechanics

The current epidemiological literature has produced mixed findings on lower extremity safety on synthetic turf compared to natural grass. More recent literature has revealed a relationship between traction and lower extremity injury. These findings paired with the mechanical traction testing literature illustrating synthetic turf presenting more significant translation and rotation traction characteristics compared to natural grass and begin to link synthetic turf to a greater incidence of lower extremity injury compared to natural grass. However, biomechanical laboratory studies have produced mixed findings when examining traction related to synthetic turf.

Cheat/Stud Influence on Foot Plantar Pressure

During the 1994 world cup soccer tournament, 38% of all members of the United States men's national soccer team sustained some form of metatarsal stress fracture or overuse injury (Knapp et al., 1998). To better understand why those athletes sustained foot injuries, Eils et al. (2004) examined twenty-one male soccer players wearing new (Nike Air Zoom Brasilia F.G.) soccer cleats. Athletes were instrumented with plantar pressure insoles, preforming four common soccer movements. The movements consisted of a controlled velocity 150 m run with pressure

measurements collected during the final 25 m. A slalom course with a horizontal distance of 40 m and a width of 7 m with three straight-line cuts one each leg, a 70% full speed sprint, and a shot on goal. In order to improve the understanding of how cleated shoes distribute pressure to different regions of the ventral foot, pressure data was broken into ten regions (medial and lateral heel, lateral and medial midfoot, medial intermediate and lateral forefoot, hallux, second toe, and toes 3-5). Data was sampled at 50 Hz and this low sampling rate resulted in less than 5 samples per stance phase for each of the ten regions. The study found during a soccer match simulated movement; the foot was exposed to a variety of different pressures depending on the movement. Cutting movements produced elevated pressure at the medial aspect of the foot as well as the heel compared to all other movements without a change in direction, where running was found to increase forefoot and toe regions pressures compared to cutting and kicking. Kicking produced elevated lateral foot pressures on the planted foot compared to all other movements.

How does synthetic turf influence pressure distribution compare to natural grass? To address this question, Ford et al. (2006) recruited seventeen male American football players to perform a slalom type of cutting movement. Players wore American football cleats (Nike Speed TD) instrumented with a plantar pressure insole (Pedar, Novel GMBH, Munich). The plantar pressure data were broken into nine regions with data collected at 99 Hz across 99 sensors. The study found synthetic turf produced significantly greater peak pressures on the lesser toes, and central forefoot relative to natural grass. On natural grass elevated pressures were observed at the

mid-forefoot and lateral midfoot compared to synthetic turf trials. The author contributed these peak pressures to elevated levels of surface hardness commonly seen on synthetic turf (hardness data was not presented). The authors noted a potential link between the contributed elevated lateral foot pressure on natural grass to “cleat catch”, resulting from the compliance of the natural surface to external load exerted on the surface by the participant.

Similarly, Bentley et al. (2011) examined the influence cleat geometry has on foot pressure distribution. The study examined twenty-nine amateur European soccer players during an indoor straight run and slalom cutting course on synthetic non-infilled turf under two cleated conditions (bladed and conventional studded) offered by the Adidas shoe model. Pressure insoles were sampled at 50 Hz, and the foot was broken into 11 regions. The study found both mean and peak pressures during the stance phase were less on the lateral aspect of the foot and hallux (only peak) when participants were wearing the bladed cleats compared to the conventional stud geometry. The bladed cleat condition produced an abnormal foot center of pressure (COP) path during the stance phase, which was a result of the increased lateral pressure and decreased hallux pressures, compared to a more common COP path running from the heel anteriorly to the hallux. The abnormality in COP and pressure can be attributed to differences in cleat geometry influencing penetration and reducing the force applied to the ventral foot.

Cleat geometry can influence foot pressure distribution during sports-related movements. How does elevated traction as a result of cleat geometry modification, specifically cleat length, influence plantar pressure during a high force production task? Carden et al. (2017) in an abstract published in Footwear Science, examined fourteen male rugby union players performing a weighted sled push wearing rugby cleats (Waitangi, Mizuno Inc. Tokyo, Japan) with three cleat lengths (13, 16, and 21mm) on synthetic turf. Kinematic and pressure data were collected (200 and 100Hz, respectively) under the three cleat conditions during the sled drive. As the cleat length increased, significant differences were observed in the dorsiflexion angle and peak pressures of the toes, mid and lateral foot, and medial and lateral heel. Taylor et al. (2018) produced similar findings when examining twenty male middle and high school American football players performing a 75% body weight sled drive task under two different cleat conditions (Adidas Scorch X FieldTurf, and Adidas Scorch X Fly Mid Football Cleat on non-infilled Polytex® USA synthetic turf). Natural grass cleats (longer studs) produced greater lateral foot pressures compared to the synthetic turf cleat with increased pressure to the hallux and midfoot. This increased pressures can potentially be a result of increased levels of traction. As the levels of traction increase, participants had the ability to generate elevated levels of plantar pressure on the surface.

Tractional Influence on Ground Reaction Forces

Computationally humans are biomechanically analyzed as interconnected dynamic structures and comprised of various biological materials that can sustain a given degree of force prior to failure. Tractional forces can be defined as "a physical process in which a tangential force is transmitted across an interface between two bodies through frictions resulting in motion, stoppage or the transmission of power." (Raymond, 2004). Thus, this section aims to present the current literature examining the influence friction, and tractional forces have on directional ground reaction forces exerted on participants during common athletic tasks.

Pedroza et al. (2010) examined the traction question by manipulating surface friction during a 135º run and pivot movement. Thirty participants were recruited to perform the 135º pivot movement on five different surfaces with a variety of coefficient of friction (CoF) ranging from 0.3 to 0.7 (0.3, 0.4, 0.5, 0.6, 0.7). Participants wore bowling shoes while the wax was applied to the vinyl and linoleum floor, allowing surface CoF alterations. The study found no significant differences in peak vertical ground reaction force (GRF) or computed CoF (anterior-posterior, AP, GRF/vertical GRF). However, qualitative feedback from participants found a surface CoF exceeding 0.5 would be the minimum surface required to complete the task safely or without biomechanical movement modification. Experimental surface yielding a CoF of 0.3 resulted in a significantly lower qualitative participant feedback score compared to the four other

experimental surfaces. Participant feedback was supported by data collectors qualitatively observed participants demonstrating a more tentative approach on surface conditions with CoF ≤ 0.4.

Previously mentioned, tractional forces possess some degree of frictional contribution and can be defined by Amonton's law of friction. The laws are comprised of three aspects: 1) friction force is directly proportional to the applied load, 2) frictional force is independent of the area of contact, and 3) kinetic friction is independent of sliding velocity (Otsuki and Matsukawa, 2013). This is the case when two independent surfaces come in contact. However, the addition of cleats to the outer sole of a shoe introduces surface penetration adding an elevated degree of complexity. An abstract from the Nike Sport Research Laboratory examined how children and adult peak traction ratios differ during a lateral cutting movement on Astroturf wearing turf shoes (Morag and Johnson, 2001). The study examined medial-lateral (ML), anterior-posterior (AP) GRF (expressed as a percent of body weight), and peak tractional forces (ratio of AP shear and vertical forces). The study found that children experienced less ML braking forces and peak braking traction compared to their larger counterparts during the stance phase of the cutting movement on synthetic turf. Thus, the normal force has the ability to influence traction characteristics on individual bases when performing the same task under the same tractional condition. However, approach velocity and synthetic turf details were not provided.

Mechanically normal force (or vertical GRF) has been found to influence AP GRF exerted on the body, and cleat geometry can alter pressure distribution and COP on the foot. McGhie and Ettema (2013) attempted to examine how these relationships were intertwined examining the directional GRF produced by twenty-two male soccer players during a jump stop and 90º cut movement wearing three different Adidas shoes (turf shoes, traditional studs, and bladed) on a 3rd generation synthetic turf (Tarkett, FieldTurf, Calhoun, Georgia). Cleat geometry, specifically rounded/traditional cleats, produced greater impact forces during both the jump stop and cut. They also examined different infill depths and found participants were exposed to reduced impact forces during trials conducted on a combination of turf shoes with shorter cleats and increased levels of infills compared to decreased infill depth, and longer cleats.

Although these studies only examined GRF produced by participants under various CoF or traction conditions, an increased degree of information can be deducted from the three preceding studies (McGhie and Ettema, 2013; Morag and Johnson, 2001; Pedroza et al., 2010). Although the abstract by Morag and Johnson (2001) was limited in methodological details, it provides support for the notion that vertical force, or mass, is a vital contributor of traction and its influence on external GRF acting on the body during human movement. Pedroza et al. (2010) qualitatively observed that low levels of CoF (≤0.4) resulted in movement modification in order to account for depressed levels of the shoe surface interaction. McGhie and Ettema (2013) illustrated that a combination of cleat geometry and infill characteristics could influence

directional forces applied to the body with respect to body weight. Although kinematics and kinetics were not collected in these studies, the studies illustrated the influence modification of the shoe surface interface has on GRF during sports-related movements.

Tractions Influence during Cutting Movements

Since the early 1900s, solid outer sole cleats have been utilized to improve traction for athletes on natural grass (Woods, 2006). John Tate Riddell was the head football coach and athletic director at Evanston Township high school in Evanston, Illinois, in the late 1920s. Mr. Riddell noticed the leather cleated shoes were not sufficiently improving his football players footing on the field of play (Woods, 2006). The solution he developed was an attachable cleat system that would allow for longer and firmer cleats to be attached to the outer sole of the shoe in order to improve the shoe-surface interaction on various turf conditions. As time moved forward, research has found that an increase in shoe-surface interaction can be harmful. Contrary to more recent epidemiological research showing increased traction can increase the incidence of lower extremity injury (Mack et al., 2019), laboratory research examining studded shoes and turf have produced mixed findings in recent years.

Kaila, (2007) examined the influence cleat geometry had on fifteen professional European soccer players during three athletic movements (straight, 30º cut and 60º cut tasks). Each participant completed three trials of each of the experimental movements for each one of

the cleat configurations (two-bladed and two traditional cleats). A Vicon plugin gait marker set was utilized for this study, with the optical data sampled at 120 Hz and GRF at 960 Hz. The study found minimal internal transverse knee moments, and knee valgus moments during both the 30 and 60º cutting movements, but significance was not observed between cleat conditions. Gehring et al. (2007) examined six male soccer players wearing bladed, and rounded cleats performed 180º turning movements on synthetic turf with no significant differences in kinematic or kinetic data. However, the study found significant increases in knee extensor electromyography (EMG) muscle activation in the rounded stud condition compared to bladed cleats. Although not statistically significant the author briefly mentions an increase in anterior-posterior (AP) GRF of 12.5% by the bladed cleats compared to rounded studs. Elevated AP reaction forces of bladed cleats are supported by mechanical testing results of Cooper et al. (2009). The mechanical test examined various cleats and translation traction with cleat oriented perpendicular to translational force (AP reaction force). The thesis found that bladed cleats produced elevated AP braking force compared to traditional rounded cleats. Brock et al. (2014) found greater peak medial GRF during the 90º cutting movement during cleated conditions compared to non-cleated, but no statistical differences in kinematic or other kinetic values during either 90º land and cut or180º cutting movements of fourteen recreationally active American football players.

A series of articles by Müller et al. (2009, 2010a, 2010b) examined various cleat stud configurations and their influence on lower extremity biomechanics. The first study examined fifteen experienced soccer players performing a 135º turning movement under four cleat configurations on a third-generation 2-Star FIFA certified synthetic turf (Müller et al., 2009). The study found cleats with the highest AP GRF during a 135º change in direction cutting movement had higher numbers of studs (detailed cleat configuration in Sterzing et al., 2009, 2008). Those same high stud cleat configurations produced significantly greater inversion foot angles (<66%, $p<0.05$) and shank flexion angle (<16.1%, $p<0.05$). Müller et al. (2010b) examined performance characteristics produced during propulsion phases of foot strike (peak vertical force, vertical force rate, AP force, the center of pressure on force plate) of the same four stud configurations during a slalom and straight-line 6 m run. The study found no significant performance differences where observed between cleat systems during the slalom and straight-line run tasks.

A series of studies out of the University of Calgary has produced interesting findings to the shoe-interface literature. Wannop et al. (2010) examined the influence two non-cleated shoes with various levels of traction (low and high traction shoe, same size 9 one with normal outer sole and other sanded smooth), have on the lower extremity during a maximum effort 45º cut on tartan track surface mounted to a force platform. The study found the high traction shoes significantly increased peak ankle external rotation moments (11%), and the knee external

rotation moments (+13%) and adduction moments (+15%). Additionally, no differences were observed between the two traction conditions for entrance and exit velocities. Luo and Stefanyshyn (2011) examined various surface CoF conditions (0.26, 0.54, 0.82, 1.13) during a V cut movement. The study found that as surface CoF increased, the thirty-two participants produced significantly greater peak experimental CoF of GRF (CoF of GRF = AP GRF/vertical GRF). Peak experimental CoF of GRF increased 58% from 0.2 to 0.5 ($p < 0.05$), 21% from 0.5 to 0.8 ($p < 0.05$), and 5% from 0.8 to 1.1. Decreased center of gravity lean angle (-21% from 0.2 to 0.5, $p < 0.05$), -8% from 0.5 to 0.8, and -2% from 0.8 to 1.1).

Stefanyshyn et al. (2010) examined twelve recreational soccer players performing maximum effort 45º cut and 180º turning movement under four shoe conditions (Adidas Nova running shoe, Copa soccer cleat, world cup soccer cleat, TRX soccer cleat) on infilled 3rd generation synthetic turf. The study found that cleat configurations producing static translational traction values greater than 1.53 resulted in increased ankle eversion moments, and increased knee abduction moments in all cleated conditions compared to Adidas Nova running shoe. This study was followed up by Schrier et al. (2014) who examined twelve male athletes performing a 5 m sprint, and a maximum effort 180º cut movement under three unique shoe- surface interface conditions (Adidas F10 training shoe and indoor track surface, training shoe and infilled synthetic turf, and Adidas F50 cleat and infilled synthetic turf). The study found the cleat condition significantly increased eversion moments (11.5%), knee abduction moments (28.5%),

knee external rotation moments (23.6%), and knee extension moments (11.3%) during the 180º turning movement compared to lab shoe on synthetic turf (moments were reported as Nm).

Wannop and Stefanyshyn (2016) examined the influence of the translational traction of a modified Adidas F10 training shoe (studs screwed into lab shoes), and synthetic turf had on the lower extremity of ten recreationally active males performing a maximum effort 90º cut and 135º cutting movement. During the 90º cut, the high translational traction cleated lab shoes significantly increased ankle moments in all three planes of motion (external rotation 30%, eversion 7%, plantarflexion 6%), and knee moments in the transverse and frontal planes (external rotation 26.9% and adduction 11.8%). Similar findings were observed during the 135º cutting movement were significantly elevated with high translational traction cleated lab shoes producing greater ankle moments (external rotation 27.2%, eversion 16.7%, plantarflexion 11.5%, respectively) and a greater knee external rotation moment of 25.9%. Finally, Wannop et al. (2019) examined how high and low traction turf surface conditions affected lower extremity mechanics of sixteen male recreationally active athletes wearing a size 10 Adidas 16.4 FXG cleated soccer shoe. The same 90º cutting design found that high traction surface significantly increased ankle external transverse plane moments (19.5%), and knee adduction moment (14%).

The preceding studies out of the University of Calgary (Luo and Stefanyshyn, 2011; Schrier et al., 2013, 2014b; Stefanyshyn et al., 2010; Wannop et al., 2012b, 2011, 2010, 2009b) used a hexapod platform in order to establish cleat and surface traction characteristics. This

method is limited by the vertical force produced by the linear actuators with normal forces ranging from 700-750N (71.38- 76.48kg). Throughout the mechanical traction testing, literature normal force has been found to be a key contributing factor of both rotational and translation traction independent of surface characteristics. Kuhlman et al. (2010) found translational and rotation traction does not differentiate between cleat systems until 888N of normal force is met, with respect to a sampling frequency of 250 Hz. Thus, cleat traction properties presented in these studies (Schrier et al., 2014b, 2014a; Stefanyshyn et al., 2010; Wannop et al., 2019; Wannop and Stefanyshyn, 2016) may have underestimated characteristic traction differences. Müller et al. (2009, 2010a, 2010b) and Wannop et al. (2019) mounted the infilled turf onto an elevated wooden box (ranging between 0.635 and 1.27 cm), with 5.08 x 10.16 cm wood infill retaining barriers. This mounting technique allowed experimental turfs to be mounted to the force plate, but potentially introduced surface height variability due to wood infill retaining barriers and infill depth and an increased degree of force platform targeting limitation.

The previous studies produced mixed laboratory findings, which potentially could be due to a lack of transparent methodological approach to examining the sport interface research question. Müller et al. (2010) introduced the notion of mounting the turf to the force plate to improve the GRF acquisition and methodologically adopted by both Schrier et al. (2014) and Wannop et al. (2019). However, Müller et al. (2010) did find significantly more substantial differences in joint moments, but no traction characteristics (linear or rotational) of the footwear

were reported in the design of the study. The kinematic and kinetic differences throughout the turf literature could be linked to an inadequate data collection technique. Song and Godøy (2016) found that the Nyquist sampling theorem which estimates an appropriate sampling rate for a continuous-time analog signal, does not apply to an optical motion tracking system using passive markers. The study found a minimum of 163 Hz was required to adequately collect passive marker locations on a 10 Hz revolution per minute motor with passive markers placed on a turning table, with lower sampling frequencies (≤100) unable to accurately identify orientation on the motorized turntable Müller et al. (2009, 2010a, 2010b) sampled at 500 Hz and found vastly larger ankle and knee angle and moment differences during similar athletic movements compared to Schrier et al. (2014) and Wannop et al. (2019). Studies by Müller et al. (2009, 2010a, 2010b), Schrier et al. (2014), and Wannop et al. (2019) had large participant mass variabilities, and normal force has been found to nonlinearly be influential in both translational and rotational cleat traction characteristics (Andreasson et al., 1986b; Heidt et al., 1996; Kent et al., 2015a, 2011; Kuhlman et al., 2010; Livesay et al., 2006; Torg et al., 1974; Villwock et al., 2009). Wannop et al. (2019) normalizing kinetic variables to participant's body mass and height which has been found to have a nonlinear relationship with GRF (Wannop et al., 2012), with Müller et al. (2009, 2010a, 2010b) normalizing to body weight (linear relationship) and Schrier et al. (2014) reporting unnormalized data.

Chapter III

Literature Review Examination and Validation of the Fundamental Lower Extremity Mobile Testing System, and Identification of Best Practice to Mount Synthetic Turf to a Force Platform

As of the 2018-19 academic year, 8.4 million high school and college student-athletes participated in interinstitutional competitive sports programs, and of which, approximately 41% participated in outdoor sports played on turf surfaces (turf-sports) (National Collegiate Athletic Association, 2019; NFSHSA, 2019). Traditionally, turf-sports have been played on natural grass turf exposed to environmental conditions. Nevertheless, since its introduction to athletics in 1965, synthetic turf has become a common alternative to natural turf (Levy et al., 1990). With between 12,000 and 13,000 active synthetic fields in the United States, and approximately 1,200 to 1,500 new systems installed each year (Synthetic Turf Council, 2019). Since the early 1970s, synthetic turf has been linked to significantly higher levels of lower extremity injury compared to natural sports turf (Stevenson and Anderson, 1981; Torg et al., 1974).

An examination of knee injuries sustained by NCAA American football players indicated non-contact posterior cruciate ligament (PCL), and anterior cruciate ligament (ACL) injury was 2.94 and 1.63 times more likely to occur on synthetic turf compared to natural sports turf (Loughran et al., 2019). The National Football League (NFL) injury surveillance data from 2012-2016 found per play athletes sustained 16% more lower extremity injuries on synthetic turf compared to natural turf (Mack et al., 2019), with non-contact foot and ankle injuries 1.46 times

more likely on synthetic turf. To account for environmental conditions, athletes utilize studded footwear to prevent foot slippage during competition and practice on natural and synthetic turf. However, the increased incidence of injury has been crudely linked to the studded footwear's inability to disengage from the synthetic surface (Lambson et al., 2007; Mack et al., 2019; Torg et al., 1974).

Numerous mechanical devices have been developed to examine the athlete-surface interface. These instruments have aimed to mimic the foot planting and pivoting, or planting and dragging across the surface in a linear movement pattern (Heidt et al., 1996; Kent et al., 2012; McNitt et al., 1997; Torg et al., 1974). Synthetic turf across cleat configurations require greater levels of torque and translational force to disassociate the studded footwear from the synthetic materials compared to natural turf (Heidt et al., 1996; Kent et al., 2012, 2015; Villwock et al., 2009). Both linear and angular variables can be linked to increased braking (anterior-posterior) ground reaction force (GRF) and the free moment (about the vertical axis of contact surface), all standard variables acquired by a force platform. However, few instruments have been examined against the gold standard in-ground force platform, and those that did have produced mixed levels of agreement (Kuhlman et al., 2010; Thoms et al., 2013; Wannop et al., 2009a). Primarily those instruments have anecdotally addressed vertical force agreement. Two studies addressed non-vertical force agreement (Thoms et al., 2013; Wannop et al., 2009a): Wannop et al. (2009) examined the agreement between a force platform and a hydraulic actuator driven, low

horizontal velocity (0.25 m/s), system traction testing instrument. Although not the primary focus of the study, the authors graphically presented a time normalized ensembled curve of the vertical and horizontal force ratio. The instrument showed a “very good agreement” between the two systems.

Thoms et al. (2013) instrument was horizontally drive by a brushless motor, and vertically by a pneumatic actuator. The system was able to produce horizontal velocities up to 1 m s^{-1}, and vertical force up to 2100 N. the system statistically over estimated horizontal force and underestimated vertical forces compared to force platform measurements. Despite the rotational traction being the most studied form of sports-turf traction (Andreasson et al., 1986a; Lambson et al., 2007; Livesay et al., 2006; Torg et al., 1974; Villwock et al., 2009), according to the literature, no study has examined the agreement between a rotational test and the free moment obtained on a force platform.

Historically, epidemiological data has driven biomechanical researchers to replicate the settings where injuries occur in an effort to understand the underlying mechanisms of the injuries. However, laboratory studies examining turf-sport athletics have primarily been performed under non-turf conditions (Sigward and Powers, 2006). Studies that have attempted to replicate the turf condition have produced mixed findings (Gdovin et al., 2018), or did not report kinetic variables (Deneweth et al., 2014). This lack of surface replication and mixed findings

could be due to the logistical complexity of appropriately preparing experimental surfaces for data collection within the laboratory setting, as well as limited literature examining methodology examining how to acquire laboratory data duly. Therefore the two objectives of this study are as followed: 1) to identify the static and dynamic levels of agreement between an in-ground force platform, and a novel mechanical surface testing device and 2) using the established level of agreement obtained during aim one as reference level of agreement, aim two looked to identify the best method to mount synthetic turf to an in-ground force platform to adequately force measurement in future laboratory biomechanics studies looking to examine the influence of the cleat-turf interface on human mechanics.

Methods

Surface Conditions

Four experimental surface conditions and two footform conditions were tested during this study. An infilled synthetic turf comprised of a turf fiber density of 32,037 g/m^3, a fiber length of 51mm, and fiber thickness (primary, secondary) of 360/100 microns (Astroturf™ rhino blend, Astroturf, Dalton, GA) was used for three experimental surface mounting conditions. Synthetic turf was prepared following manufacturer recommendations with styrene-butadiene rubber infill 41±2 mm, and 0.45 kg of silica sand per 0.3 m^2. Experimental systems were mounted to a piece

of 60 x 60cm, and 12.7mm thick aluminum plate mounted through four threaded holes on the force platform. The four surface mounting conditions were as followed:

1. Surface condition 1: Control surface with aluminum plate only, used to establish the levels of agreement between the force platform and fLEX.
2. Surface condition 2: Turf mounting method 1 - A piece of 60 x 60 cm turf mounted to an aluminum plate, used in surface condition 1, using double-sided carpet tape (Model 442063, Duck Brand In.).
3. Surface condition 3: Turf mounting method 2 - A decoupled piece (cut to fit force platform, independent of surrounding turf) of synthetic turf adhered via Construction Adhesive (The Gorilla Glue Company, Cincinnati, OH) to aluminum plate used in surface condition 1.
4. Surface condition 4: Turf mounting method 3 - A coupled piece (Uniform piece of turf expanding around force platform) of synthetic turf adhered via Construction Adhesive (The Gorilla Glue Company, Cincinnati, OH) to an aluminum plate. The surrounding turf was mounted to a 1.27 cm thick wood floorboard (1.2 x 2.4 m) with a 62 x 62 cm square-cut in the center for the aluminum plate.

Footform Conditions

The rigid footform was a custom attachment that allowed mounting of either cleat/court shoe outer sole or standardized cleatform to an aluminum mounting plate. Further details on footform conditions are provided below:

1. Footform Condition 1: The outer sole of a court shoe (non-branded Adidas "experimental" basketball shoe) rigidly mounted to an aluminum plate (Kent et al., 2012) (Figure 1).
2. Footform Condition 2: The standardized cleatform is a 2.54 cm thick aluminum structure with recessed fitting for mounting plate. The base of the footform consists of six 15 mm aluminum studs. The cleatform was designed and used to limit any variability related to shoe material degradation or slippage related mounting techniques. This setup also allows for direct and equitable comparisons between experimental surfaces (Figure 2).



Figure 1.Court Shoe Footform

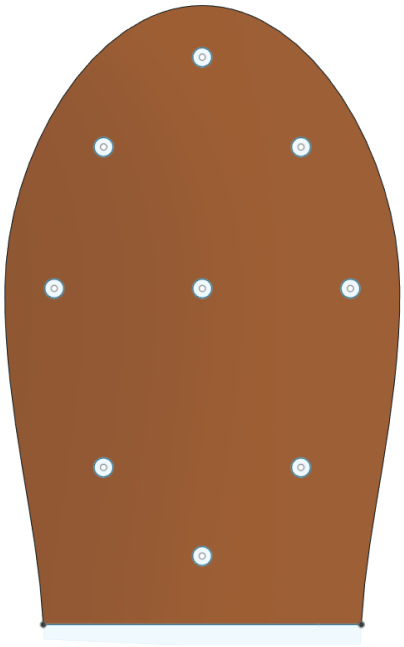


Figure 2.The cleatform with threaded holes for detachable studs.

Instrumentation

A novel mobile testing system (fLEX, fundamental lower extremity testing instrument) was designed to examine sports surface properties. fLEX is comprised of two independent testing systems, translational and rotational, with the ability to quantify static and dynamic traction characteristics of experimental interfaces (the combination of footform and surface). fLEX utilizes four linear actuated wheels for mobility and weights >5000 N.

The translational system is comprised of an interchangeable footform rigidly attached to a vertical pneumatic actuator. The vertical actuator is rigidly attached to a linear carriage mounted too low friction linear bearings with a horizontal pneumatic actuator threaded into the posterior aspect of the carriage. The two linear actuators can produce up to 5000N of force (Figure 3). The vertical actuator was positioned with a perpendicular orientation to the horizontal actuator; this orientation resulted in the footform and sensor aligned parallel to the impacting surface. A three-component quartz piezoelectric force ring (260A03, Piezotronics, Inc. Depew, NY) was rigidly mounted to the footform mounting plate. The sensor was mounted corresponding to a common biomechanical force platform orientation following a right-hand coordinate system X-Y-Z orientation with X = medial-lateral (+/-), Y = anterior-posterior (+/-), and Z = vertical (up+/down-).

The rotational system utilizes the same interchangeable footform as the translational system. The footform is rigidly attached to a torque actuating structure with low friction vertical linear bearing shafts and a pneumatic actuator applying vertical force up to 5000N. The torque structure is composed of a pneumatic rotary actuator capable of producing up to 225 Nm of torque with a dual flange reaction torque sensor (FUTEK Advanced Sensor Technology, Inc. Irvine, CA) mounted between actuator and footform (Figure *4*).

The test systems are controlled, and signals (analog and digital) were acquired via compact DAQ chassis (cDAQ-9178, National Instruments, Austin, TX). A custom program was written in LabView (version 19, National Instruments, Austin, TX, USA) to control the systems. Analog fLEX data was collected within the LabVIEW program, and an ASCII file was produced for each trial. Analog force platform data (BP600600 American Mechanical Technology Inc., Watertown, MA, USA) were collected via the Vicon Giganet data acquisition system and Nexus software (Version 2.9, Vicon Motion Analysis Inc., Oxford, UK). Data collection of both force platforms and fLEX were started at the same time using a synchronized start trigger generated by the compact DAQ chassis, and both systems acquired data at 5000 Hz. Each channel of the triaxial load cell was factory calibrated with sensor linearity of <0.1% and measurement uncertainty of ±1% the sensors full-scale capabilities (± 444.82 N for Z, and ± 177.92 N for X and Y), in addition, linearity was verified with free weight hang for X and Y components (Figure

68 and Figure 69, Appendix D). The torque sensor was locked at 45º and calibrated using rotary actuator pressure, and the result showed an adjusted R^2 of 0.999 (Figure *70* and Figure *71*, Appendix D).

Experimental Testing Protocols

Each experimental interface combination (See Table 1) were tested 60 times; five trials for each of the three experimental loading conditions corresponding to 2.5 times the theoretical body weight (BW) of a 55 kg (539.5N * 2.5BW = 1348 N), 75 kg (1838N), and 95 kg (2329 N) athlete; and four experimental movement tests including two static and two dynamic movements.

Table 1. Interface Conditions

		Footform 1 **(Court Shoe)**	Footform 2 **(Standardized Cleatform)**
Aim 1: Identify instrument force platform agreement	Control Condition	Interface Condition 1	NA
Aim 2: Examine Mounting Techniques	Surface Mounting Method 1 (Decoupled - Double Sided Tape)	Interface Condition 2	Interface Condition 3
	Surface Mounting Method 2 (Decoupled - Adhesive to Aluminum Mount)	Interface Condition 4	Interface Condition 5
	Surface Mounting Method 3	Interface Condition 6	Interface Condition 7

(Uniform - Adhesive to Aluminum Mount)		

Static Translational Tests

The fLEX translational system applied vertical forces corresponding to 2.5 times of theoretical body weights of a participant of 55 kg (1348 N), 75 kg (1838 N), and 95 kg (2329 N). The 2.5 BW loading coefficient was chosen based on the peak BW normalized vertical GRF during running trials at 6.0 m/s (Keller et al., 1996). Once vertical force was achieved, horizontal force was incrementally increased by 75 N every 100 ms until it reached 1500 N (force platform limit), or the cleat surface interface bound was exceeded, and footform displaced > 10 cm. Five trials for each loading condition and interface condition were performed.

Static Rotational Tests

The fLEX rotational system applied vertical forces corresponding to 2.5 times of theoretical body weights of a participant of 55 kg (1348 N), 75 kg (1838 N), and 95 kg (2329 N). Once vertical force was achieved, a rotational torque was incrementally increased 5 Nm every 100 ms until maximum torque was applied (225 Nm), or footform completed a full 90º rotation. Five trials for each loading condition and interface condition were performed

Dynamic Translation Tests

To better simulate a running forefoot strike, dynamic trials were conducted on the experimental surfaces. The fLEX translational system initiated horizontal motion as a result of pressure applied to the horizontal actuator, succeeded by the application of pressure to the vertical actuator corresponding to one of the three loading conditions. The footform impacted the surface for an average of 180 ms before returning to the starting position. Five trials for each loading condition and interface condition were performed.

Dynamic Rotational Tests

In a similar effort, the dynamic rotational test aimed to simulate a counterclockwise foot rotation during a cutting task on the experimental surface conditions. The fLEX rotational system initiated vertical motion corresponding to the required pressure to produce experimental loads. 200 ms after vertical motion began, the rotary actuator applied a 225 Nm torque. The footform impacted the surface for an average of 280 ms before returning to the starting position. Five trials for each loading condition and interface condition were performed on each testing surface.

Data Processing (Data Acquisition Validation)

Force platform and fLEX data were imported into MATLAB (version R2019b, MathWorks Inc., Natick, MA, USA) for data processing and analysis. Both force platform and fLEX signals were independently filtered using a fourth-order zero-lag low-pass Butterworth

filter with various cutoff frequencies ranging from 20 to 200 Hz (see detailed filtering process and results in appendix C) This cutoff frequency range was due to the exploratory nature of the study. Due to the differences in sensor orientation of fLEX with respect to the force platform, shear forces for both were examined as a resultant force, computed as the resultant force of the anterior-posterior and medial-lateral (APML-R) force components. Dependent variables of translational tests included peak vertical force (VF1) and APML-R force. Dependent variables for the rotational tests included the peak free moment (T_z) from the force platform, and peak torque from the fLEX system.

Equation 1. Free Moment Calculation

$$T_z = M_z - \left(COP_x * F_y - COP_y * F_x\right)$$

M_z, is the moment about the Z-axis measure by the force platform, COP_X is the X-coordinate of the force application point, COP_Y is the Y-coordinate of the force application point, F_y is the mediolateral force or force in the Y direction, and F_X is the anterior-posterior force or force in the X-direction.

Statistical Analysis (Data Acquisition Validation)

To investigate the levels of agreement between the force platform and fLEX, a Bland and Altman (BA) analyses were conducted (Bland and Altman, 1986). BA plots were generated in MATLAB for each experimental surface and individual interface combinations for each discrete

variable. Agreement between the two instruments was summarized by calculating the bias of the systems estimated by mean difference and standard deviation of differences. Shapiro-Wilk test was used to assess normality. The distribution of the differences within each plot was calculated with the 95% limits of agreement: upper and lower limits corresponded to the mean difference ±1.96 standard deviation. Absolute and relative biases and limits of agreement were reported (Bland and Altman, 1999). The force platform was used as the reference measurement system, or true measurement, with bias differences illustrating fLEX measurement differences from the force platform (Krouwer, 2008). Thus, the absolute bias results were presented as the absolute measured difference from the force platform (Appendix A), and the relative bias results were presented as a percent difference from the force platform (Appendix B). The addition of the relative bias was to account for the large magnitude of the variables. Positive and negative differences identified over and under estimation by fLEX. Additionally, to assess statistical differences between the measurement systems, a paired-sample t-test was run with on each BA analysis with an alpha level of 0.05 set *a priori*. T-tests were run on each individual measurement for all dependent variables with all loading rates included within the analysis. Data for interface condition one was analyzed prior to experimental surface mounting conditions. This was to establish a baseline level of agreement to be compared with the experimental surface mounting conditions.

In addition to the traditional BA graphical presentation, the novel Bland-Altman multi-variable relative spider plot (BASP) were generated for this study. The BASP were generated in MATLAB to examine multiple relative BA graphs within a single figure graphically. Like the BA plot, a relative axis (the top middle axis) used the force platform as the "gold standard" or reference measurement. The solid black zero line identifies 0 relative differences between systems. All dependent variables on the BASP have an independent relative axis. Each axis has the relative mean bias plus upper and lower limits of agreement. This allows all dependent variables to be plotted on the same figure making visually easier and more convenient for multiple variable interpretations.

Results

Descriptive data and all paired-samples t-tests results for each experimental interface combination were presented in Table 2-6. P values of the t-test results were reported to identify significant differences between measurement systems for each interface condition below with the BA results.

During the static tests of the interface condition 1 (control condition; Figure 6), mean relative and absolute bias data of the BA analysis showed that fLEX underestimated the peak free moment of the force platform by -0.02% (absolute bias of 0.18 Nm, $p = 0.96$ (t-test), Table 2). In the dynamic tests, it overestimated the peak free moment by 0.05% (0.01 Nm, $p = 0.99$,

Table 3). The fLEX overestimated APML-R of the force platform by 5.48% (20.78 N, p = 0.64, Table 4) during static tests, and by 3.8% (35.85 N, p = 0.96, Table 5) during dynamic tests. fLEX overestimated the peak vertical force of the force platform by 0.18% (6.82 N, p = 0.58, Table 6) during dynamics tests. Additionally, no statistically significant differences were observed for any control condition measurements.

During the static tests of interface condition 2 (Figure 7), mean relative and absolute bias data of the BA analysis showed that fLEX significantly overestimated the peak free moment of the force platform by 6.99 % (4.33 Nm, p<0.01, Table 2). In the dynamic tests, it underestimated the peak free moment by 0.41 % (-0.19 Nm, p = 0.9, Table 3). fLEX significantly overestimated APML-R of the force platform by 3.75 % (17.83 N, p<0.01, Table 4) during static tests and significantly overestimated by 1.33% (9.29 N, p=0.03, Table 5) during dynamic tests. fLEX significantly overestimated the peak vertical force of the force platform by 2.9 % (61.11 N, p < 0.01, Table 6) during dynamics tests. fLEX static peak torque, static and dynamic shear forces were found to be significantly different from force platform measurements.

During the static tests of interface condition 3 (Figure 8), mean relative and absolute bias data of the BA analysis showed that fLEX significantly overestimated the peak free moment of the force platform by 10.17% (6.17 Nm, p= 0.01, Table 2). In the dynamic tests, it underestimated the peak free moment by 16.4 % (-11.37 Nm, p=0.9, Table 3). The fLEX

significantly overestimated APML-R of the force platform by 20.51 % (180.82 N, $p<0.01$, Table 4) during static tests and overestimated by 40.99 % (292.38 N, $p<0.01$, Table 5) during dynamic tests. fLEX significantly overestimated the peak vertical force of the force platform by 10.35 % (158.04 N, $p <0.01$, Table 6) during dynamics tests. Dynamic peak torque was not significantly different between the two systems.

During the static tests of interface condition 4 (Figure 9), mean relative and absolute bias data of the BA analysis showed that fLEX significantly overestimated the peak free moment of the force platform by 3.23 % (1.66 Nm, $p<0.01$, Table 2). In the dynamic tests, it overestimated the peak free moment by 3.01 % (2.09 Nm, $p = 0.35$, Table 3). The fLEX overestimated APML-R of the force platform by 3.51 % (16.74 N, $p = 0.08$,Table 4) during static tests and significantly overestimated by 9.46 % (85.32 N, $p<0.01$, Table 5) during dynamic tests. fLEX overestimated the peak vertical force of the force platform by 0.06 % (7.87 N, $p = 0.64$, Table 6) during dynamics tests. Static peak torque and dynamic shear forces measurements were different between the two systems.

During the static tests of interface condition 5 (Figure 10), mean relative and absolute bias data of the BA analysis showed that fLEX overestimated the peak free moment of the force platform by 3.83 % (2.46 Nm, $p=0.06$, Table 2). In the dynamic tests, it underestimated the peak free moment by 0.1 % (0.19 Nm, $p = 0.86$, Table 3). The fLEX significantly overestimated

APML-R of the force platform by 10.7 % (81.66 N, $p<0.01$, Table 4) during static tests and overestimated by 4.1 % (56.49 N, $p= 0.06$, Table 5) during dynamic tests. fLEX underestimated peak vertical force of the force platform by 4.7 % (-88.5 N, $p = 0.69$, Table 6) during dynamics tests. All measurements, except static shear force, were not different between measurement systems.

During the static tests of interface condition 6 (Figure 11), mean relative and absolute bias data of the BA analysis showed that fLEX significantly overestimated the peak free moment of the force platform by 17.74 % (8.8 Nm, $p<0.01$, Table 2). In the dynamic tests, fLEX significantly overestimated the peak free moment by 15.49 % (9.07 Nm, $p<0.01$, Table 3). The fLEX significantly overestimated APML-R of the force platform by 37.51 % (184.15 N, $p<0.01$, Table 4) during static tests and significantly overestimated by 39.4 % (174.59 N, $p<0.01$, Table 5) during dynamic tests. fLEX underestimated peak vertical force of the force platform by 1.1 % (–15.99 N, $p = 0.17$, Table 6) during dynamics tests. All measurements, except vertical force, were found to be different between measurement systems.

During the static tests of interface condition 7 (Figure 12), mean relative and absolute bias data of the BA analysis showed that fLEX significantly overestimated the peak free moment of the force platform by 62.65 % (28.73 Nm, $p<0.01$, Table 2). In the dynamic tests, it overestimated the peak free moment by 3.44 % (-2.06 Nm, $p = 0.87$, Table 3). The fLEX

significantly overestimated APML-R of the force platform by 48.2 % (271.7 N, $p<0.01$, Table 4) during static tests and significantly overestimated by 57.97 % (294.18 N, $p<0.01$, Table 5) during dynamic tests. fLEX underestimated peak vertical force of the force platform by 10.61 % (-222.15 N, $p <0.01$, Table 6) during dynamics tests. All measurements were found to be different between measurement systems.

Discussion

The first aim of this study was to establish the levels of agreement between a force platform and a novel mechanical surface testing instrument (fLEX) during static and dynamic tests. To achieve this, fLEX performed a series of tests on a force platform, termed interface condition 1 (court shoe and aluminum mounting plate). fLEX was found to have high levels of agreement with the force platform for all measured dependent variables (Torque-free moment, vertical force, and shear force). During rotational tests, fLEX was found to have a systematic bias of <1%. Translational tests, fLEX was found to have a vertical system bias of 0.81%, and shear bias of 3.8% with agreement ranges within ±4.5% and ±14%.

Previous literature examining mechanical surface testing instrument agreement with an in-ground force platform have found significant differences for both shear and vertical force measurements (Thoms et al., 2013). However, no fLEX system measurements, during the control condition, were found to be significantly different from the in-ground force platform. Previous

systems have positioned shear force measurement sensors at the horizontal actuator-carriage interface (Figure 3). This sensor location results in a force measurement with a substantially vertical position offset from the surface. However, fLEX's force measurements are acquired within the footform located just above the testing surface, which significantly reduces the vertical offset. This offset reduction resulted in no significant differences for either shear or vertical force measurements of fLEX compared to the force platform. Additionally, no previous study, to our knowledge, has examined the agreement between the free moment of a force platform and the rotational torque of a mobile surface testing instrument. The high level of agreement between fLEX's rotational system and force platform free moment may be a result of the design of the rigid rotational structure and sensor calibration at the footform level. Torque shaft measurements must be positioned perpendicularly to the force platform during data collection in order to achieve the high levels of agreement between the two systems. Overall, fLEX showed high levels of agreement between the in-ground force platform for all forces and torques. These high levels of agreement also identified the best possible level of agreement for the examination of the subsequent aim of the study (please see practical application for fLEX in chapter IV).

Using the established level of agreement obtained during aim one as a reference level of agreement, aim two looked to identify the best method to mount synthetic turf to an in-ground force platform. The force platform used in this study was equipped with four threaded holes. All

experimental conditions utilized a mounting plate bolted onto the force platform through these holes. The first of the three mounting methods placed an independent or decoupled, piece of synthetic turf mounted onto the mounting plate with double-sided tape. The second and third mounting methods glued the synthetic turf to the aluminum plate. In mounting method two, the synthetic turf was cut out from the surrounding turf. In mounting method three, the synthetic turf was not cut out and was a uniform piece attached to the force platform and its surrounding floor surface. The uniform piece was glued to an aluminum mounting plate, and surrounding turf was attached to the elevated wood subflooring with a hole cut to fit the force platform. Our results found that mounting method 2 produced the highest level of agreement between the two systems.

The test results using the mounting method 2 with a decoupled piece of synthetic turf glued to the aluminum plate in interface conditions 4 and 5, found rotational system biases for both the court shoe and standard cleatform the most similar to the results in interface condition one (<1%) but did produce slightly larger agreement range ±10%. Translation vertical force system biases were equally good as the control condition (<1%), with similar increases in agreement range as the rotational tests ±18%. This method produced the lowest shear force system bias (<9%), but with a ±20% agreement range. Although shear measurements were higher than the control condition, the increased rigidity of the glued synthetic turf backing resulted in the highest level of agreement for all experimental mounting conditions.

The mounting method 1 with decoupled and taped surface for interface conditions 2 and 3, were found to be the second most effective method for mounting synthetic turf to the force platform. This method has been used previously, examining the cleat-turf interface on synthetic turf in a laboratory setting (Brock, 2012; Gdovin et al., 2018). Both studies examined cleated footwear with a control court shoe condition. Turf mounting condition two variables were found to be adequate in acquiring force platform data with mean biases for torque ranging from 1-9%, vertical force 1-5%, and shear forces 2-25%, respectively.

During the first high load, static rotational trials for interface condition three, the torsional force produced by fLEX's standard cleatform exceeded the adhesive capabilities of the tape, resulting in the synthetic turf being disassociated from the aluminum plate. This is problematic because, without the adhesive pulling on the surface of the aluminum plate, the force platform free moment may be prone to interference due to the disassociation. Additionally, once the adhesive failed, all subsequent tests resulted in turf disassociation. Prior to dynamic translational tests, the old tape pieces were removed and replaced with new pieces of adhesive tape on the aluminum surface. However, during the first static trial at the medium load, the adhesive failed once again. In BA Figure 21, the medium and high loading conditions produced shear forces less than to the lowest loading condition.

The initial tape failure resulted in the synthetic turf mounting bond being compromised for all subsequent static and dynamic trials independent of the vertical load. This compromised bond created an inability by both systems to quantify the true surface interface an athlete would experience in the field of play. In addition, the compromised bonding capability of the tape resulted in significant variability in vertical force measurements at peak torque. The adhesive failure can be a result of the polypropylene fibers threaded through the turf backing. The threading pattern created an inconsistent turf backing limiting the bonding areas between the synthetic turf and the aluminum mounting surface. Additionally, during dynamic translational tests, it was observed that the edges of the decouple turf would flip up during the contact phase.

During early trials, the decoupled tape technique did show the potential to be a viable method to mount an experimental surface to the force platform. However, this method, as executed in this study, was not found to be the best method to examine cleated footwear, which has been found to have high traction coefficients greater than 1 (Heidt et al., 1996). The high traction of interface condition 3 (cleatform-tape) resulted in a compromised bond between the synthetic turf and the mounting plate. The compromised bond resulted in peak torque magnitudes equivalent to the non-cleated control condition, and significantly less than interface condition 5 (glued counterpart, -78.1 vs. -89.6 Nm, -69.2 vs. -104.1 Nm, and -79 vs. -114.4 Nm). Failure of this bond can significantly influence the accuracy and reliability of acquiring experimental forces and torque exerted on a participant during laboratory studies. If future studies elect to utilize this

mounting technique, an increased awareness needs to be placed on the synthetic turf bond throughout the data collection session. If, at any point, within the data collection, the synthetic turf disassociates from the force platform, this was a sign that tapes bonding capabilities had been compromised. The removal of the compromised tape and reapplication of new tape must be performed.

The mounting method 3 using uniform synthetic turf rigidly mounted to an aluminum plate in the interface condition 6 and 7, found moderate to high levels of vertical force agreement (1-4%) for both footform conditions during translational movement. Peak torques and shear force measurements exhibited the lowest agreement of all mounting conditions, with a torque agreement range of 8-61%, and a shear force agreement range of 22-46%. However, during dynamic torque tests for interface condition 7 (Figure 58, Appendix B), low and medium loading conditions showed absolute agreement similar to interface condition 5 (independent-glued cleatform). However, during the high loading condition fLEX and the force platform agreement was substantially more difference than medium and low load conditions. Thus, a potential shift of the surrounding wood structure could have influence force platform measurements during testing. This potential shifting of the support structure occurred during the controlled testing environment, in which the support structure was exposed to minimal motion during testing. This is not a realistic expectation for future laboratory studies. The potential structural shift, along

with limited system agreement, creates a significant methodological limitation to this approach. Please see practical mounting applications in chapter IV.

The primary limitation to this study was the shear force measurement range of the force platform. Within the literature, cleated footwear can produce shear forces superseding vertical force (Heidt et al., 1996). Therefore, the shear force measurement range of the force platform for the two highest vertical loads was insufficient. This resulted in static shear force agreement measurements collected before the cleat-surface interface bound was exceeded for mounting conditions 2 and 3. Secondly, movement tests were conducted in the order of the smallest to largest vertical load, and synthetic turf infill displacement was not addressed until the completion of each movement. These limitations may have resulted in the high variability in peak torque and shear force measurements. This increased variability was not observed during the interface condition one test. Therefore, potential future research examining infill stability should be addressed in order to select a more stable/repeatable infill synthetic turf combination, or laboratory procedure to decrease traction variability.

The fLEX system's limitation was observed during dynamic translational tests. During the examination of the mounting methods, fLEX was observed to overestimate shear force at a greater magnitude than the related static tests. These increases in shear force magnitude observed by fLEX may be a result of system deformation. The translation test schematic diagram (Figure

3) showed a pneumatic actuator perpendicular to the floor with the triaxial load cell attached at the cleatform. The high shear forces applied during the dynamic tests may have resulted in the carriage structure (which the vertical actuator is attached) deforming. This deformation would result in clockwise rotation (with respect to Figure 3) of the triaxial load cell, consequently resulting in vertical force being experienced by the Y force component. This clockwise rotation can be observed by the vertical force measurement present in Figure 5. During early contact, the agreement between the two systems presents high agreement, but as cleatform engagement increases, an increase in the vertical force is observed by fLEX, and not by the force platform. During static trials, a maximum shear force of 1500 N was horizontally applied, compared to a shear force greater than 4000 N during dynamic tests. The court shoe utilized during control trials was unable to produce these high magnitude shear forces observed during cleatform trials in which the surface interface could exceed one and produce a more noticeable system deformation.

Conclusion

The agreement between the force platform and the mobile testing instrument (fLEX) observed during aim one, found fLEX to be a viable mobile instrument for assessing vertical and shear forces (<4%) as well as torque (<1%) exerted on an athlete via the shoe-surface interface. Aim two of this study found as mounting rigidity increases on an independent sample of an

experimental infilled synthetic turf, so does the level of agreement between the two systems. Mounting condition 2 was found to produce the most similar levels of agreement to the control condition, mounting condition 3 was found to have the poorest levels of agreement. Mounting condition 1 fell between 2 and 3 but was unable to acquire shear and peak torques observed in the mounting condition 2. Therefore, in order to acquire reliable ground reaction force and moment data during future laboratory studies, a rigid interface between the synthetic turf and the force platform must be in place, or else authors should take caution when interpreting kinetic data.

CHAPTER IV

PRACTICAL APPLICATIONS

fLEX Practical Applications

*Until fLEX translational or rotational variables are linked to human injury data (directly via controlled laboratory studies, or examination of onsite cleat-turf interface athletic injuries), all practical applications are theoretical.

High levels of traction at the shoe-turf interface are generally believed to be linked to non-contact lower extremity injuries (Lambson et al., 2007; Mack et al., 2019; Skovron et al., 1990; Torg et al., 1974). Post-injury cleat-turf analysis studies have found interface conditions exhibiting high rotational traction result in a higher incidence of lower extremity injuries (Lambson et al., 2007; Mack et al., 2019; Torg et al., 1974). Studies examining footwear traction have found that as rotational and translational traction increases body weight normalized anterior-posterior ground reaction force increases (Müller et al., 2009; Wannop et al., 2010), ankle moments increase in all three planes of motion (Wannop and Stefanyshyn, 2016), and knee moments increase in all three planes of motion (Wannop and Stefanyshyn, 2016). Wannop et al. (2019) found a cleat-turf rotation interface difference of 3.6 Nm can significantly increase peak ankle external rotation moment and angular impulse, as well as increased peak adduction knee moment. However, cleat-turf interface values were not clearly defined. Additionally, interface characteristics were quantified using a steward platform (Fichter, 1986) with applied normal load of 650 N. This method makes direct comparisons difficult at this time.

Mounting Methods Applications

The square footage of a football field is 5,350 m^2. A synthetic turf football field is comprised of 24 field width strips (> 48.8 m) broken into approximately 4.572 m segments. Segments are joined with a hook and loop fabric adhered to the turf backing. Most synthetic turf

companies recommend 0.45-0.91 kg of silica sand per 0.3 m^2 added to the system to weigh the surface down and fill gaps between fibers (Levy et al., 1990). This recommendation atop a synthetic American football field results in the cumulative sand load between 26,127 to 52,254 kg. Additionally, according to the literature, there is no scientific evidence that a synthetic turf system installed meeting manufacture sand recommendation should experience slippage between the turf backing and neighboring surface. Therefore, during laboratory studies, synthetic turf using recommended infill procedures, along with mounting method two (turf backing glued to mounting plate), can be termed a real-world replication at the rigidly mounted locations. Mounting method one cannot be termed a successful real-world replication due to the turf disassociating during cleatform condition. Although mounting method one is more convenient it did not outperform mounting method two. Thus, synthetic turf research requires a greater time commitment to setup and preparation to appropriately examine the cleat-turf interface.

List of References

Andreasson, G., Lindenberger, U., Renström, P., Peterson, L., 1986a. Torque developed at simulated sliding between sport shoes and an artificial turf. Am. J. Sports Med. 14, 225–230. https://doi.org/10.1177/036354658601400308

Andreasson, G., Lindenberger, U.L.F., Renström, P., Peterson, L., 1986b. Torque developed at simulated sliding between sport shoes and an artificial turf. Am. J. Sports Med. 14, 225–230. https://doi.org/10.1177/036354658601400308

Arendt, E., Dick, R., 1995. Knee Injury Patterns Among Men and Women in Collegiate Basketball and Soccer: NCAA Data and Review of Literature. Am. J. Sports Med. 23, 694–701. https://doi.org/10.1177/036354659502300611

Beaulieu, M.L., Lamontagne, M., Xu, L., 2008. Gender differences in time-frequency EMG analysis of unanticipated cutting maneuvers. Med. Sci. Sports Exerc. 40, 1795–1804. https://doi.org/10.1249/MSS.0b013e31817b8e9e

Bland, J., Altman, D.G., 1986. Statistical methods for assessing agreement between two methods of clinical measurement. Lancet 1, 307–310. https://doi.org/10.1016/S0140-6736(86)90837-8

Bland, J.M., Altman, D.G., 1999. Measuring agreement in method comparison studies. Stat. Methods Med. Res. 8, 135–160. https://doi.org/10.1177/096228029900800204

Boden, B.P., Dean, C.S., Feagin, J.A., Garrett, W.E., 2000. Mechanisms of anterior cruciate ligament injury. Orthopedics 23, 573–578. https://doi.org/10.3928/0147-7447-20000601-15

Bowers, K.D., Martin, R.B., 1976. Turf-toe: a shoe-surface related football injury. Med. Sci. Sports 8, 81–83.

Brock, E., Zhang, S., Milner, C., Liu, X., Brosnan, J.T., Sorochan, J.C., 2014. Effects of two football stud configurations on biomechanical characteristics of single-leg landing and cutting movements on infilled synthetic turf. Sport. Biomech. 13, 362–379. https://doi.org/10.1080/14763141.2014.965727

Brock, E.A., 2012. Biomechanical Differences of Two Common Football Movement Tasks in

Studded and Non-Studded Shoe Conditions on Infilled Synthetic.

Carden, P., Bru, B., Jones, A., Dixon, S., 2017. Influence of rugby surface type and boot stud length on lower limb biomechanical variables associated with Achilles tendinopathy during Rugby Union specific movements. Footwear Sci. 9, S132–S134. https://doi.org/10.1080/19424280.2017.1314379

Comstock, R.D., Pierpointm, L., 2019. National High School Sports-Related Injury Surveillance Study 2018-2019 School Year, NATIONAL HIGH SCHOOL SPORTS-RELATED INJURY SURVEILLANCE STUDY. https://doi.org/10.1017/CBO9781107415324.004

Comstock, R.D., Pierpointm, L., Arakkal, A., 2019. National High School Sports-Related Injury Surveillance Study 2017-2018 School Year, Center for Injury Research & Policy. https://doi.org/10.1017/CBO9781107415324.004

Cooper, B.S., 2009. Traction characteristics of cleated athletic shoes at various angles of internal rotation on artificial turf. Thesis.

Deneweth, J.M., Pomeroy, S.M., Russell, J.R., McLean, S.G., Zernicke, R.F., Bedi, A., Goulet, G.C., 2014. Position-specific hip and knee kinematics in NCAA football athletes. Orthop. J. Sport. Med. 2, 1–10. https://doi.org/10.1177/2325967114534591

Doller, J., Strother, S., 1978. Turf toe: an acute inflammatory response to athletic activity on artificial playing surfaces. J. Am. Podiatr. Med. Assoc. 68, 512–514.

Dragoo, J.L., Braun, H.J., Harris, A.H.S., 2013. The effect of playing surface on the incidence of ACL injuries in national collegiate athletic association American football. Knee 20, 191–195. https://doi.org/10.1016/j.knee.2012.07.006

Eils, E., Streyl, M., Linnenbecker, S., Thorwesten, L., Völker, K., Rosenbaum, D., 2004. Characteristic Plantar Pressure Distribution Patterns during Soccer-Specific Movements. Am. J. Sports Med. 32, 140–145. https://doi.org/10.1177/0363546503258932

Ekstrand, J., Timpka, T., Hagglund, M., Karlsson, J., 2006. Risk of injury in elite football played on artificial turf versus natural grass: a prospective two-cohort study. Br. J. Sports Med. 40, 975–980. https://doi.org/10.1136/bjsm.2006.027623

Faunø, P., Jakobsen, B.W., 2006. Mechanism of anterior cruciate ligament injuries in soccer. Int. J. Sports Med. 27, 75–79. https://doi.org/10.1055/s-2005-837485

Ford, K.R., Manson, N.A., Evans, B.J., Myer, G.D., Gwin, R.C., Heidt, R.S., Hewett, T.E., 2006. Comparison of in-shoe foot loading patterns on natural grass and synthetic turf. J. Sci. Med. Sport 9, 433–440. https://doi.org/10.1016/j.jsams.2006.03.019

Ford, K.R., Myer, G.D., Toms, H.E., Hewett, T.E., 2005. Gender differences in the kinematics of unanticipated cutting in young athletes. Med. Sci. Sports Exerc. 37, 124–129. https://doi.org/10.1249/01.MSS.0000150087.95953.C3

Fuller, C.W., Dick, R.W., Corlette, J., Schmalz, R., 2007. Comparison of the incidence, nature and cause of injuries sustained on grass and new generation artificial turf by male and female football players. Part 2: Training injuries. Br. J. Sports Med. 41, 20–26. https://doi.org/10.1136/bjsm.2007.037275

Gdovin, J., Williams, C., Wilson, S., Luginsland, L., Allen, C.R., Wade, C., Garner III, J.C., 2018. Influences of Athletic Footwear on Ground Reaction Forces During A Sidestep Cutting Maneuver on Artificial Turf. Int. J. Kinesiol. Sport. Sci. 6, 30. https://doi.org/10.7575/aiac.ijkss.v.6n.2p.30

Gehring, D., Rott, F., Stapelfeldt, B., Gollhofer, A., 2007. Effect of soccer shoe cleats on knee joint loads. Int. J. Sports Med. 28, 1030–1034. https://doi.org/10.1055/s-2007-965000

Griffin, L.Y., Agel, J., Albohm, M.J., Arendt, E.A., Dick, R.W., Garrett, W.E., Garrick, J.G., Hewett, T.E., Huston, L., Ireland, M.L., Johnson, R.J., Kibler, W.B., Lephart, S., Lewis, J.L., Lindenfeld, T.N., Mandelbaum, B.R., Marchak, P., Teitz, C.C., Wojtys, E.M., 2000. Noncontact anterior cruciate ligament injuries: risk factors and prevention strategies. J. Am. Acad. Orthop. Surg. https://doi.org/10.5435/00124635-200005000-00001

Grund, T., Senner, V., 2010. Traction behavior of soccer shoe stud designs under different game-relevant loading conditions. Procedia Eng. 2, 2783–2788. https://doi.org/10.1016/j.proeng.2010.04.066

Grund, T., Senner, V., Grube, K., 2007. Development of a test device for testing soccer boots under gamerelevant highrisk loading conditions. Sport. Eng. 10, 55–63.

https://doi.org/10.1007/bf02844202

Gwinn, D.E., Wilckens, J.H., McDevitt, E.R., Ross, G., Kao, T.C., 2000. The relative incidence of anterior cruciate ligament injury in men and women at the United States Naval Academy. Am. J. Sports Med. https://doi.org/10.1177/03635465000280012901

Hanson, A.M., Padua, D.A., Blackburn, J.T., Prentice, W.E., Hirth, C.J., 2008. Muscle activation during side-step cutting maneuvers in male and female soccer athletes. J. Athl. Train. 43, 133–143. https://doi.org/10.4085/1062-6050-43.2.133

Hawkins, P., 1984. Developments in synthetic grasses. Turf Manag. July, 23–25.

Heidt, R.S., Dormer, S.G., Cawley, P.W., Scranton, P.E., Losse, G., Howard, M., 1996. Differences in friction and torsional resistance in athletic shoe-turf surface interfaces. Am. J. Sports Med. 24, 834–842. https://doi.org/10.1177/036354659602400621

Hirsch, C., Lewis, J., 1965. Experimental ankle-joint fractures. Acta Orthop. 36, 408–417. https://doi.org/10.3109/17453676508988650

Kaila, R., 2007. Influence of modern studded and bladed soccer boots and sidestep cutting on knee loading during match play conditions. Am. J. Sports Med. 35, 1528–1536. https://doi.org/10.1177/0363546507300257

Keller, T.S., Weisberger, A.M., Ray, J.L., Hasan, S.S., Shiavi, R.G., Spengler, D.M., 1996. Relationship between vertical ground reaction force and speed during walking, slow jogging, and running. Clin. Biomech. https://doi.org/10.1016/0268-0033(95)00068-2

Kent, R., Crandall, J., Forman, J., Lessley, D., Lau, A., Garson, C., 2012. Development and assessment of a device and method for studying the mechanical interactions between shoes and playing surfaces in situ at loads and rates generated by elite athletes. Sport. Biomech. 11, 414–429. https://doi.org/10.1080/14763141.2011.650188

Kent, R., Forman, J., Lessley, D., Crandall, J., 2011. Characterization of Athletic Shoe-Surface Mechanics in situ at Loads and Rates Relevant to Game Situations. Ircobi Conf. 40–50.

Kent, R., Forman, J.L., Crandall, J., Lessley, D., 2015a. The mechanical interactions between an American football cleat and playing surfaces in-situ at loads and rates generated by elite

athletes: a comparison of playing surfaces. Sport. Biomech. 14, 1–17. https://doi.org/10.1080/14763141.2015.1024277

Kent, R., Forman, J.L., Lessley, D., Crandall, J., 2015b. The mechanics of American football cleats on natural grass and infill-type artificial playing surfaces with loads relevant to elite athletes. Sport. Biomech. 14, 246–257. https://doi.org/10.1080/14763141.2015.1052749

Knapp, T.P., Mandelbaum, B.R., Garrett, J., 1998. Why are stress injuries so common in the soccer player? Clin. Sports Med. https://doi.org/10.1016/S0278-5919(05)70123-X

Koga, H., Nakamae, A., Shima, Y., Iwasa, J., Myklebust, G., Engebretsen, L., Bahr, R., Krosshaug, T., 2010. Mechanisms for noncontact anterior cruciate ligament injuries: Knee joint kinematics in 10 injury situations from female team handball and basketball. Am. J. Sports Med. 38, 2218–25. https://doi.org/10.1177/0363546510373570

Krouwer, J.S., 2008. Why Bland-Altman plots should use X, not (Y + X)/2 when X is a reference method. Stat. Med. 27, 778–780. https://doi.org/10.1002/sim.3086

Kuhlman, S., Sabick, M., Pfeiffer, R., Cooper, B., Forhan, J., 2010. Effect of loading condition on the traction coefficient between shoes and artificial turf surfaces. Proc. Inst. Mech. Eng. Part P J. Sport. Eng. Technol. 224, 155–165. https://doi.org/10.1243/17543371JSET56

Lambson, R.B., Barnhill, B.S., Higgins, R.W., 2007. Football Cleat Design and Its Effect on Anterior Cruciate Ligament Injuries. Am. J. Sports Med. 24, 155–159. https://doi.org/10.1177/036354659602400206

Landry, S.C., McKean, K.A., Hubley-Kozey, C.L., Stanish, W.D., Deluzio, K.J., 2007. Neuromuscular and lower limb biomechanical differences exist between male and female elite adolescent soccer players during an unanticipated run and crosscut maneuver. Am. J. Sports Med. 35, 1901–1911. https://doi.org/10.1177/0363546507307400

Lehner, S., Dießl, C., Chang, D., Senner, V., 2013. Optimization of a foot model for the evaluation of the injury risk during cutting movements in football. Procedia Eng. 60, 325–330. https://doi.org/10.1016/j.proeng.2013.07.010

Levy, I., Skovron, M., Agel, J., 1990. Living with artificial grass: A knowledge update. Part 1: Basic Science. Am. J. Sports Med. 18, 406–413.

Levy, I.M., Skovron, M.L., Agel, J., Levy, I.M., Agel, J., Skovron, M.L., Agel, J., 1990. Living with artificial grass: A knowledge update. Part 1: Basic Science. Am. J. Sports Med. 18, 406–413. https://doi.org/10.1177/036354659001800511

Livesay, G.A., Reda, D.R., Nauman, E.A., 2006. Peak torque and rotational stiffness developed at the shoe-surface interface: The effect of shoe type and playing surface. Am. J. Sports Med. 34, 415–422. https://doi.org/10.1177/0363546505284182

Loughran, G.J., Vulpis, C.T., Murphy, J.P., Weiner, D.A., Svoboda, S.J., Hinton, R.Y., Milzman, D.P., 2019. Incidence of Knee Injuries on Artificial Turf Versus Natural Grass in National Collegiate Athletic Association American Football: 2004-2005 Through 2013-2014 Seasons. Am. J. Sports Med. 036354651983392. https://doi.org/10.1177/0363546519833925

Luo, G., Stefanyshyn, D., 2011. Identification of critical traction values for maximum athletic performance. Footwear Sci. 3, 127–138. https://doi.org/10.1080/19424280.2011.639807

Mack, C.D., Hershman, E.B., Anderson, R.B., Coughlin, M.J., McNitt, A.S., Sendor, R.R., Kent, R.W., 2019. Higher Rates of Lower Extremity Injury on Synthetic Turf Compared With Natural Turf Among National Football League Athletes: Epidemiologic Confirmation of a Biomechanical Hypothesis. Am. J. Sports Med. 47, 189–196. https://doi.org/10.1177/0363546518808499

Mattingly, T., 2018. UT Vols' 1968 opener featured John Ward's debut, artificial turf. News Sentin. NA.

McGhie, D., Ettema, G., 2013. Biomechanical analysis of surface-athlete impacts on third-generation artificial turf. Am. J. Sports Med. 41, 177–185. https://doi.org/10.1177/0363546512464697

McLean, S.G., Huang, X., Van Den Bogert, A.J., 2005. Association between lower extremity posture at contact and peak knee valgus moment during sidestepping: Implications for ACL injury. Clin. Biomech. 20, 863–870. https://doi.org/10.1016/j.clinbiomech.2005.05.007

McLean, S.G., Lipfert, S.W., Van Den Bogert, A.J., 2004. Effect of gender and defensive opponent on the biomechanics of sidestep cutting. Med. Sci. Sports Exerc. 36, 1008–1016.

https://doi.org/10.1249/01.MSS.0000128180.51443.83

McNitt, A., Middour, R., Waddington, D., 1997. Development and Evaluation of a Method to Measure Traction on Turfgrass Surfaces. J. Test. Eval. 25, 99–107. https://doi.org/10.1520/jte11329j

Messina, D.F., Farney, W.C., DeLee, J.C., 1999. The incidence of injury in Texas high school basketball: A prospective study among male and female athletes. Am. J. Sports Med. https://doi.org/10.1177/03635465990270030401

Meyers, M.C., 2017. Incidence, Mechanisms, and Severity of Match-Related Collegiate Men's Soccer Injuries on FieldTurf and Natural Grass Surfaces. Am. J. Sports Med. 45, 708–718. https://doi.org/10.1177/0363546516671715

Meyers, M.C., 2010. Incidence, Mechanisms, and Severity of Game-Related College Football Injuries on FieldTurf Versus Natural Grass. Am. J. Sports Med. 38, 687–697. https://doi.org/10.1177/0363546509352464

Meyers, M.C., Barnhill, B.S., 2004. Incidence, causes, and severity of high school football injuries on FieldTurf versus natural grass: A 5-year prospective study. Am. J. Sports Med. https://doi.org/10.1177/0363546504266978

Morag, E., Johnson, D., 2001. Traction requirements of young soccer players. Proc. V Symp. Footwear Biomech. Gr. 62–63.

Müller, C., Sterzing, T., Lake, M., Milani, T.L., 2010a. Different stud configurations cause movement adaptations during a soccer turning movement. Footwear Sci. 2, 21–28. https://doi.org/10.1080/19424281003685702

Müller, C., Sterzing, T., Lange, J., Milani, T.L., 2010b. Comprehensive evaluation of player-surface interaction on artificial soccer turf. Sport. Biomech. 9, 193–205. https://doi.org/10.1080/14763141.2010.511679

Müller, C., Sterzing, T., Milani, T.L., Lake, M., 2009. Influence of different stud configurations on lower extremity kinematics and kinetics during a soccer turning movement. Footwear Sci. 1, 82–83. https://doi.org/10.1080/19424280903059695

Myklebust, G., Engebretsen, L., Brækken, I.H., Skjølberg, A., Olsen, O.E., Bahr, R., 2003. Prevention of anterior cruciate ligament injuries in female team handball players: A prospective intervention study over three seasons. Clin. J. Sport Med. https://doi.org/10.1097/00042752-200303000-00002

National Collegiate Athletic Association, 2019. 2018-19 NCAA Sports Sponsorship and Participation Rates Report.

NFSHSA, 2019. 2018-19 High School Athletics Participation Survey [WWW Document]. Natl. Fed. State High Sch. Assoc. URL https://www.nfhs.org/articles/participation-in-high-school-sports-registers-first-decline-in-30-years/

Olson, D.E., Sikka, R.S., Hamilton, A., Krohn, A., 2011. Football injuries: current concepts. Curr Sport. Med Rep 10, 290–298. https://doi.org/10.1249/JSR.0b013e31822d4029

Otsuki, M., Matsukawa, H., 2013. Systematic breakdown of Amontons' law of friction for an elastic object locally obeying Amontons' law. Sci. Rep. https://doi.org/10.1038/srep01586

Pedroza, A., Fernandez, S., Heidt, R., Kaeding, C., 2010. Evaluation of the shoe-surface interaction using an agility maneuver. Med. Sci. Sports Exerc. 42, 1754–1759. https://doi.org/10.1249/MSS.0b013e3181d7d307

Pollard, C.D., Davis, I.M.C., Hamill, J., 2004. Influence of gender on hip and knee mechanics during a randomly cued cutting maneuver. Clin. Biomech. https://doi.org/10.1016/j.clinbiomech.2004.07.007

R. Gdovin, J., C. Williams, C., J. Wilson, S., A. Luginsland, L., Allen, C.R., Wade, C., Garner III, J.C., 2018. Influences of Athletic Footwear on Ground Reaction Forces During A Sidestep Cutting Maneuver on Artificial Turf. Int. J. Kinesiol. Sport. Sci. 6, 30–36. https://doi.org/10.7575/aiac.ijkss.v.6n.2p.30

Raymond, G.B., 2004. Mechanical Wear Fundamentals and Testing, Revised and Expanded, Marcel Dekker Inc., USA. https://doi.org/doi:10.1201/9780203021798.fmatt

Robbins, D.H., Schneider, L.W., Snyder, R.G., Pflug, M., Haffner, M., 1983. Seated posture of vehicle occupants, in: SAE Technical Papers. https://doi.org/10.4271/831617

School Enrollment in the United States, 2018. U.S. Census Bureau (2018).

Schrier, N., Wannop, J.W., Worobets, J., Stefanyshyn, D., 2013. Effects of artificial turf on performance and ground contact kinetics during a sprint acceleration. Footwear Sci. 5, S101–S103. https://doi.org/10.1080/19424280.2013.799582

Schrier, N.M., Wannop, J.W., Lewinson, R.T., Worobets, J., Stefanyshyn, D., 2014a. Shoe traction and surface compliance affect performance of soccer-related movements. Footwear Sci. 6, 69–80. https://doi.org/10.1080/19424280.2014.886302

Schrier, N.M., Wannop, J.W., Lewinson, R.T., Worobets, J., Stefanyshyn, D., 2014b. Shoe traction and surface compliance affect performance of soccer-related movements. Footwear Sci. 6, 69–80. https://doi.org/10.1080/19424280.2014.886302

Serensits, T.J., McNitt, A.S., 2014. Comparison of Rotational Traction of Athletic Footwear on Varying Playing Surfaces Using Different Normal Loads. Ats 11, 0. https://doi.org/10.2134/ats-2013-0073-rs

Sigward, S., Powers, C., 2006. The influence of experience on knee mechanics during side-step cutting in females. Clin. Biomech. 21, 740–747. https://doi.org/10.1016/j.clinbiomech.2006.03.003

Sigward, S.M., Cesar, G.M., Havens, K.L., 2015. Predictors of frontal plane knee moments during side-step cutting to 45 and 110 degrees in men and women: Implications for anterior cruciate ligament injury. Clin. J. Sport Med. 25, 529–534. https://doi.org/10.1097/JSM.0000000000000155

Sigward, S.M., Pollard, C.D., Havens, K.L., Powers, C.M., 2012. Influence of sex and maturation on knee mechanics during side-step cutting. Med. Sci. Sports Exerc. 44, 1497–1503. https://doi.org/10.1249/MSS.0b013e31824e8813

Sigward, S.M., Powers, C.M., 2006. The influence of gender on knee kinematics, kinetics and muscle activation patterns during side-step cutting. Clin. Biomech. 21, 41–48. https://doi.org/10.1016/j.clinbiomech.2005.08.001

Skovron, M.L., Levy, I.M., Agel, J., 1990. Living with artificial grass: a knowledge update. Part 2: Epidemiology. Am. J. Sports Med. https://doi.org/10.1177/036354659001800511

Song, M.H., Godøy, R.I., 2016. How fast is your body motion? Determining a sufficient frame rate for an optical motion tracking system using passive markers. PLoS One 11, 1–14. https://doi.org/10.1371/journal.pone.0150993

Stefanyshyn, D.J., Lee, J.S., Park, S.K., 2010. The influence of soccer cleat design on resultant joint moments. Footwear Sci. 2, 13–19. https://doi.org/10.1080/19424280903535454

Sterzing, T., Müller, C., Hennig, E.M., Milani, T.L., 2009. Actual and perceived running performance in soccer shoes: A series of eight studies. Footwear Sci. 1, 5–17. https://doi.org/10.1080/19424280902915350

Sterzing, T., Müller, C., Schwanitz, S., Odenwald, S., Milani, T.L., 2008. Discrepancies between mechanical and biomechanical measurements of soccer shoe traction on artificial turf. Int. Conf. Biomech. Sport. 339–342.

Stevenson, M.J., Anderson, B.D., 1981. The effects of playing surfaces on injuries in college intramural touch football. J. Natl. Intramural Recreat. Sport. Assoc. 5, 59–64.

Synthetic Turf Council, 2019. Synthetic Turf Council: About Synthetic Turf.

Taylor, J.B., Ford, K.R., Schmitz, R.J., Ross, S.E., Ackerman, T.A., Shultz, S.J., 2018. Sport-specific biomechanical responses to an ACL injury prevention programme: A randomised controlled trial. J. Sports Sci. 36, 2492–2501. https://doi.org/10.1080/02640414.2018.1465723

Thoms, A.W., Brosnan, J.T., Paquette, M.R., Zhang, S., Sorochan, J.C., 2013. A New Device for Simulating Athlete-to-Surface Interactions on Natural and Synthetic Turf. J. Test. Eval. 41, 20120103. https://doi.org/10.1520/jte20120103

Torg, J.S., Quedenfeld, T., 1971. Effect of shoe type and cleat length on incidence and severity of knee injuries among high school football players, Research Quarterly of the American Association for Health, Physical Education and Recreation. https://doi.org/10.1080/10671188.1971.10615058

Torg, J.S., Quedenfeld, T.C., Landau, S., 1974. The shoe-surface interface and its relationship to football knee injuries. Am. J. Sports Med. 2, 261–269. https://doi.org/10.1177/036354657400200502

Uhorchak, J.M., Scoville, C.R., Williams, G.N., Arciero, R.A., St. Pierre, P., Taylor, D.C., 2003. Risk Factors Associated with Noncontact Injury of the Anterior Cruciate Ligament. A Prospective Four-Year Evaluation of 859 West Point Cadets, in: American Journal of Sports Medicine. https://doi.org/10.1177/0363546503031006180 1

Villwock, M.R., Meyer, E.G., Powell, J.W., Fouty, A.J., Haut, R.C., 2009. Football playing surface and shoe design affect rotational traction. Am. J. Sports Med. 37, 518–525. https://doi.org/10.1177/0363546508328108

Wannop, J.W., Foreman, T., Madden, R., Stefanyshyn, D., 2019. Influence of the composition of artificial turf on rotational traction and athlete biomechanics. J. Sports Sci. 0, 1–8. https://doi.org/10.1080/02640414.2019.1598923

Wannop, J.W., Luo, G., Stefanyshyn, D., 2011. Effect of normal load, speed and moisture on footwear traction. Footwear Sci. 3. https://doi.org/10.1080/19424280.2011.575834

Wannop, J.W., Luo, G., Stefanyshyn, D., 2009a. Wear influences footwear traction properties in canadian high school football. Footwear Sci. 1, 121–127. https://doi.org/10.1080/19424280903410062

Wannop, J.W., Luo, G., Stefanyshyn, D., 2009b. Traction properties of footwear in canadian high school football. Footwear Sci. 1, 105–107. https://doi.org/10.1080/19424280903063523

Wannop, J.W., Luo, G., Stefanyshyn, D.J., 2012a. The effect of normal load, speed and moisture on footwear traction. Footwear Sci. 4, 37–43. https://doi.org/10.1080/19424280.2011.653992

Wannop, J.W., Luo, G., Stefanyshyn, D.J., 2012b. Footwear traction at different areas on artificial and natural grass fields. Sport. Eng. 15, 111–116. https://doi.org/10.1007/s12283-012-0091-x

Wannop, J.W., Stefanyshyn, D.J., 2016. The effect of translational and rotational traction on lower extremity joint loading. J. Sports Sci. 34, 613–620. https://doi.org/10.1080/02640414.2015.1066023

Wannop, J.W., Worobets, J.T., Stefanyshyn, D.J., 2010. Footwear traction and lower extremity

joint loading. Am. J. Sports Med. 38, 1221–1228. https://doi.org/10.1177/0363546509359065

Whitehurst, J.R., 1968. The Astrodome turf and lower extremity injuries. J. Am. Coll. Health Assoc. 17, 136–137.

Woods, J., 2006. John Tate Tiff [WWW Document]. Genealogy.com.

Appendices

Appendix A: Tables and Figures

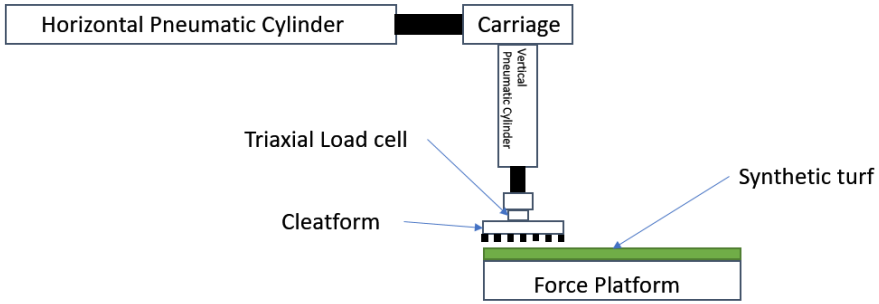


Figure 3. The fLEX translational test schematic diagram.

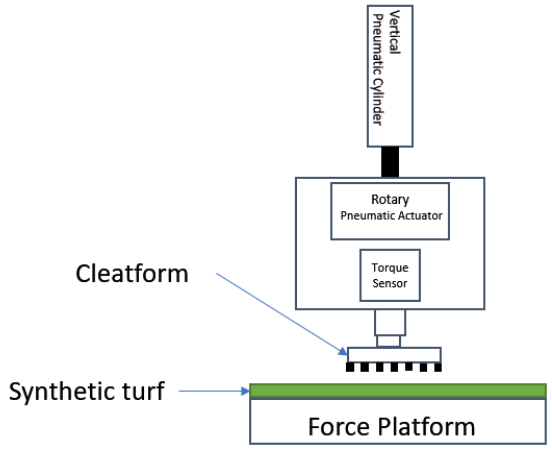


Figure 4. The fLEX rotational test schematic diagram.

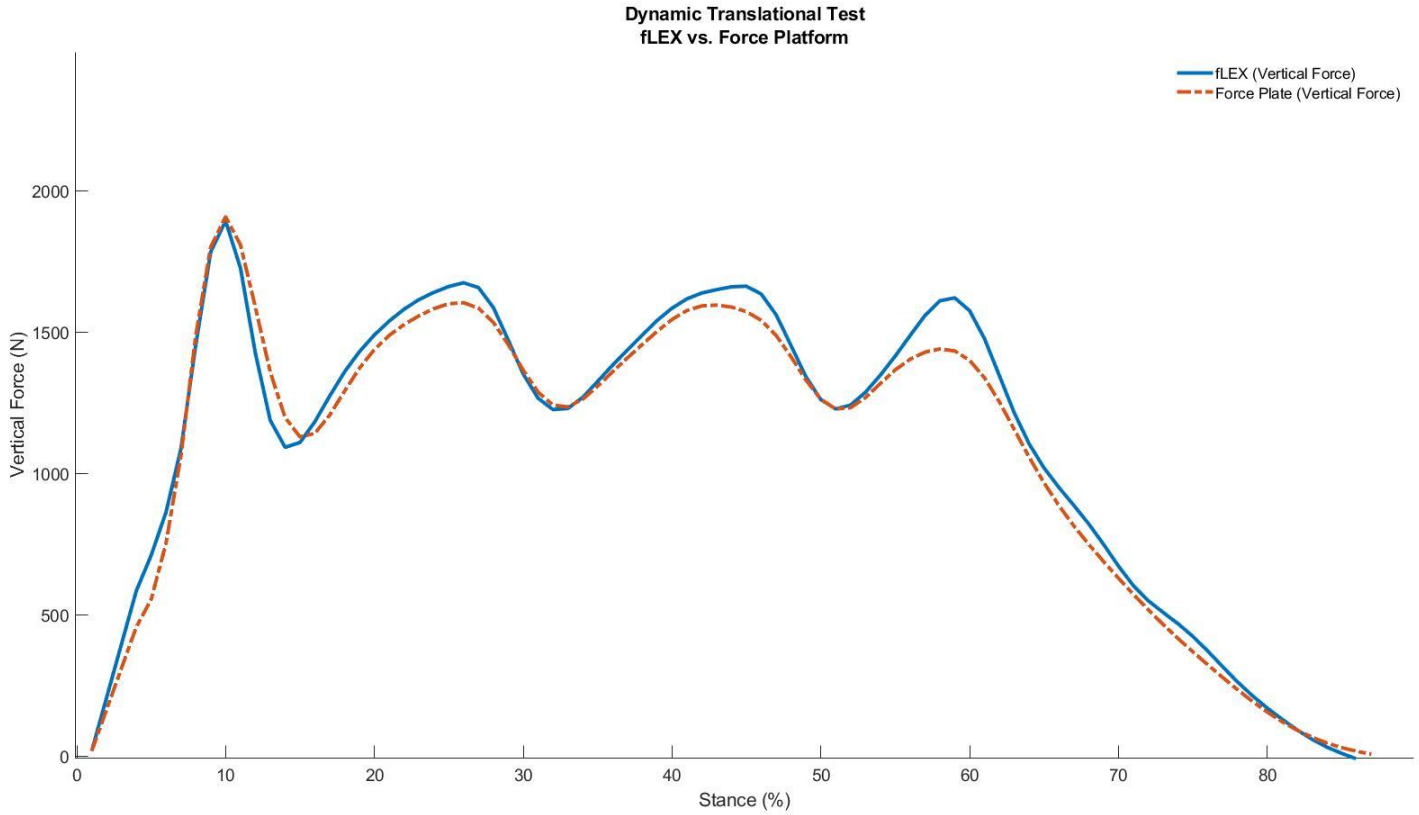


Figure 5. Impact Normalized Vertical Force.

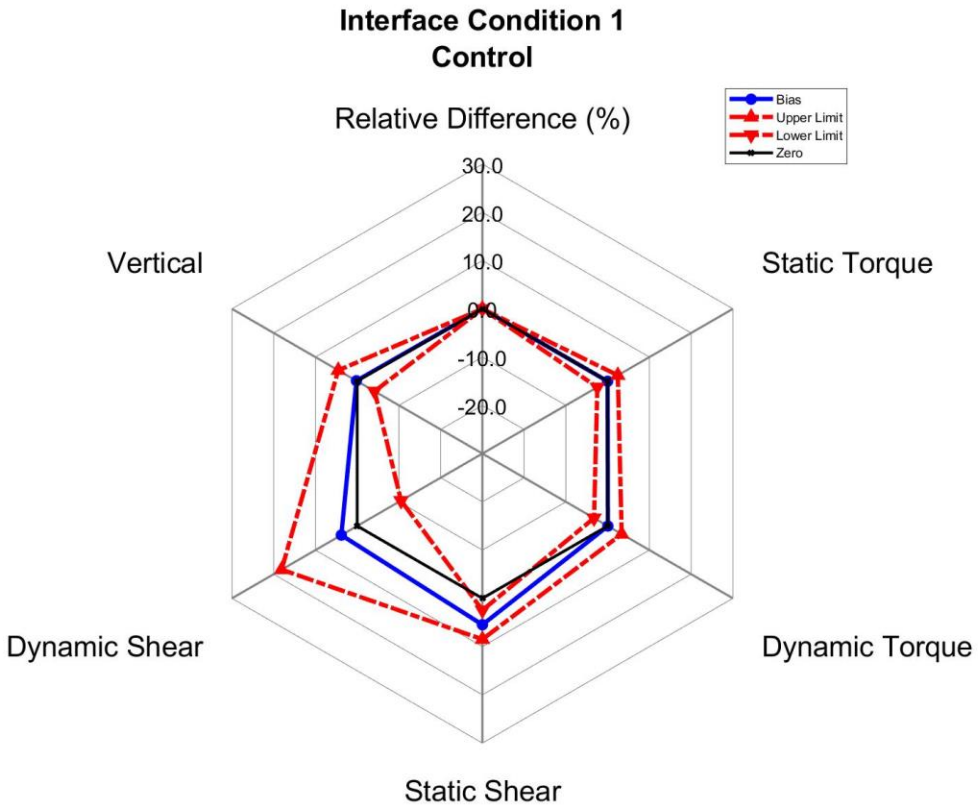


Figure 6. BASP Control Condition

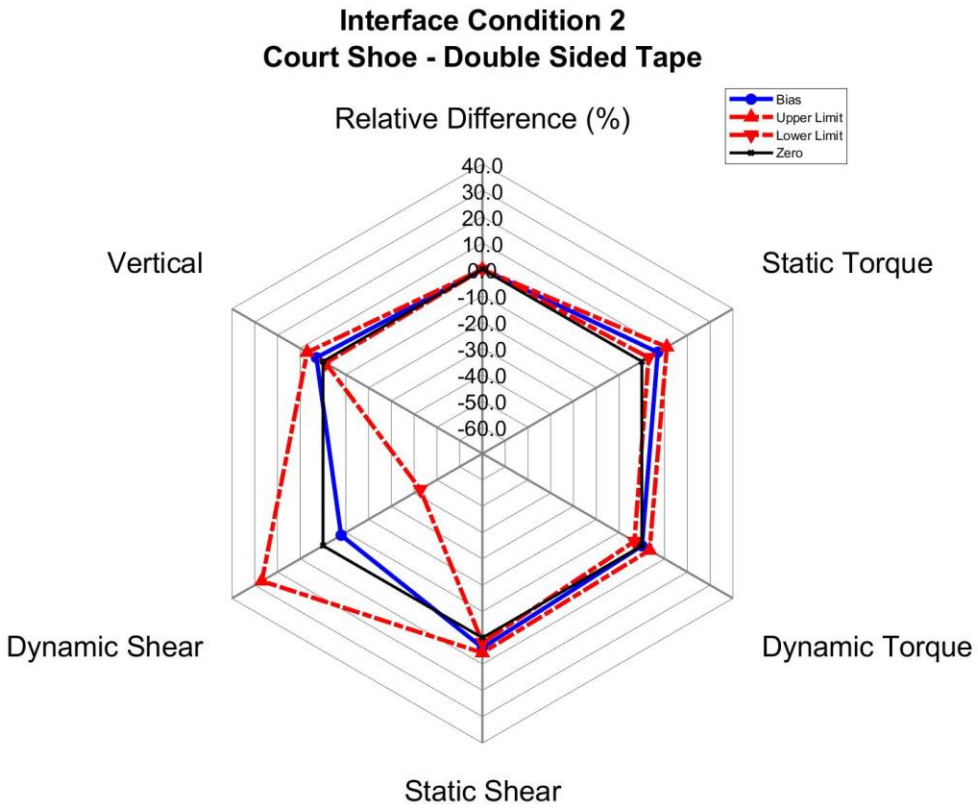


Figure 7. Interface Condition 2 (Tape-Court Shoe)

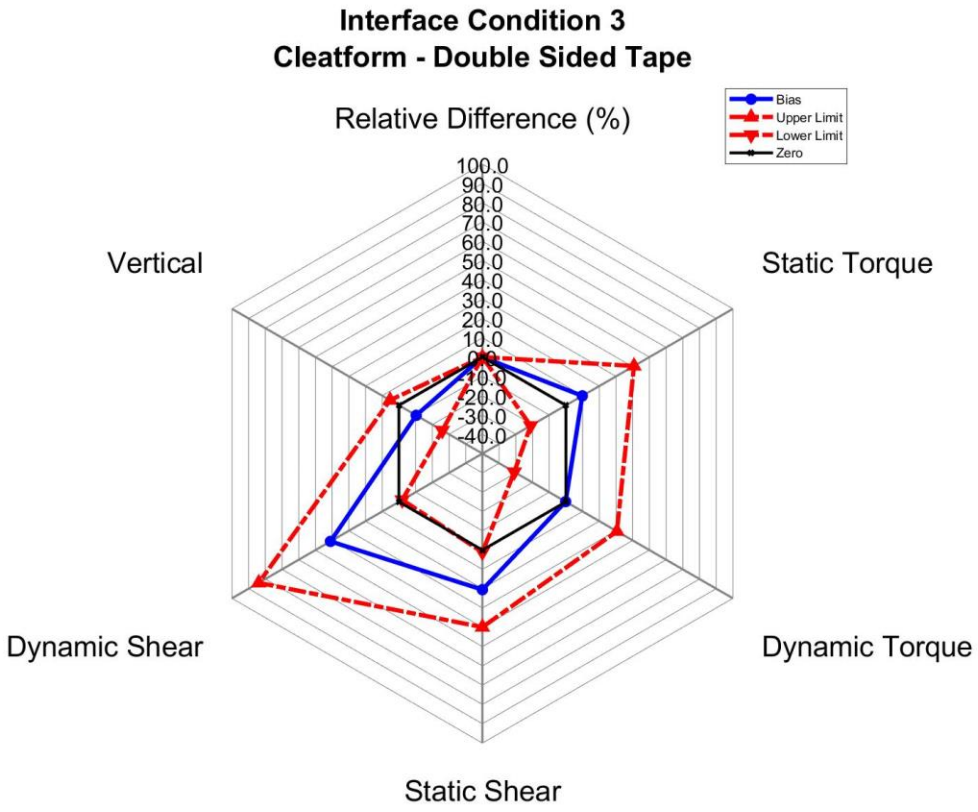


Figure 8. Interface Condition 3 (Tape -Cleatform)

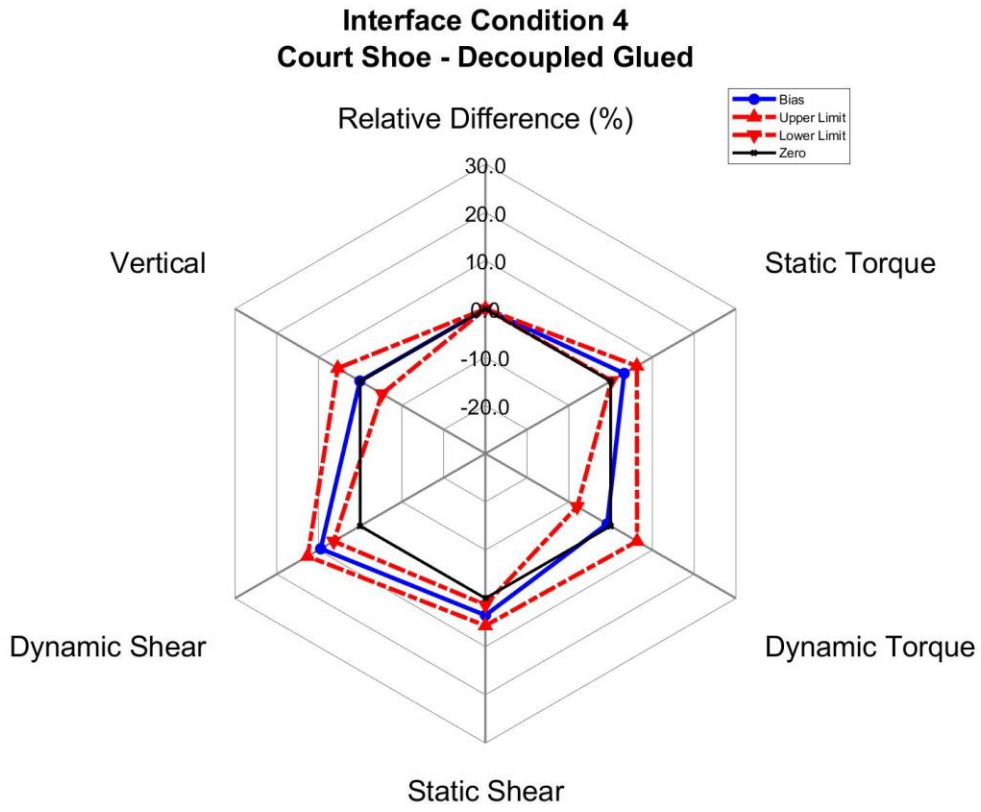


Figure 9. Interface Condition 4 (Decoupled Glued - Court)

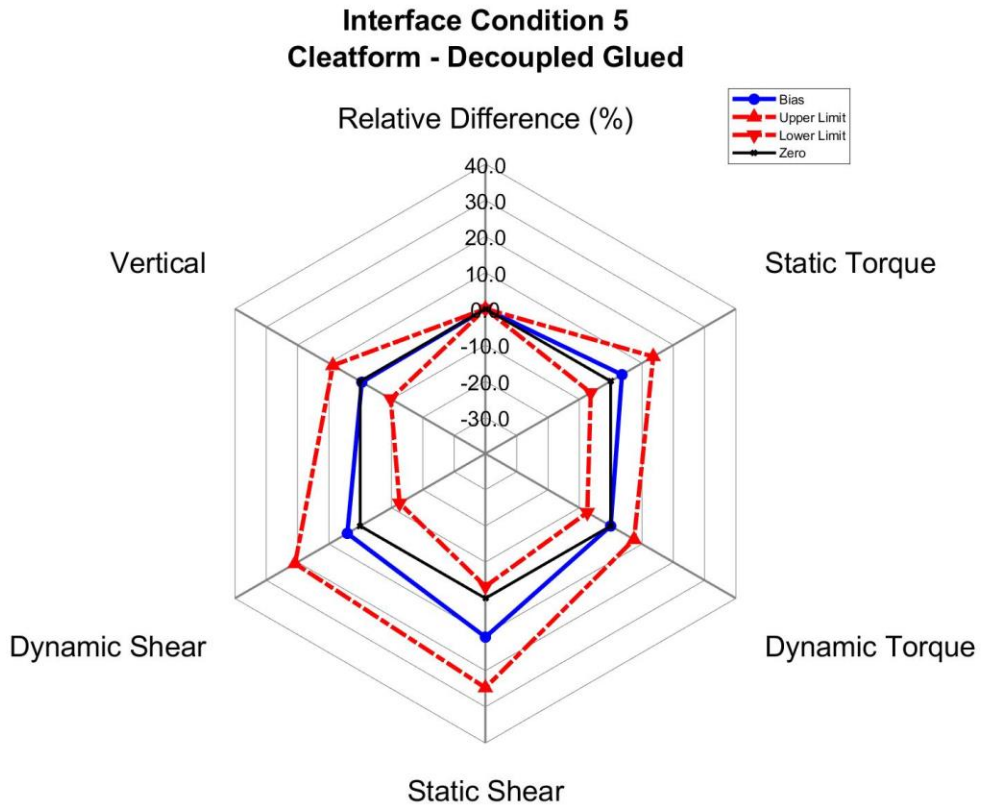


Figure 10. Interface Condition 5 (Decoupled Glued - Cleatform)

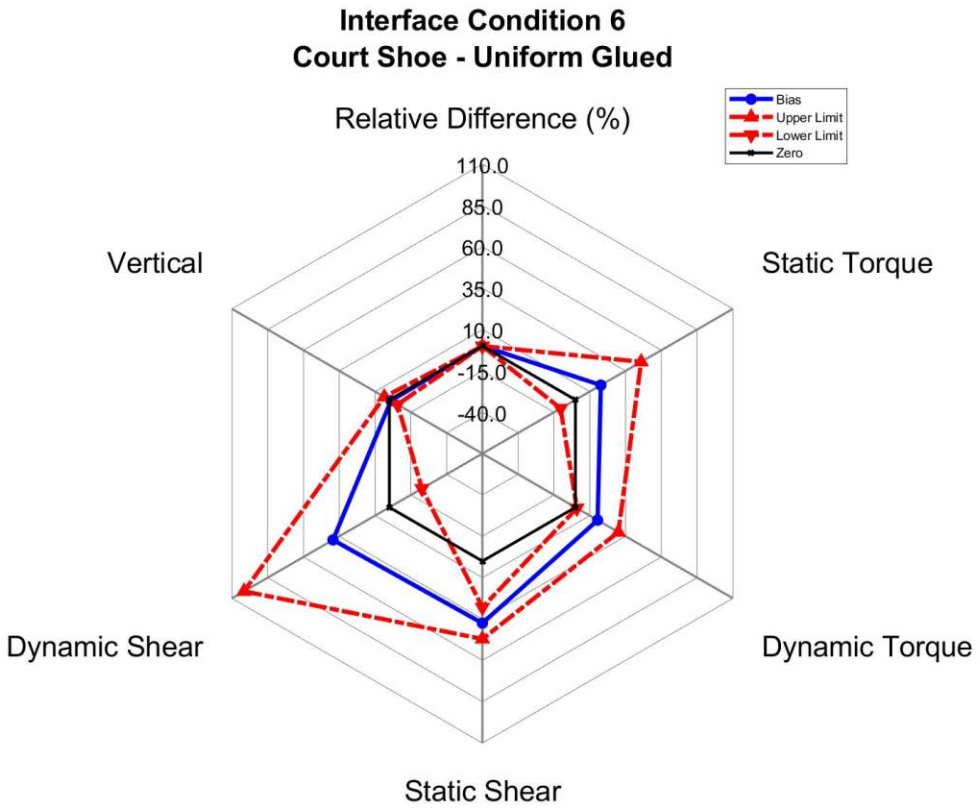


Figure 11. Interface Condition 6 (Uniform Glued - Court)

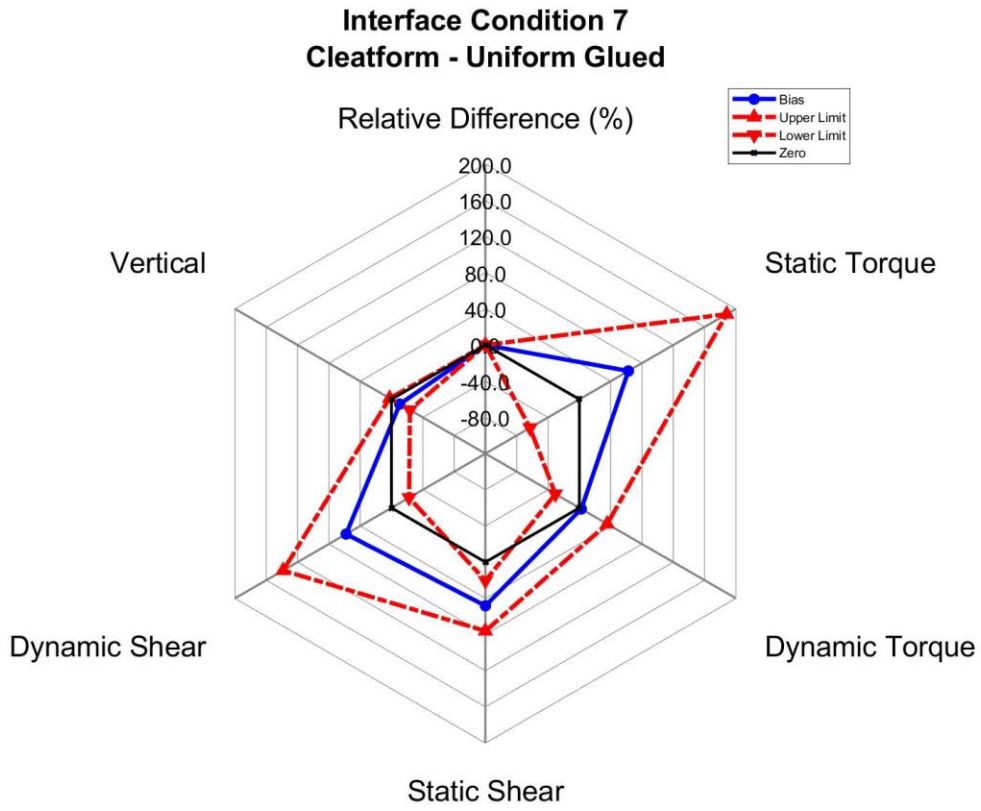


Figure 12. Interface Condition 7 (Uniform Glued – Cleatform)

Table 2. Static Peak Torque (Nm).

Test Condition	fLEX	Force Platform	% Bias	Absolute bias	Upper limit (%)	Lower limit (%)	P value
Interface Condition 1 (Control)	-74.32	-74.50	-0.02	-0.18	2.44	-2.48	0.96
Interface Condition 2 (Taped-Court Shoe)	-64.07	-59.74	6.99	4.33	10.99	2.99	**<0.01**
Interface Condition 3 (Tape-Cleatform)	-85.31	-79.14	10.17	6.17	41.75	-21.13	**0.01**
Interface Condition 4 (Independent Glued-Court shoe)	-58.15	-56.48	3.23	1.66	6.28	0.19	**<0.01**
Interface Condition 5 (Independent Glued-Cleatform)	-88.28	-85.81	3.83	2.46	13.89	-6.36	0.06
Interface Condition 6 (Uniform Glued-Court shoe)	-63.05	-53.89	17.74	8.80	45.91	-10.42	**<0.01**
Interface Condition 7 (Uniform Glued-Cleatform)	-76.25	-47.53	62.65	28.73	188.31	-63.02	**<0.01**

Table 3. Dynamic Peak Torque (Nm).

Test Condition	fLEX	Force Platform	% Bias	Absolute bias	Upper limit (%)	Lower limit (%)	P value
Interface Condition 1 (Control)	-87.34	-87.35	0.05	0.01	3.36	-3.26	0.98
Interface Condition 2 (Taped-Court Shoe)	-69.78	-69.96	-0.41	-0.19	3.57	-3.61	0.9
Interface Condition 3 (Tape-Cleatform)	-62.28	-73.65	-16.44	-11.37	29.40	-62.27	0.9
Interface Condition 4 (Independent Glued-Court shoe)	-72.79	-70.70	3.01	2.09	8.22	-2.71	0.35
Interface Condition 5 (Independent Glued-Cleatform)	-99.02	-99.22	-0.01	-0.19	7.47	-7.46	0.86
Interface Condition 6 (Uniform Glued-Court shoe)	-71.42	-62.35	15.49	9.07	29.96	1.02	<**0.01**
Interface Condition 7 (Uniform Glued-Cleatform)	-96.56	-94.49	3.44	2.06	36.18	-30.59	0.87

Table 4. Static Shear Force (N)

Test Condition	fLEX	Force Platform	% Bias	Absolute bias	Upper limit (%)	Lower limit (%)	P value
Interface Condition 1 (Control)	445.73	424.94	5.48	20.78	8.49	2.46	0.64
Interface Condition 2 (Taped-Court Shoe)	514.79	496.97	3.75	17.83	5.70	1.81	**<0.01**
Interface Condition 3 (Tape-Cleatform)	1115.15	934.33	20.51	180.82	39.93	1.09	**0.01**
Interface Condition 4 (Independent Glued-Court shoe)	547.99	531.26	3.51	16.74	5.67	1.36	0.08
Interface Condition 5 (Independent Glued-Cleatform)	933.42	851.76	10.71	81.66	24.72	-3.29	**<0.01**
Interface Condition 6 (Uniform Glued-Court shoe)	679.40	495.25	37.51	184.15	47.07	27.95	**<0.01**
Interface Condition 7 (Uniform Glued-Cleatform)	854.57	582.86	48.24	271.70	76.09	20.39	**<0.01**

Table 5. Dynamic Shear Force (N)

Test Condition	fLEX	Force Platform	% Bias	Absolute bias	Upper limit (%)	Lower limit (%)	P value
Interface Condition 1 (Control)	986.84	950.99	3.80	35.85	18.10	-10.51	0.96
Interface Condition 2 (Taped-Court Shoe)	1129.13	1138.41	-1.33	-9.29	23.60	-20.94	**0.03**
Interface Condition 3 (Tape-Cleatform)	976.81	684.43	40.99	292.38	83.95	-1.98	<**0.01**
Interface Condition 4 (Independent Glued-Court shoe)	984.45	899.13	9.46	85.32	12.57	6.35	<**0.01**
Interface Condition 5 (Independent Glued-Cleatform)	1256.08	1199.59	4.10	56.49	20.79	-12.60	0.06
Interface Condition 6 (Uniform Glued-Court shoe)	1001.58	826.99	39.40	174.59	101.53	-22.73	<**0.01**
Interface Condition 7 (Uniform Glued-Cleatform)	1046.41	752.22	57.97	294.18	138.45	-22.51	<**0.01**

Table 6. Dynamic Vertical Force (N)

Test Condition	fLEX	Force Platform	% Bias	Absolute bias	Upper limit (%)	Lower limit (%)	P value
Interface Condition 1 (Control)	2018.11	2011.29	0.18	6.82	4.52	-4.16	0.58
Interface Condition 2 (Taped-Court Shoe)	2071.39	2010.27	2.90	61.11	6.95	-1.15	<**0.01**
Interface Condition 3 (Tape-Cleatform)	1518.06	1676.10	10.35	158.04	5.30	-26.00	<**0.01**
Interface Condition 4 (Independent Glued-Court shoe)	1989.42	1981.55	0.06	7.87	5.37	-5.25	0.64
Interface Condition 5 (Independent Glued-Cleatform)	1776.15	1864.71	-4.74	-88.57	4.37	-13.85	0.69
Interface Condition 6 (Uniform Glued-Court shoe)	1919.82	1935.81	-1.09	-15.99	3.54	-5.72	0.17
Interface Condition 7 (Uniform Glued-Cleatform)	1896.75	2118.90	-10.61	-222.15	2.31	-23.54	<**0.01**

Appendix B: Relative Bland-Altman Plots

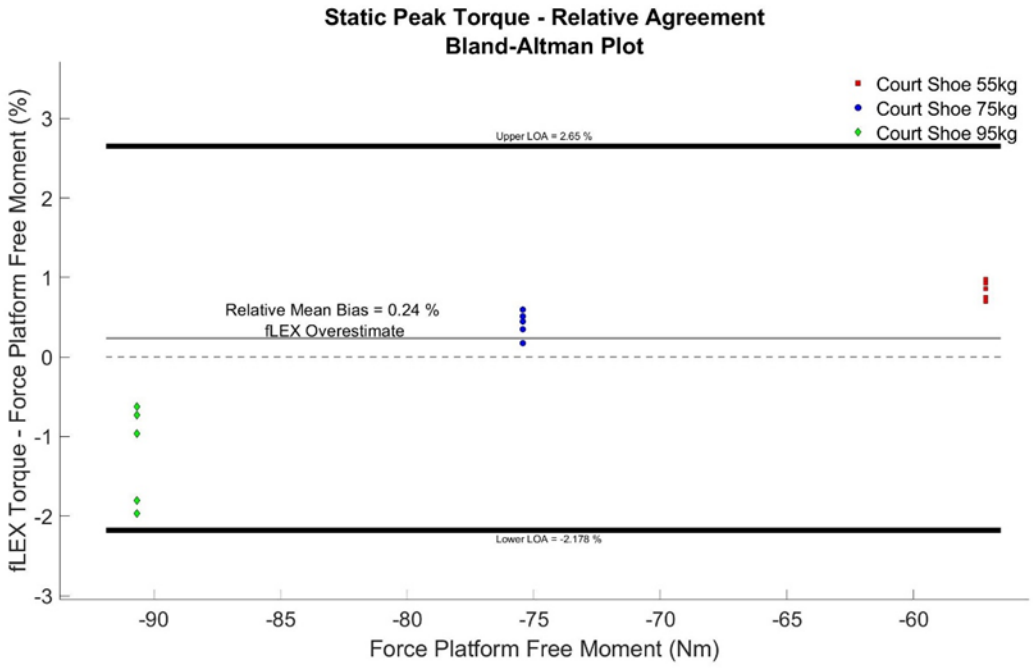


Figure 13. Peak Torque Agreement during Static Tests, Interface Condition 1 (Control)

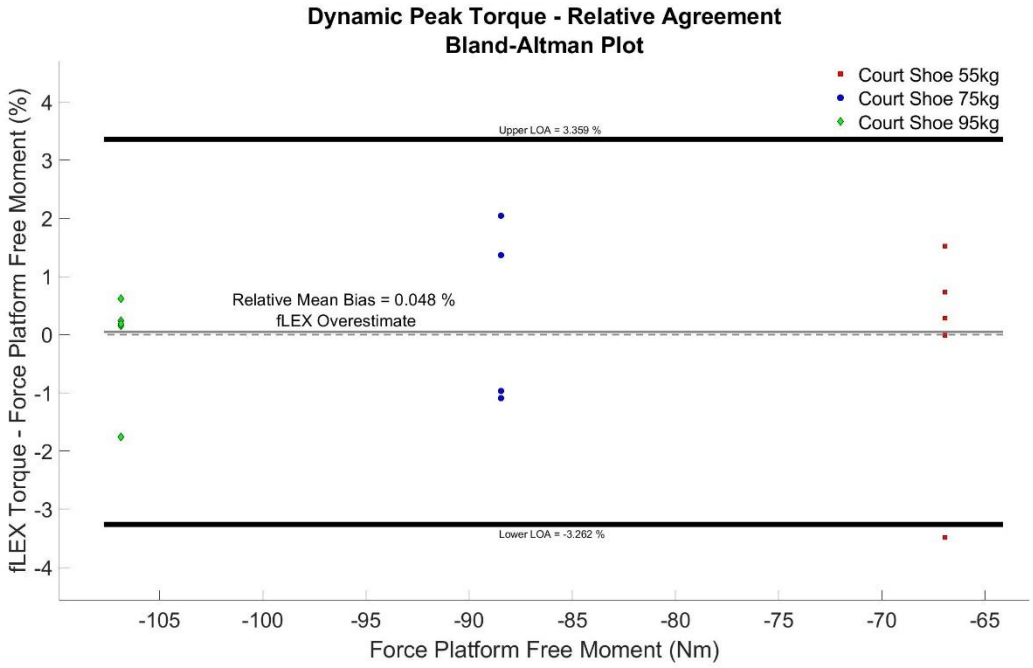


Figure 14. Peak Torque Agreement during Dynamic Tests, Interface Condition 1 (Control)

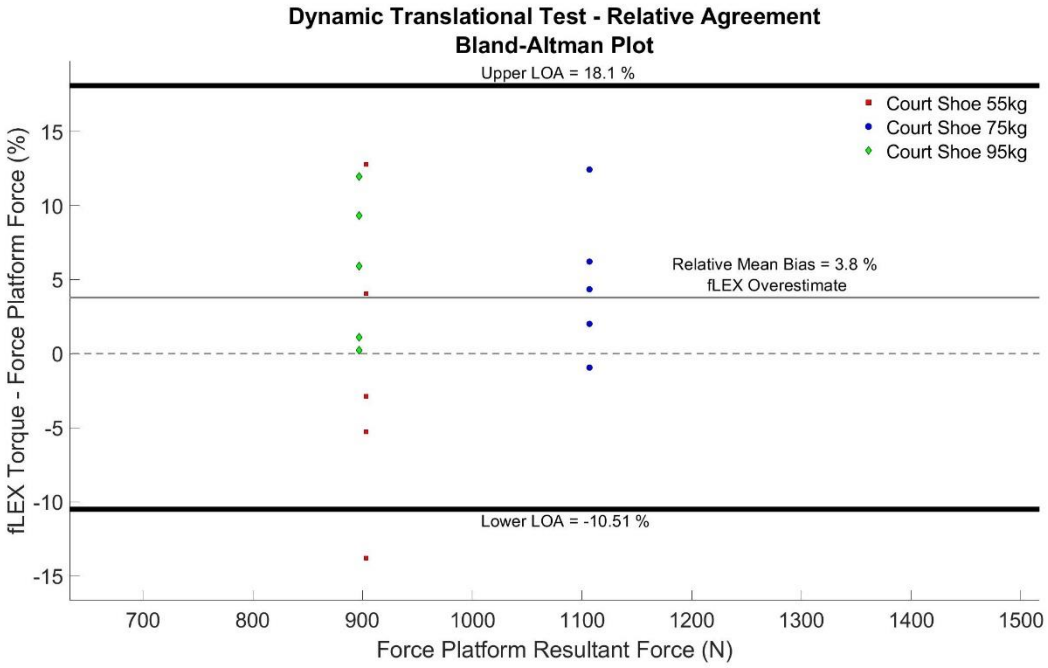


Figure 15. Resultant Force Agreement during Dynamic Test, Interface Condition 1 (Control)

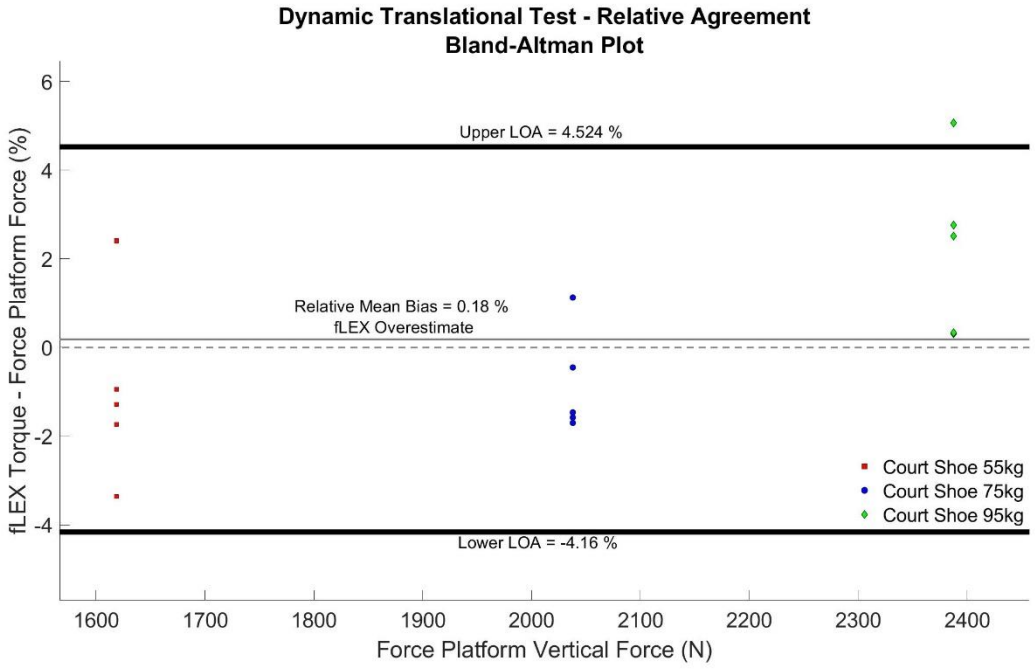


Figure 16. Vertical Force Agreement during Dynamic Test, Interface Condition 1 (Control)

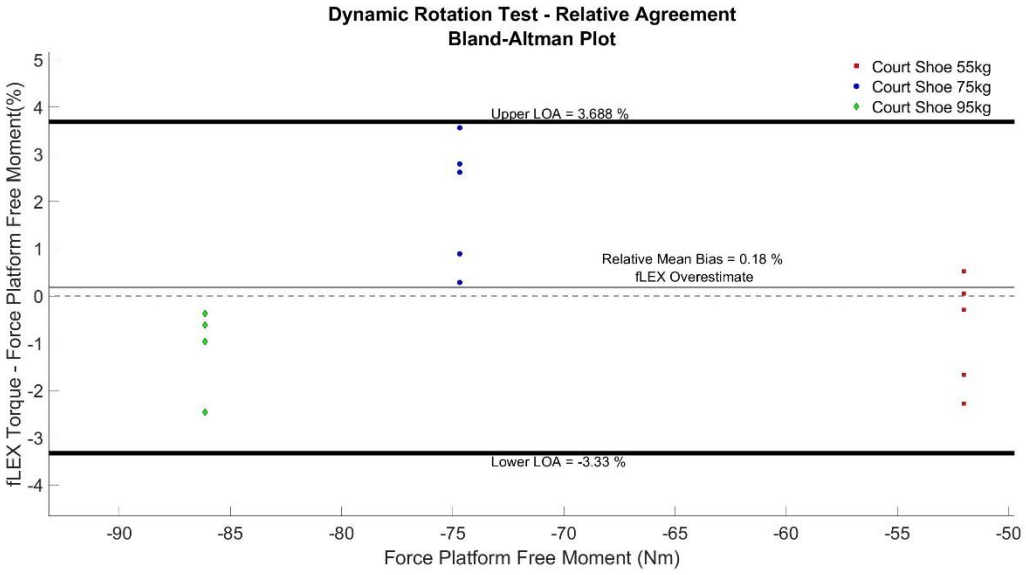


Figure 17. Peak Torque Agreement during Dynamic Tests, Interface Condition 2 (Taped-Court)

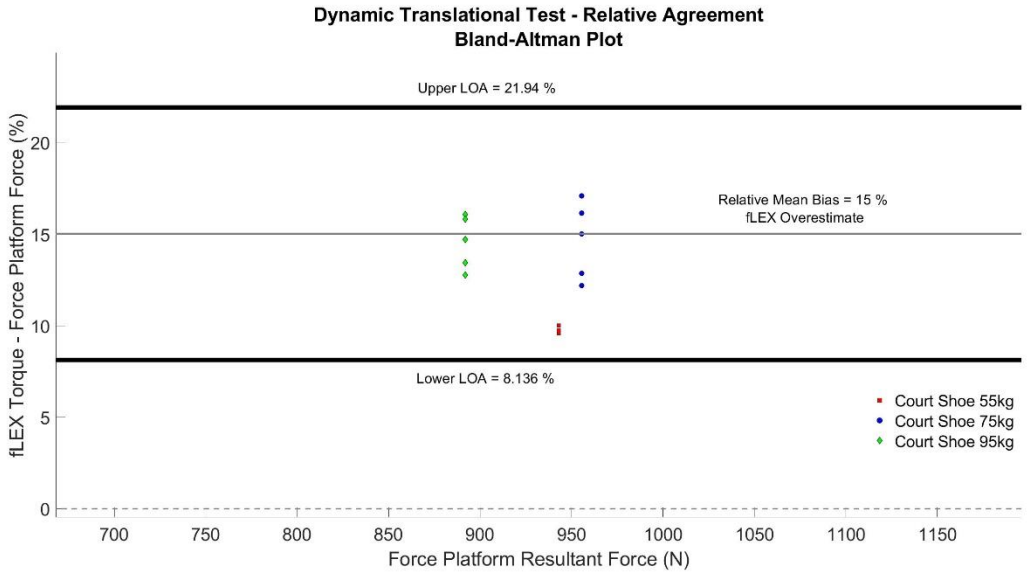


Figure 18. Resultant Force Agreement during Dynamic Test, Interface Condition 2 (Taped-Court)

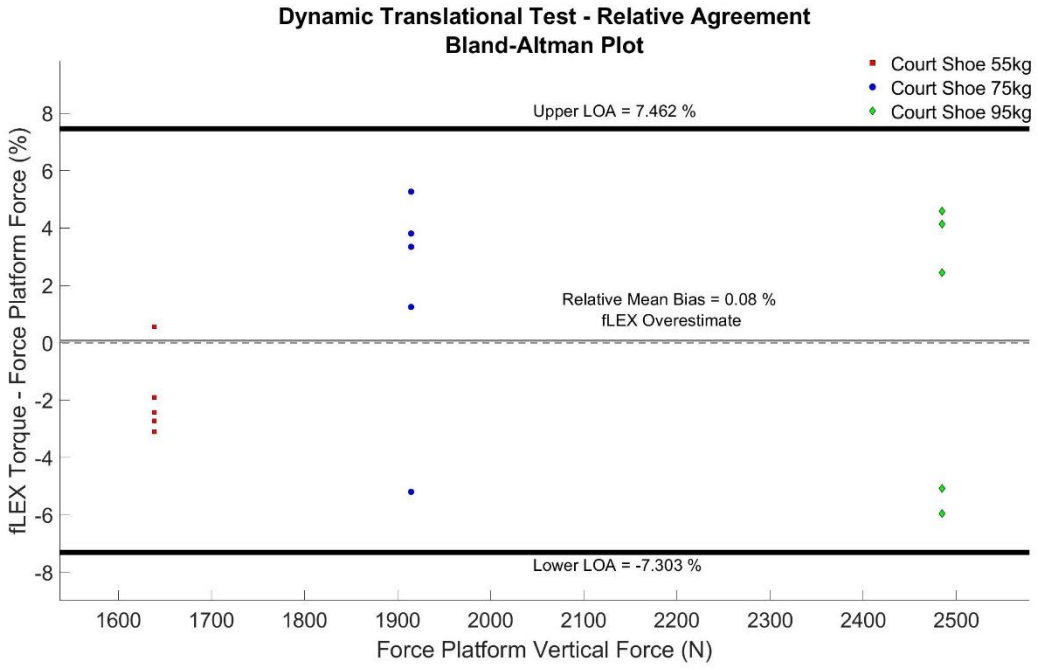


Figure 19. Vertical Force Agreement during Dynamic Test, Interface Condition 2 (Taped-Court)

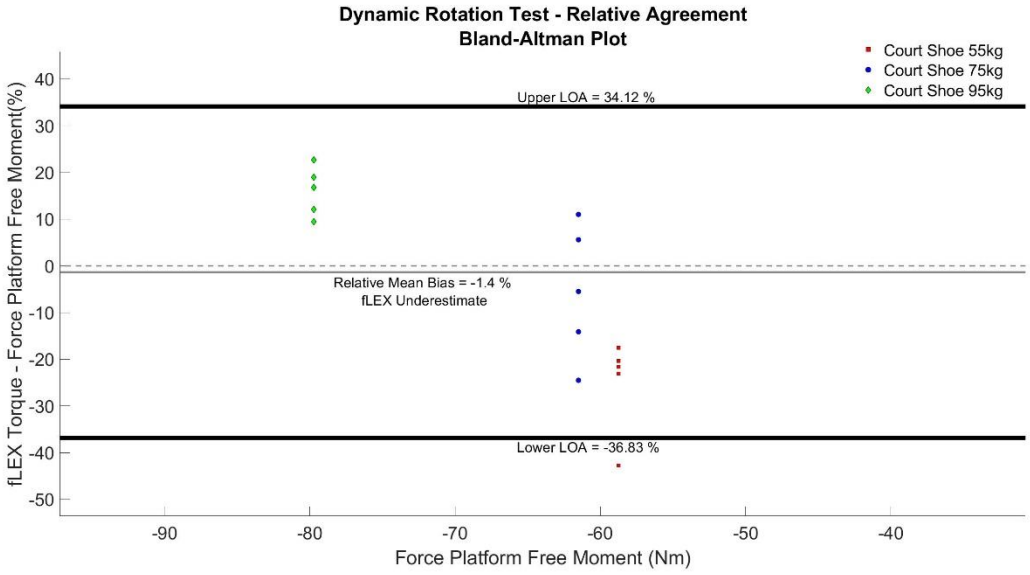


Figure 20. Peak Torque Agreement during Dynamic Tests, Interface Condition 3 (Taped-Cleat)

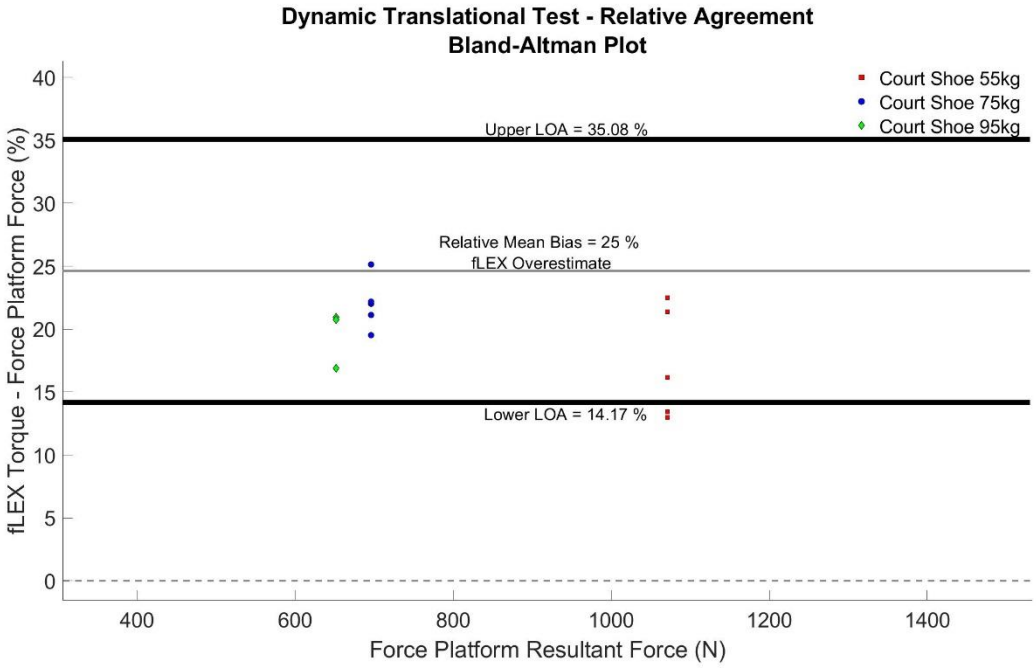


Figure 21. Resultant Force Agreement during Dynamic Test, Interface Condition 3 (Taped-Cleat)

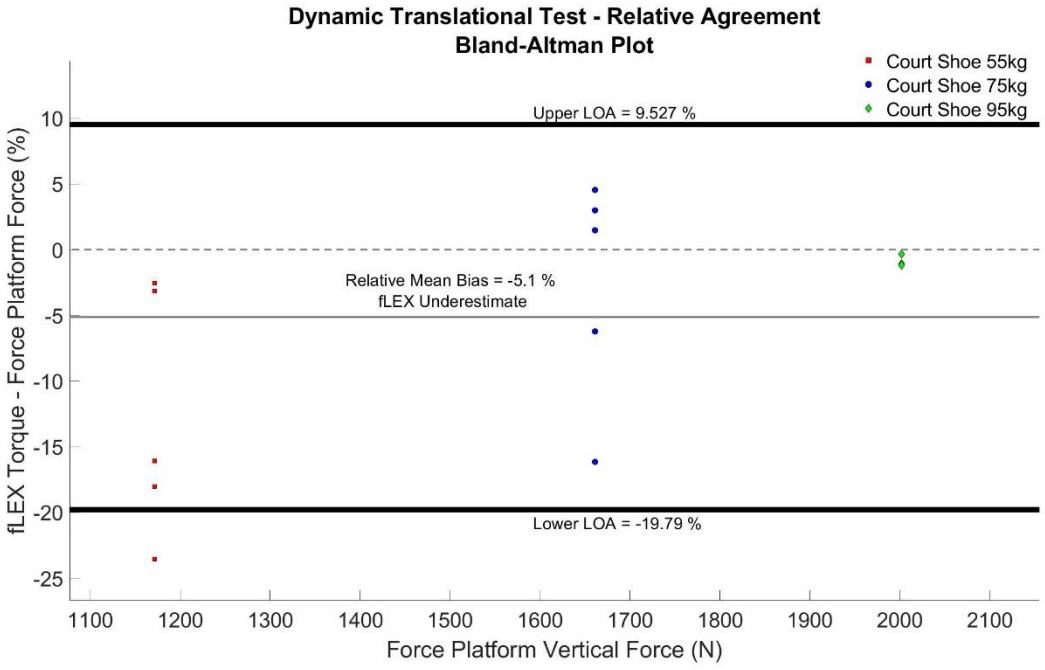


Figure 22. Vertical Force Agreement during Dynamic Test, Interface Condition 3 (Taped-Cleat)

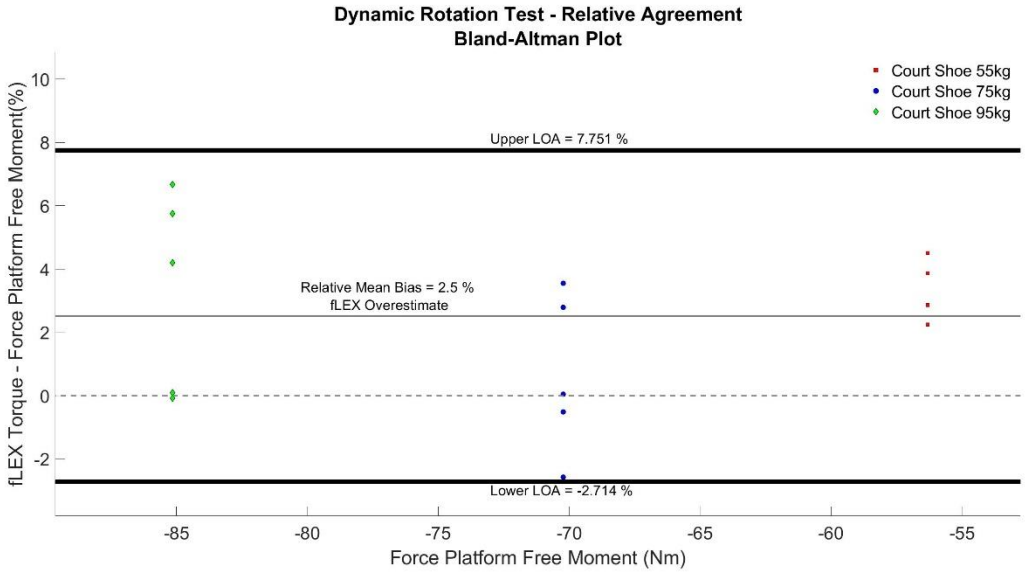


Figure 23. Peak Torque Agreement during Dynamic Tests, Interface Condition 4 (Independent Glue-Court)

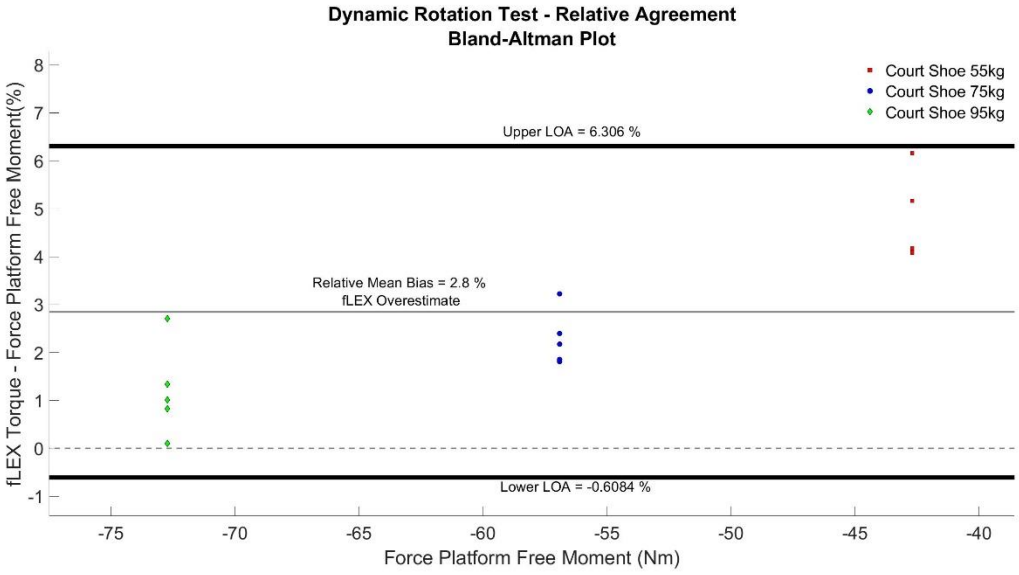


Figure 24. Peak Torque Agreement during Static Tests, Interface Condition 4 (Independent Glue-Court)

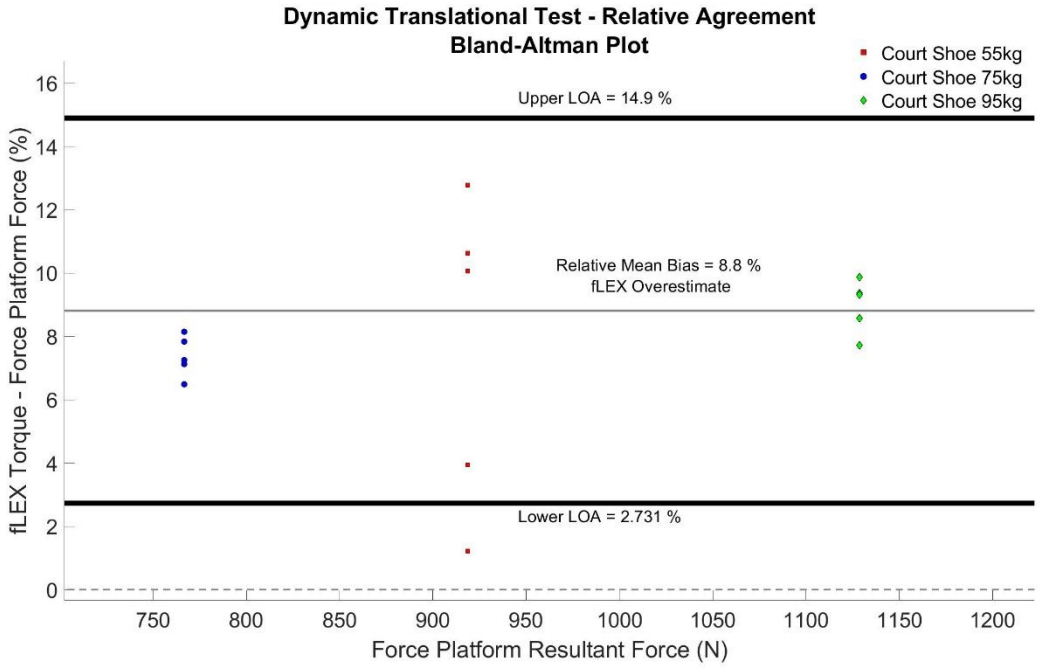


Figure 25. Resultant Force Agreement during Dynamic Test, Interface Condition 4 (Independent Glue-Court)

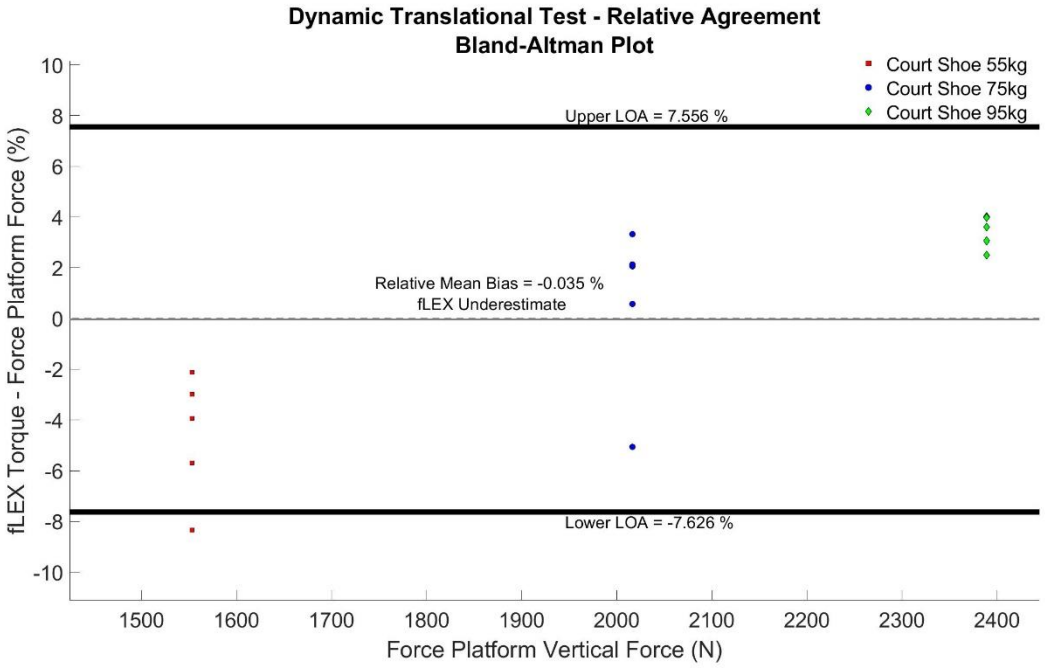


Figure 26. Vertical Force Agreement during Dynamic Test, Interface Condition 4 (Independent Glue-Court)

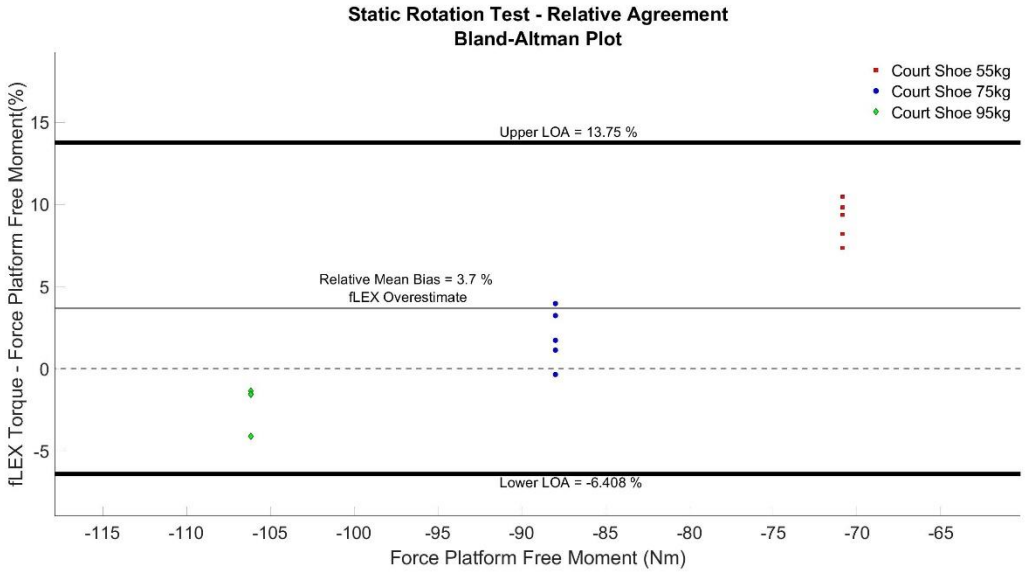


Figure 27. Peak Torque Agreement during Static Tests, Interface Condition 5 (Independent Glue-Cleat)

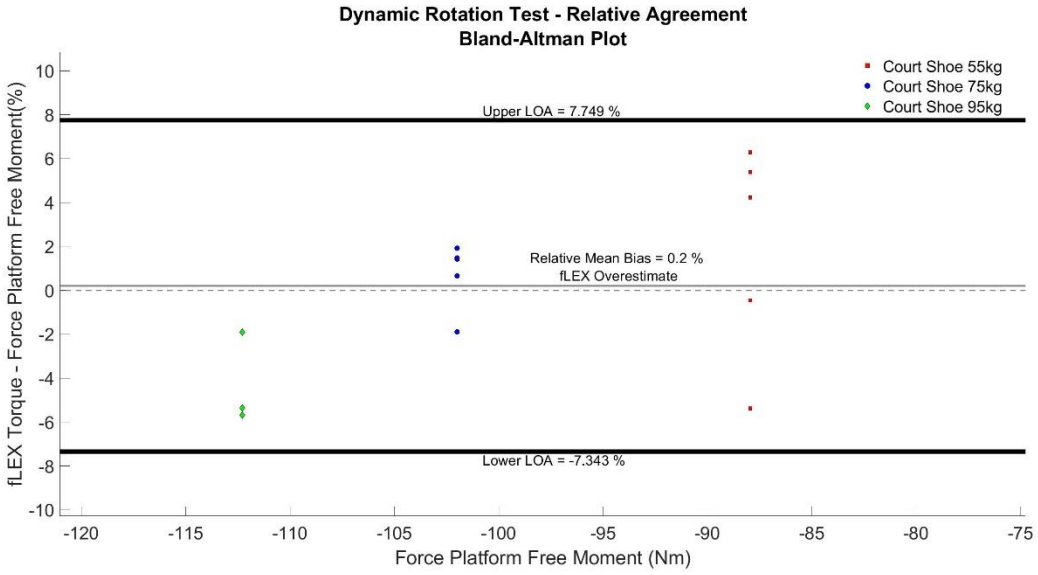


Figure 28. Peak Torque Agreement during Dynamic Tests, Interface Condition 5 (Independent Glue-Cleat)

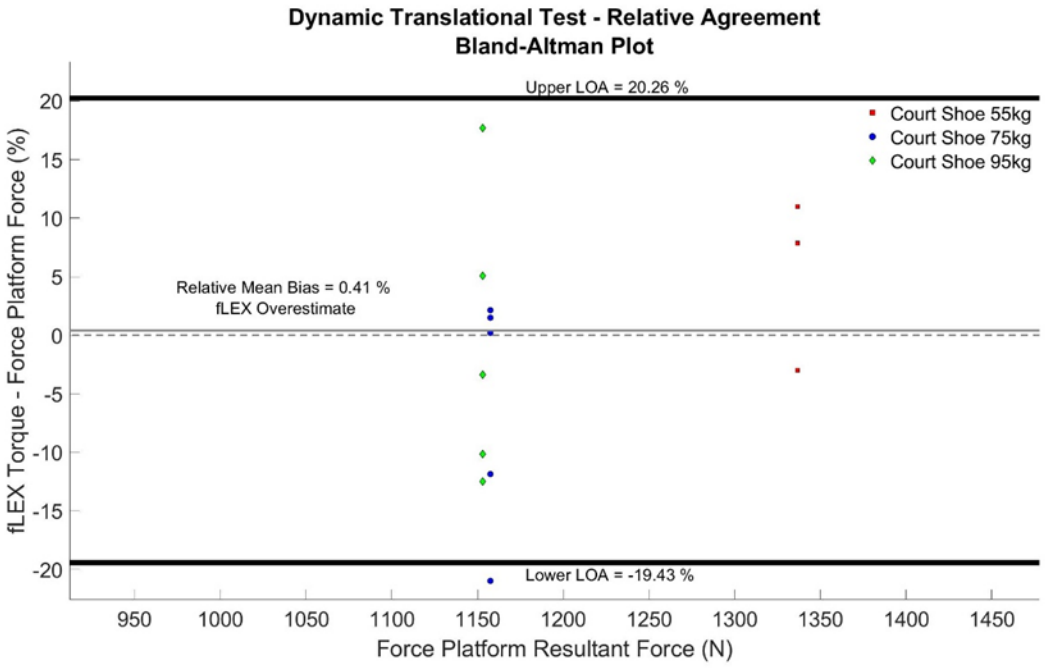


Figure 29. Resultant Force Agreement during Dynamic Test, Interface Condition 5 (Independent Glue-Cleat)

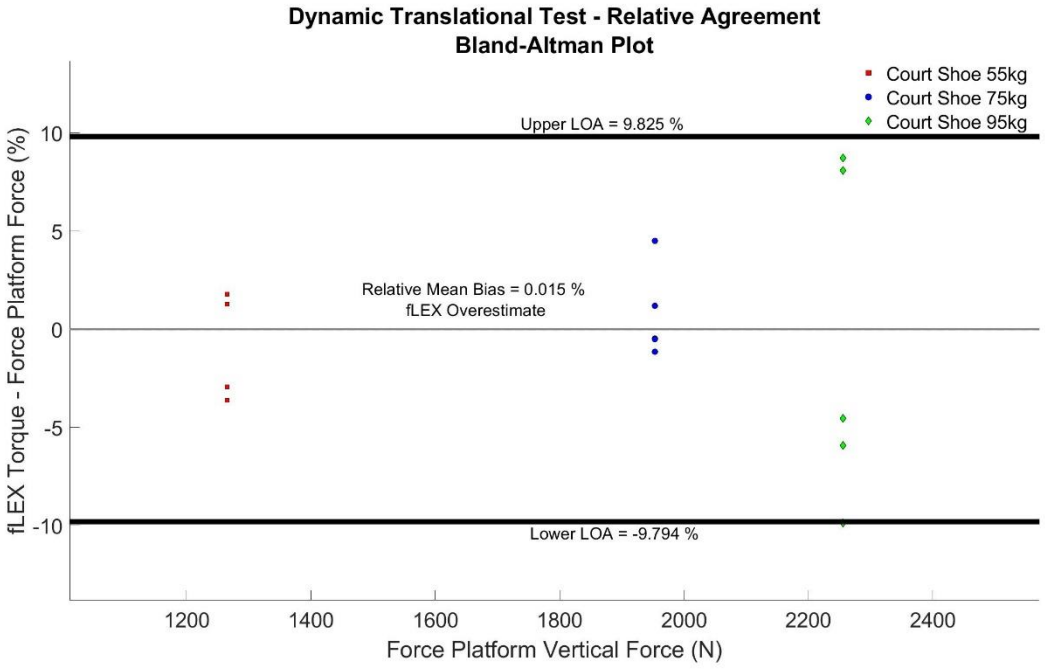


Figure 30. Vertical Force Agreement during Dynamic Test, Interface Condition 5 (Independent Glue-Cleat)

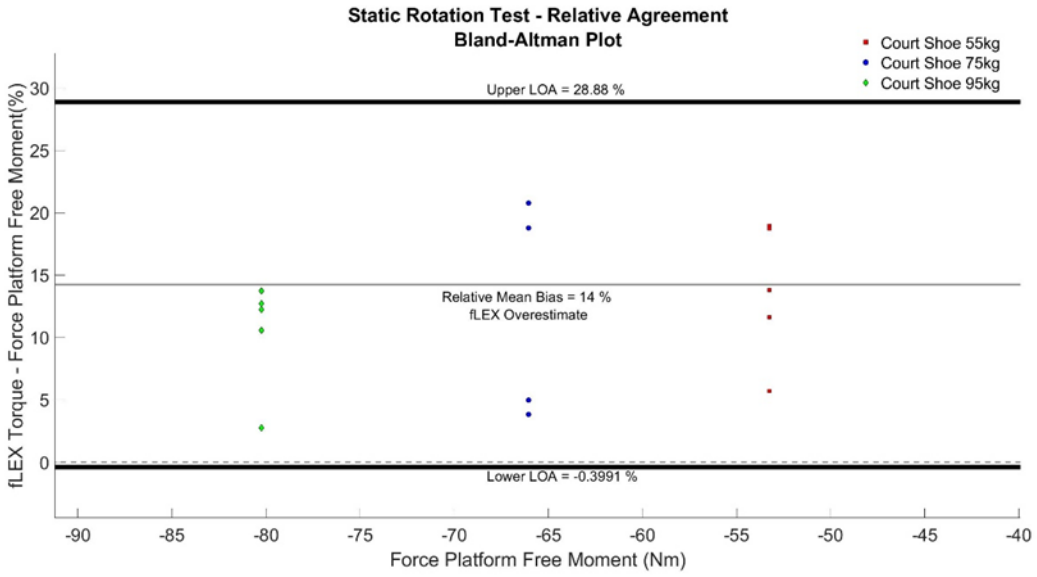


Figure 31.Peak Torque Agreement during Dynamic Tests, Interface Condition 6 (Uniform Glue-Court)

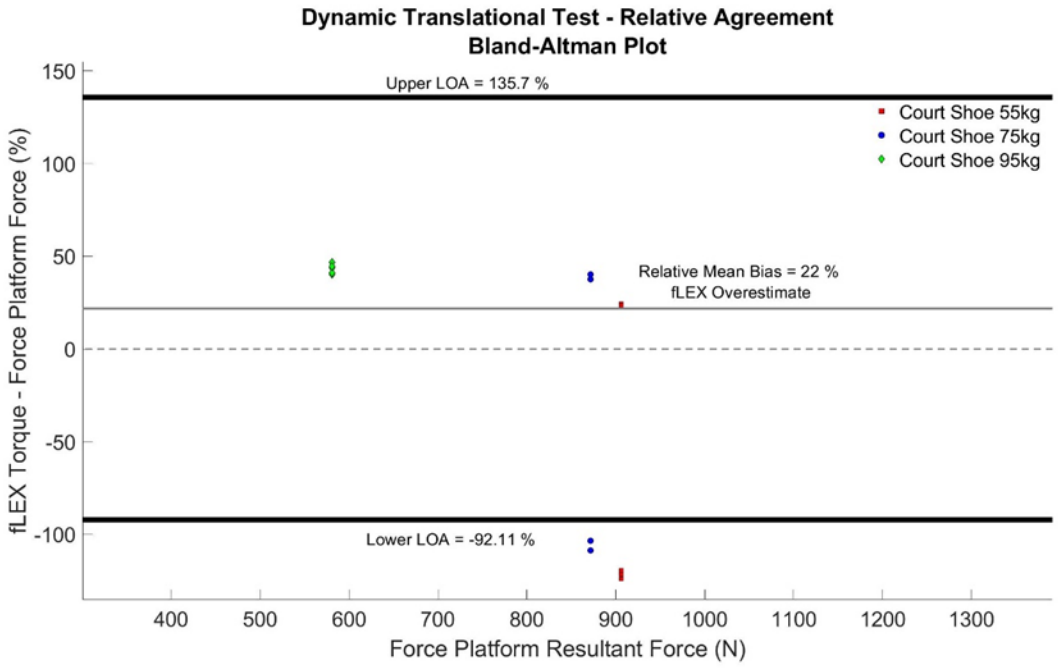


Figure 32. Resultant Force Agreement during Dynamic Test, Interface Condition 6 (Uniform Glue-Court)

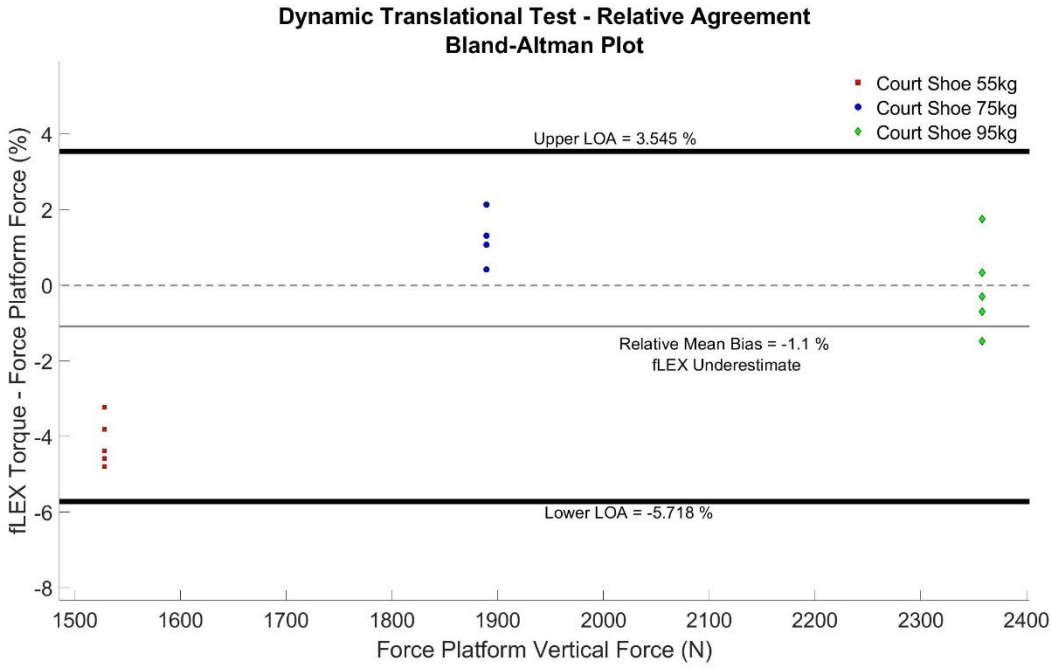


Figure 33. Vertical Force Agreement during Dynamic Test, Interface Condition 6 (Uniform Glue-Court)

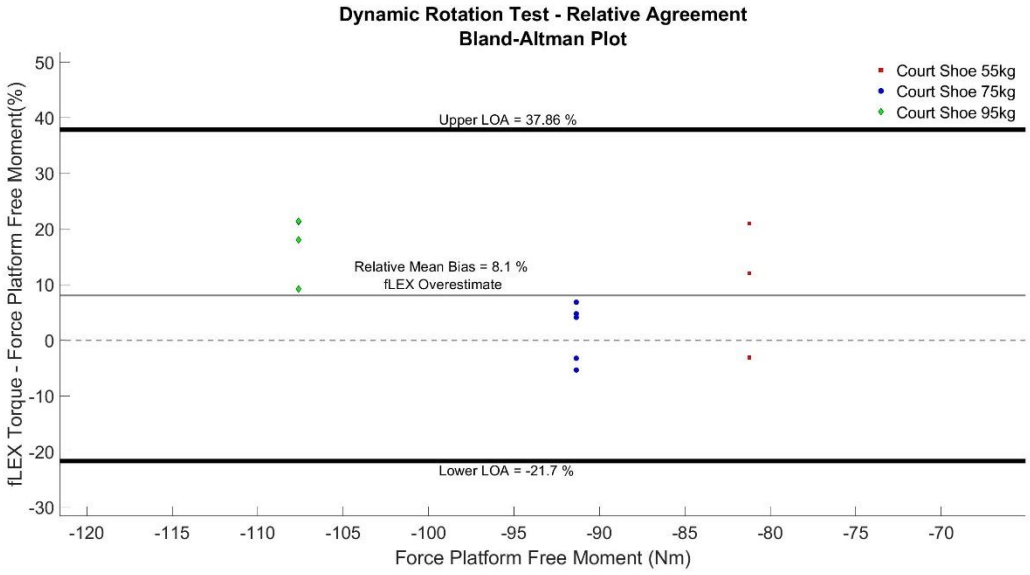


Figure 34. Peak Torque Agreement during Dynamic Tests, Interface Condition 7 (Uniform Glue-Cleat)

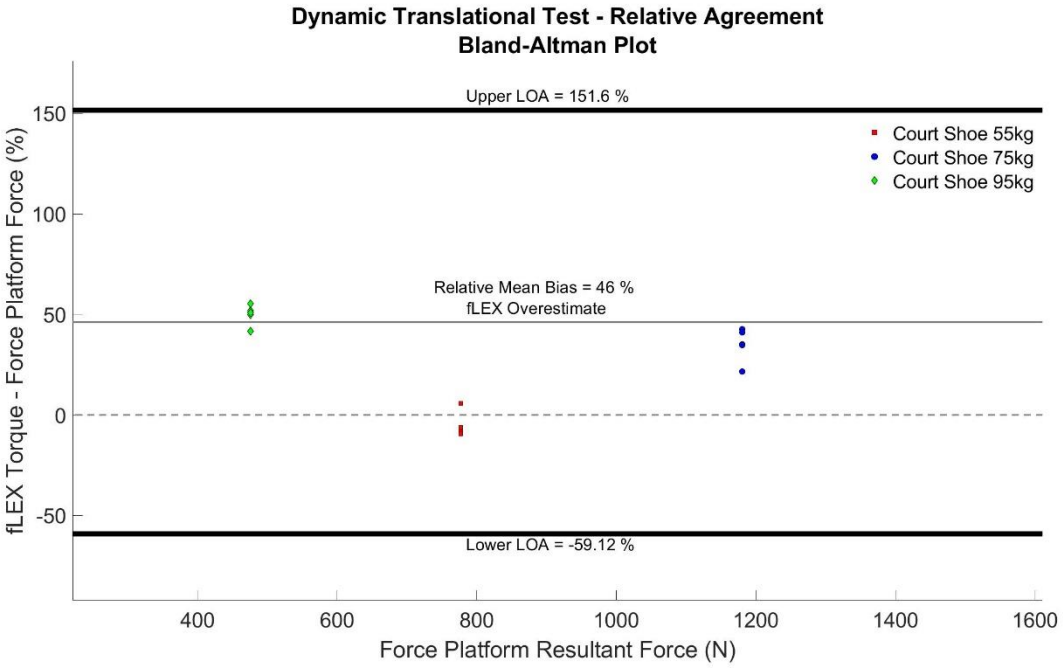


Figure 35. Resultant Force Agreement during Dynamic Test, Interface Condition 7 (Uniform Glue-Cleat)

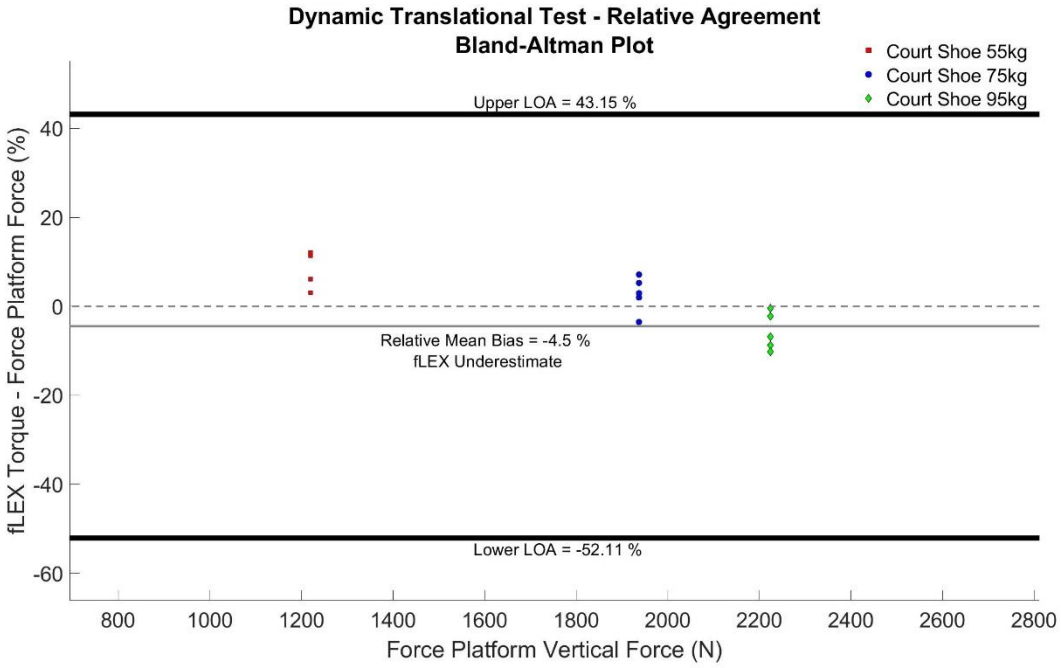


Figure 36. Vertical Force Agreement during Dynamic Test, Interface Condition 7 (Uniform Glue-Cleat)

Appendix C: Absolute Bland-Altman Plot

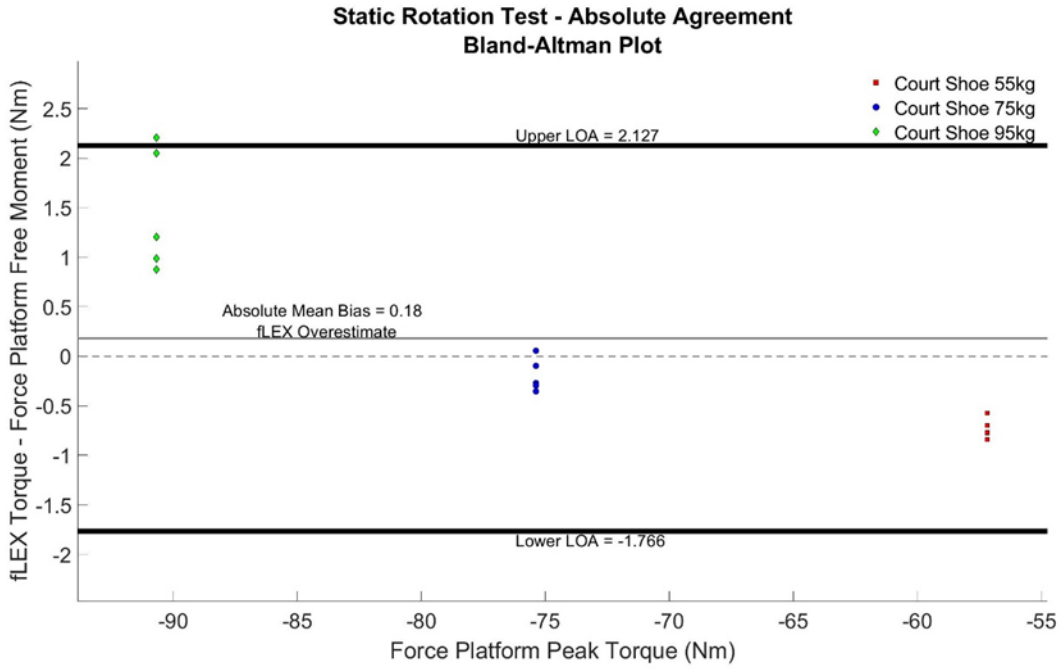


Figure 37. Peak Torque Agreement during Static Tests, Interface Condition 1 (Control)

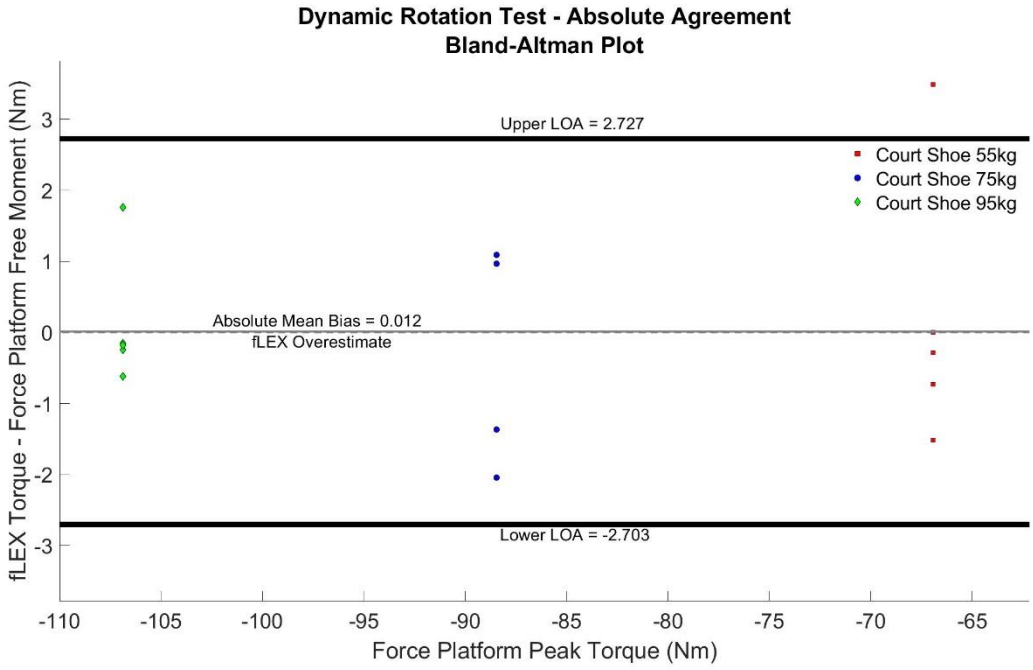


Figure 38. Peak Torque Agreement during Dynamic Tests, Interface Condition 1 (Control)

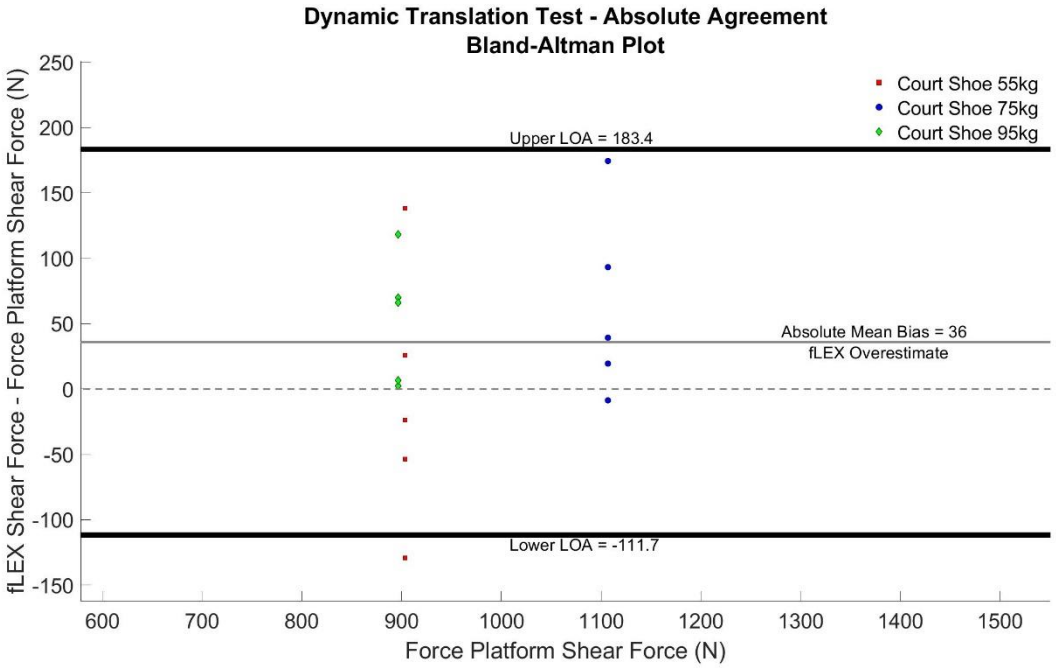


Figure 39. Resultant Force Agreement during Dynamic Test, Interface Condition 1 (Control)

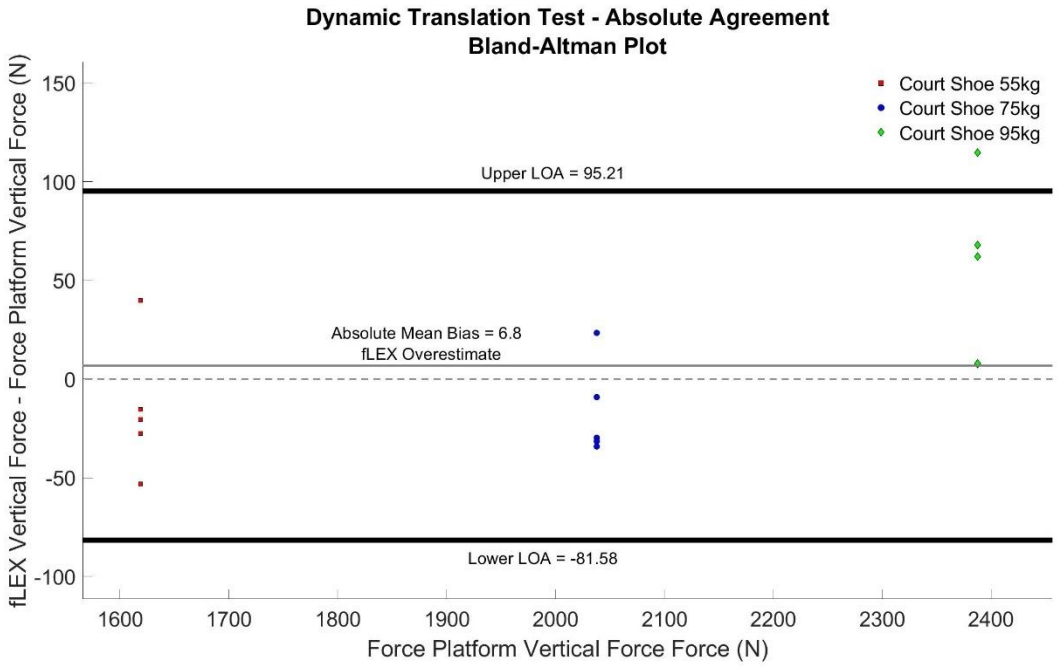


Figure 40. Vertical Force Agreement during Dynamic Test, Interface Condition 1 (Control)

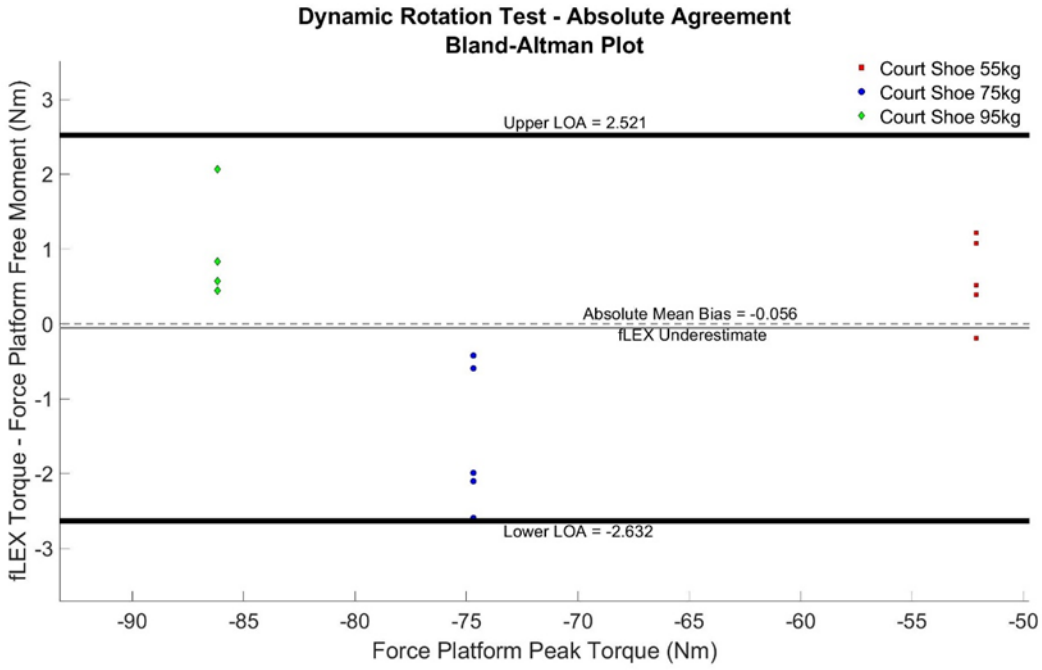


Figure 41.Peak Torque Agreement during Dynamic Tests, Interface Condition 2 (Tape-Court)

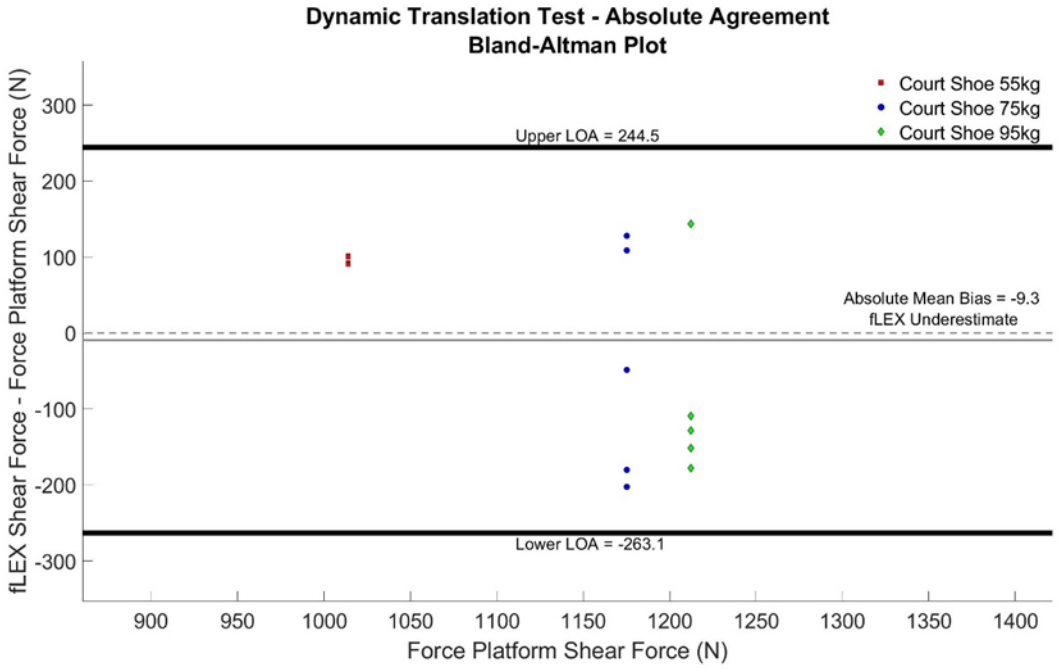


Figure 42. Resultant Force Agreement during Dynamic Test, Interface Condition 2 (Tape-Court)

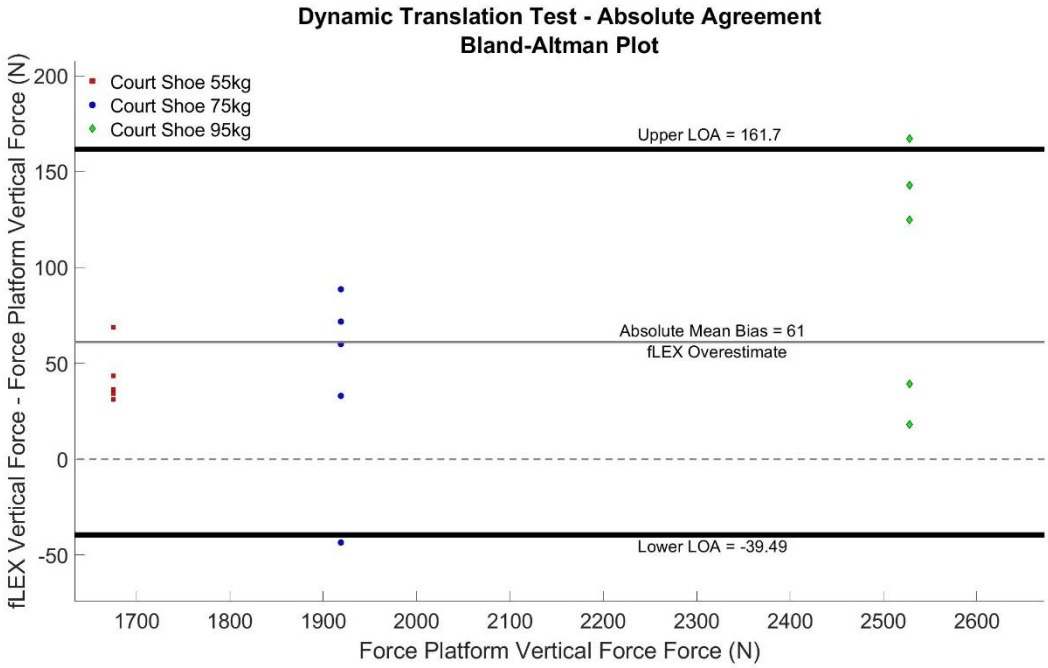


Figure 43. Vertical Force Agreement during Dynamic Test, Interface Condition 2 *(Tape-Court)*

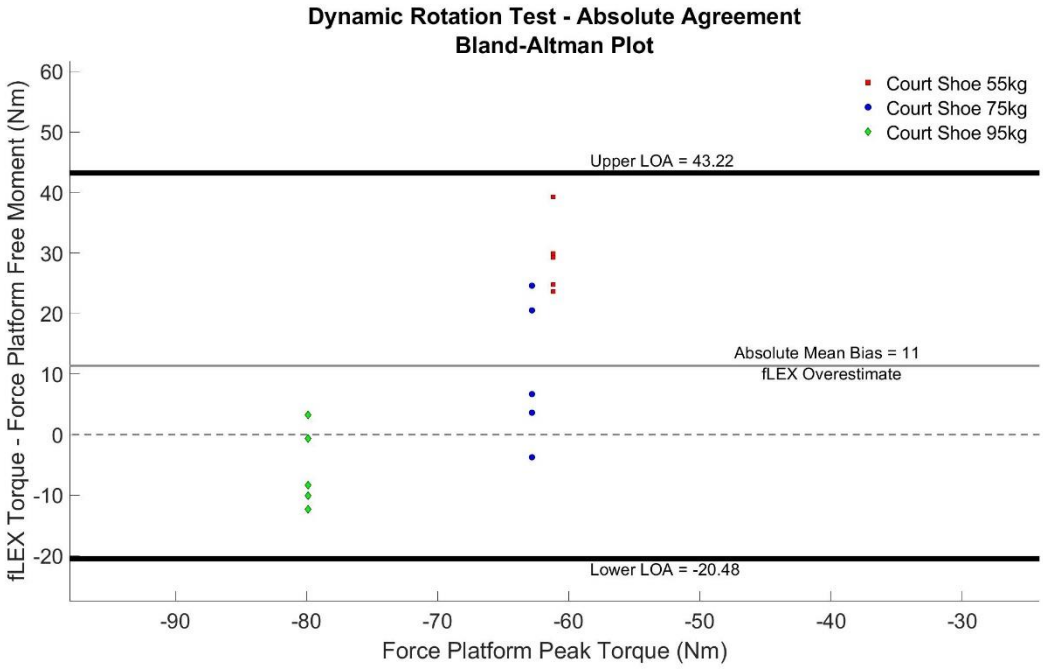


Figure 44. Peak Torque Agreement during Dynamic Tests, Interface Condition 3 *(Tape-Cleat)*

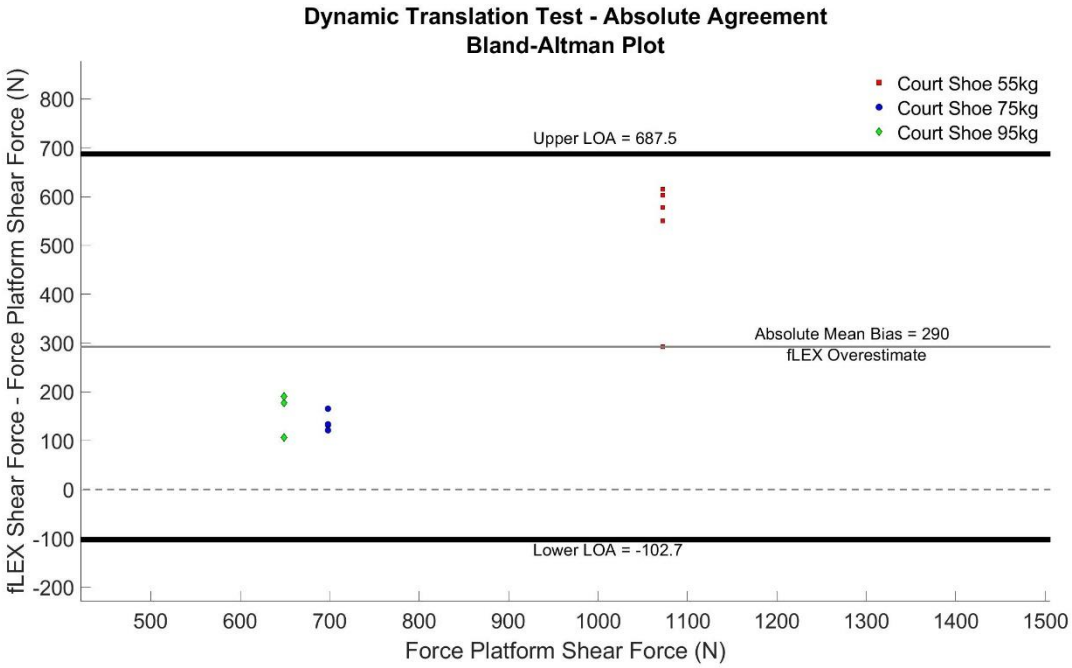


Figure 45. Resultant Force Agreement during Dynamic Test, Interface Condition 3 *(Tape-Cleat)*

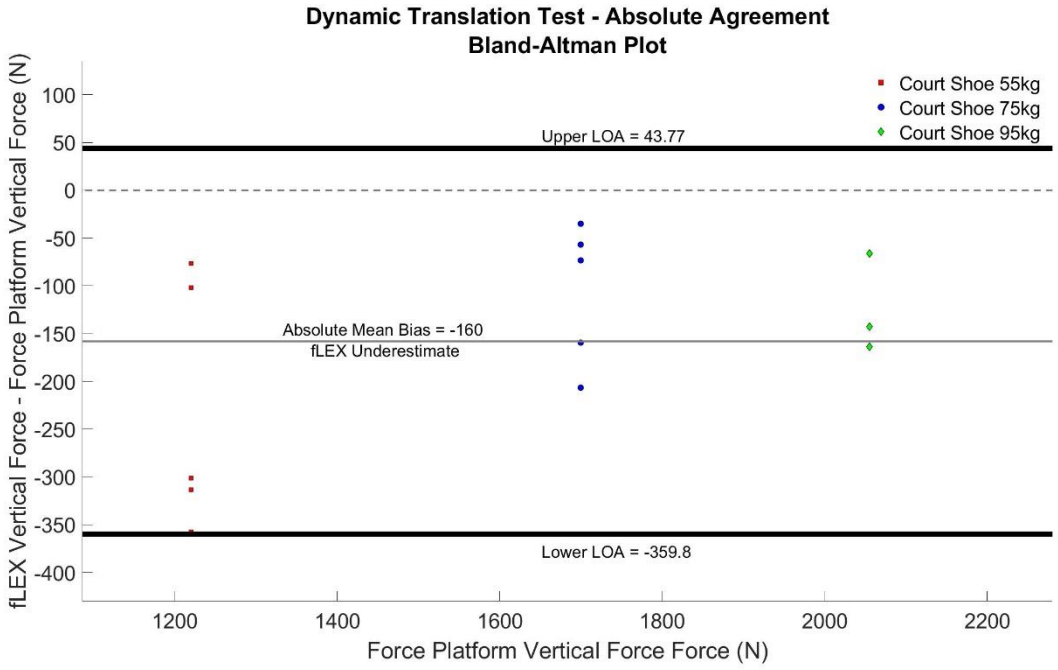


Figure 46. Vertical Force Agreement during Dynamic Test, Interface Condition 3 *(Tape-Cleat)*

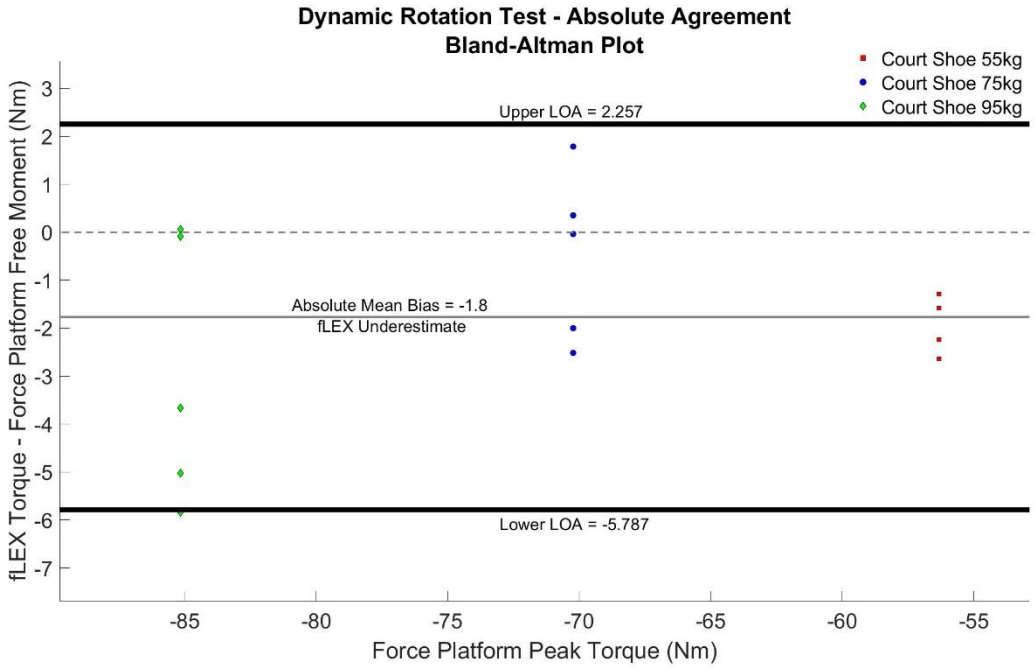


Figure 47. Peak Torque Agreement during Dynamic Tests, Interface Condition 4 (Independent Glue-Court)

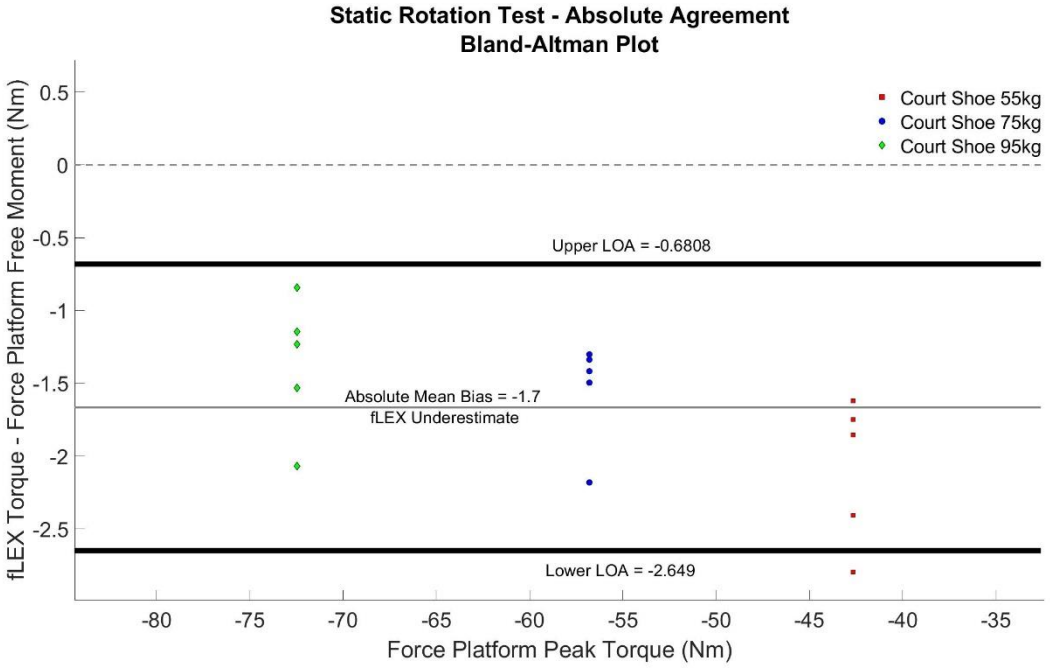


Figure 48. Peak Torque Agreement during Static Tests, Interface Condition 4 (Independent Glue-Court)

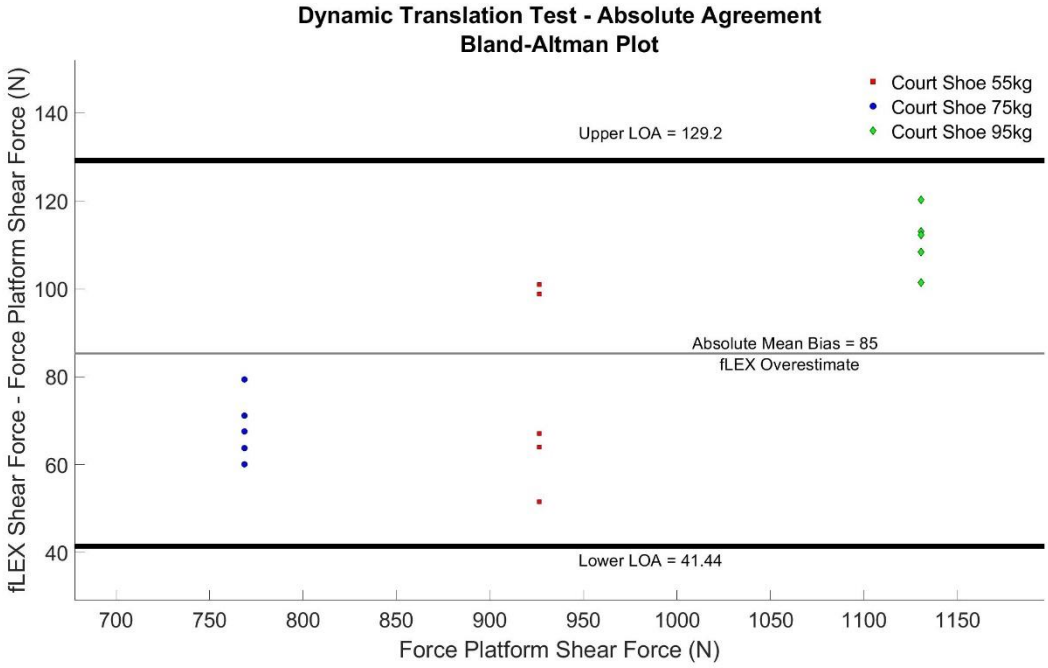


Figure 49. Resultant Force Agreement during Dynamic Test, Interface Condition 4 (Independent Glue-Court)

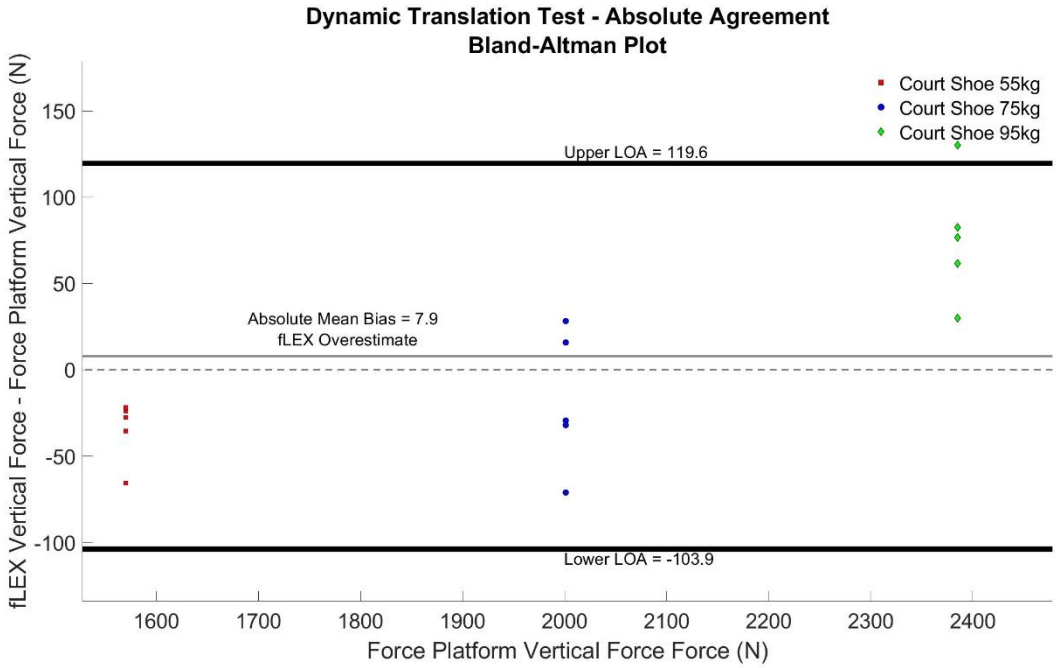


Figure 50. Vertical Force Agreement during Dynamic Test, Interface Condition 4 (Independent Glue-Court)

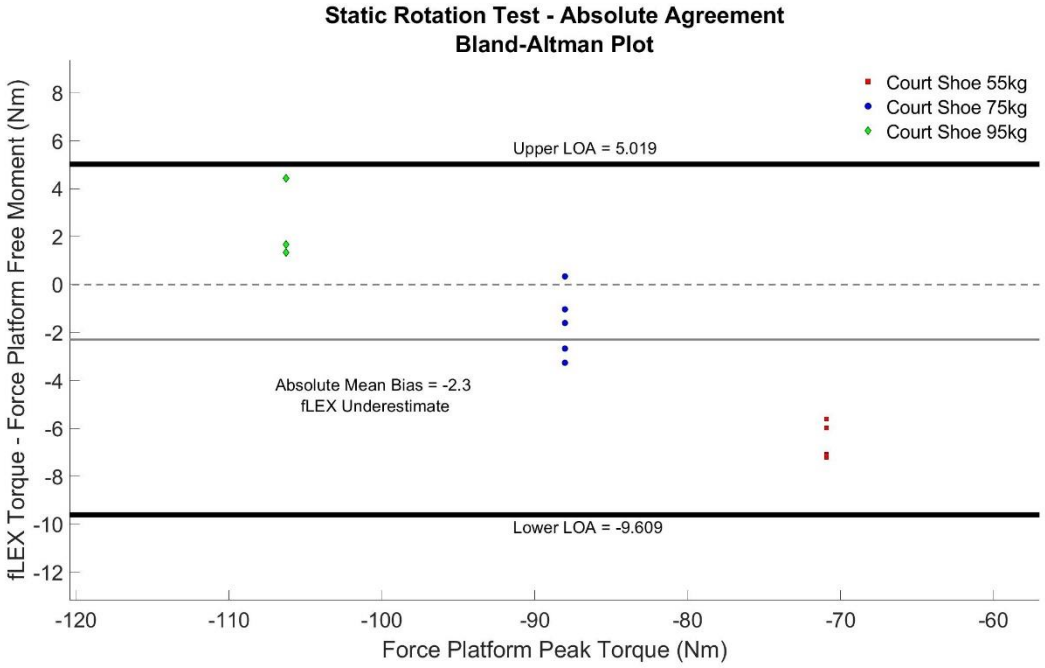


Figure 51. Peak Torque Agreement during Static Tests, Interface Condition 5 (Independent Glue-Cleat)

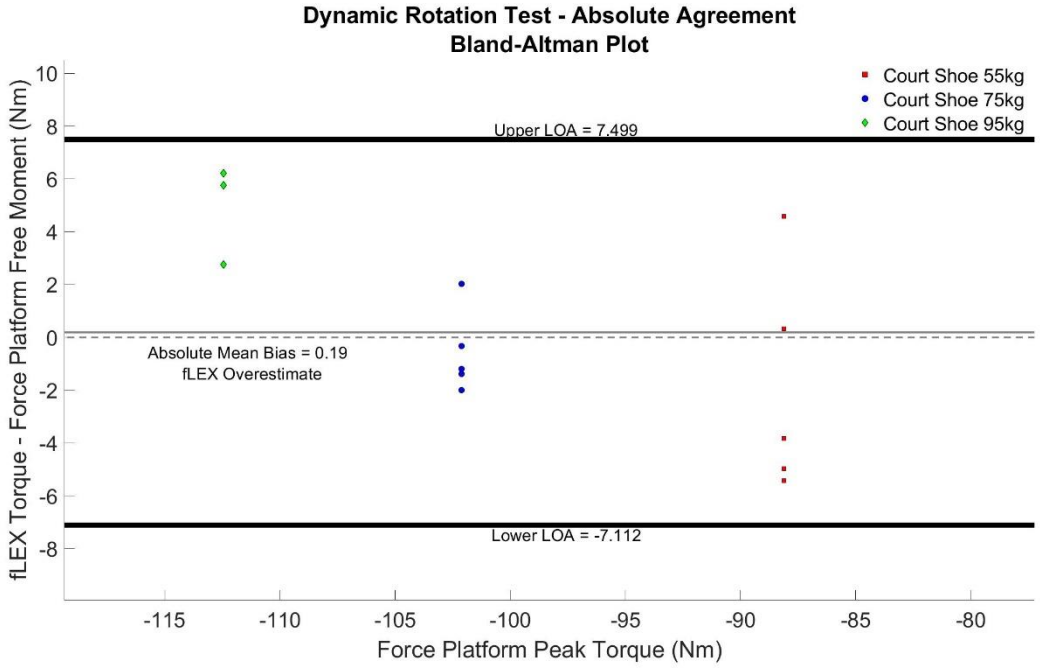


Figure 52. Peak Torque Agreement during Dynamic Tests, Interface Condition 5 (Independent Glue-Cleat)

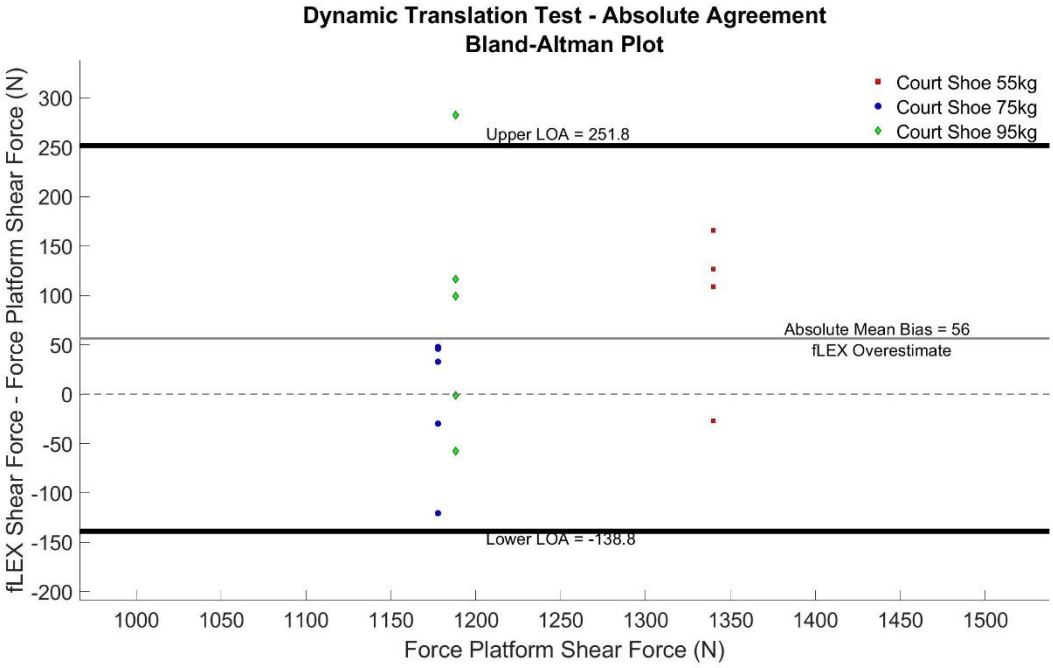


Figure 53. Resultant Force Agreement during Dynamic Test, Interface Condition 5 (Independent Glue-Cleat)

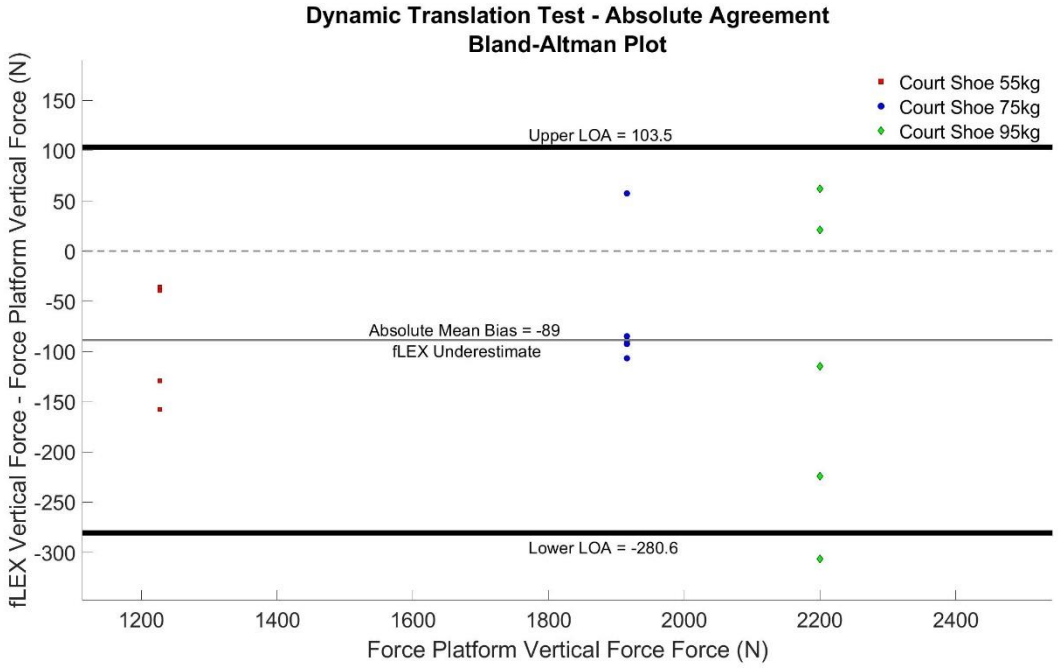


Figure 54. Vertical Force Agreement during Dynamic Test, Interface Condition 5 (Independent Glue-Cleat)

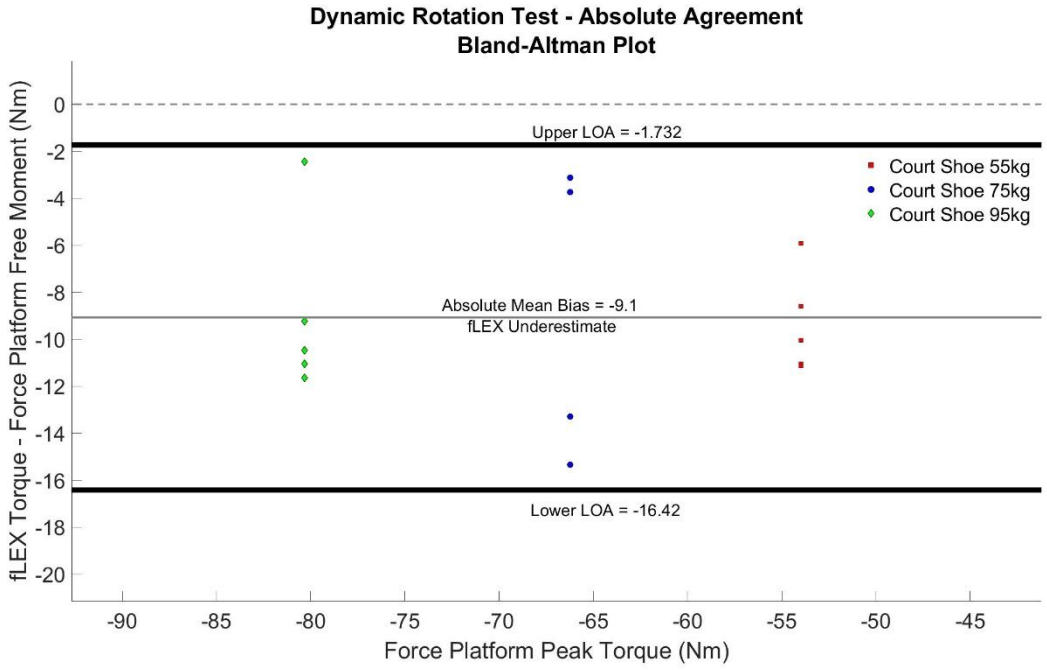


Figure 55. Peak Torque Agreement during Dynamic Tests, Interface Condition 6 (Uniform Glue-Court)

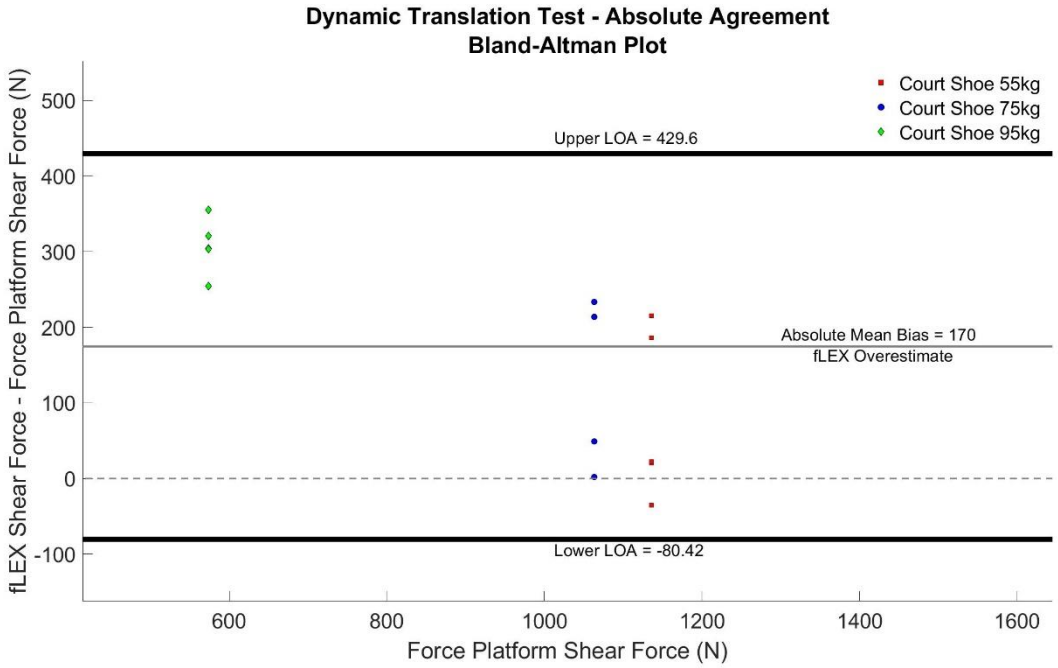


Figure 56. Resultant Force Agreement during Dynamic Test, Interface Condition 6 (Uniform Glue-Court)

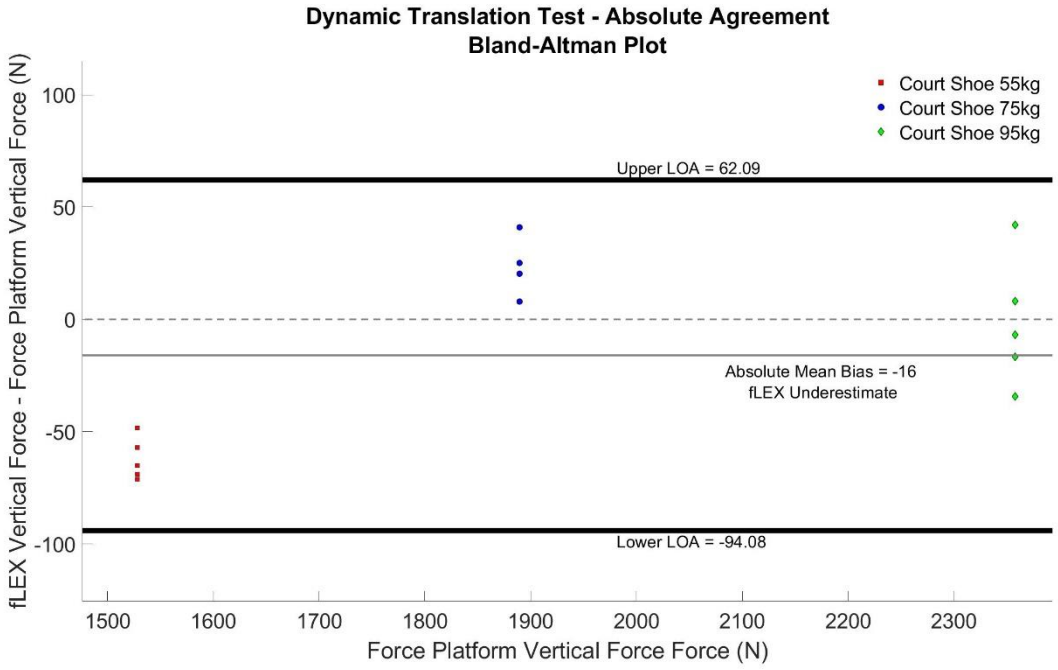


Figure 57. Vertical Force Agreement during Dynamic Test, Interface Condition 6 (Uniform Glue-Court)

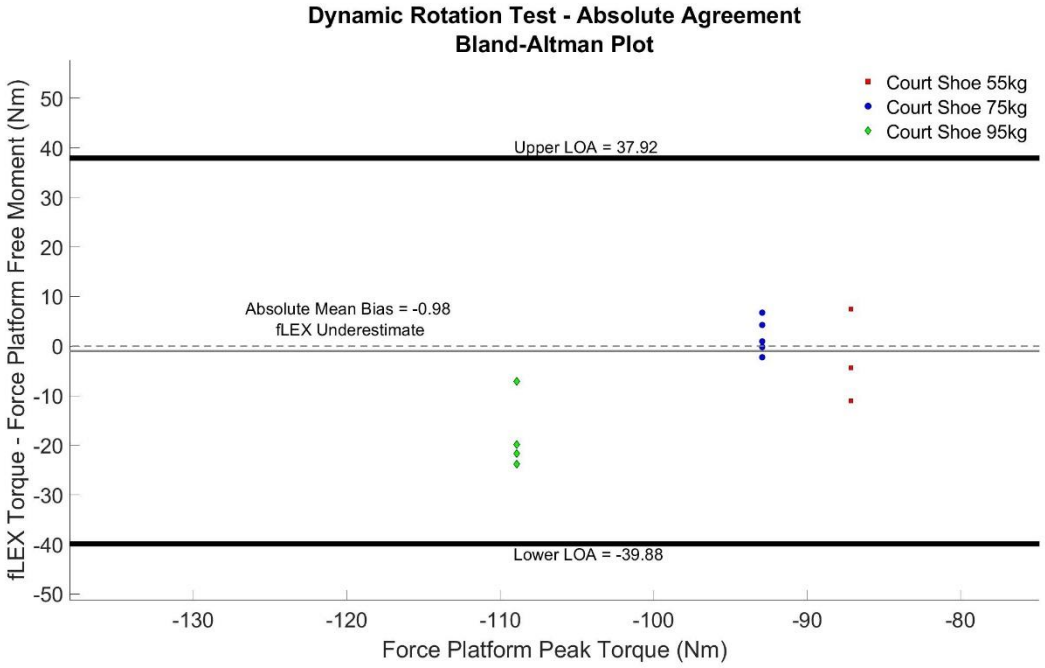


Figure 58. Peak Torque Agreement during Dynamic Tests, Interface Condition 7 (Uniform Glue-Cleat)

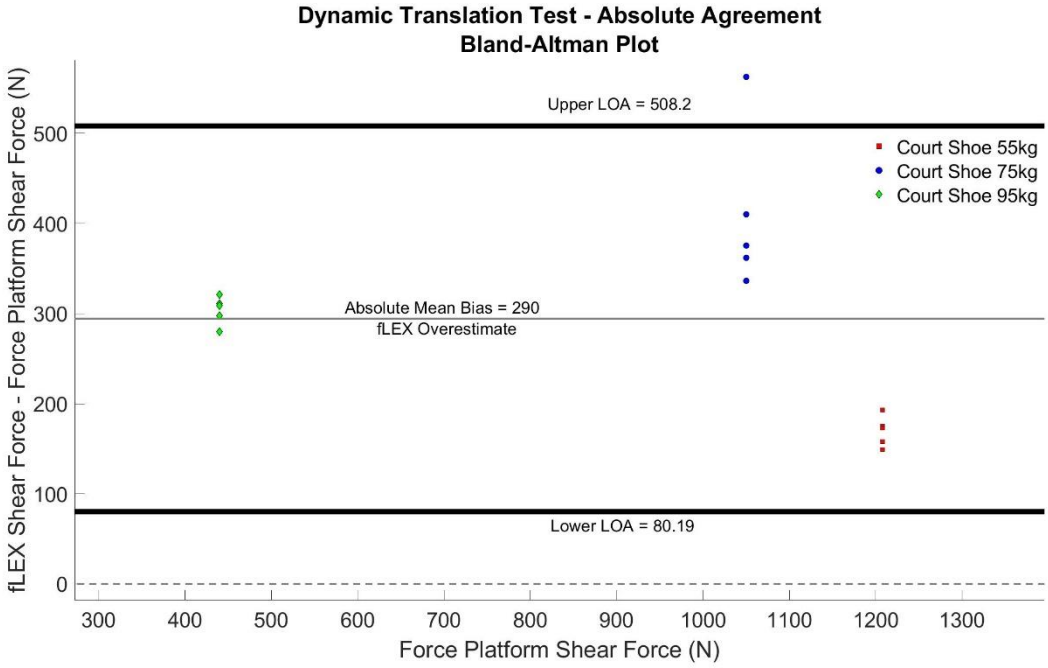


Figure 59. Resultant Force Agreement during Dynamic Test, Interface Condition 7 (Uniform Glue-Cleat)

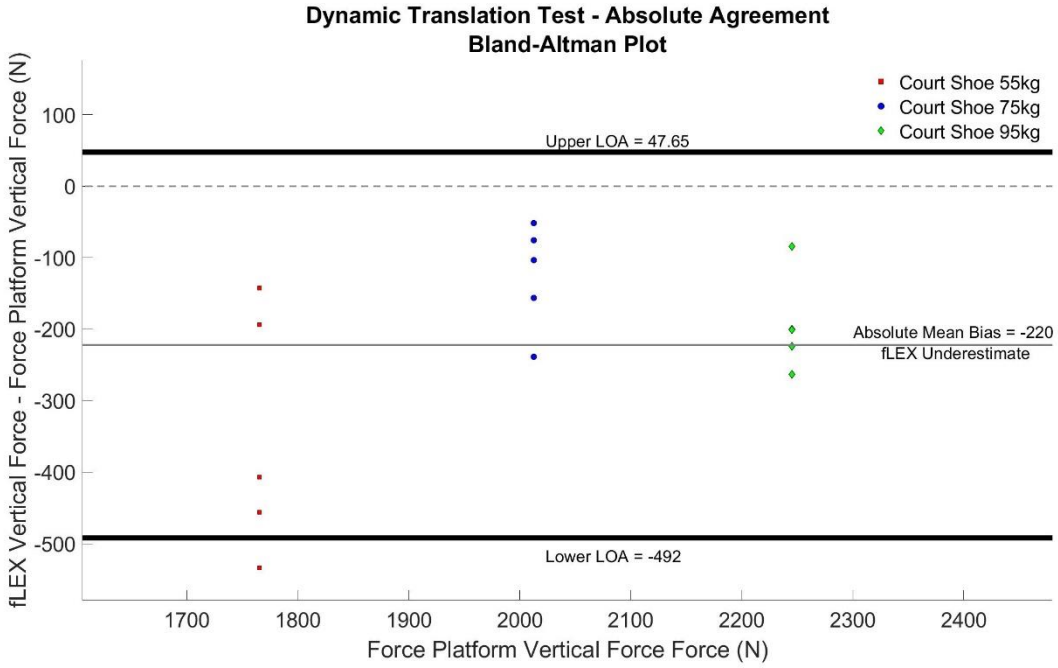


Figure 60. Vertical Force Agreement during Dynamic Test, Interface Condition 7 (Uniform Glue-Cleat)

Appendix D: Filtering

Detailed Filtering Process

Results from the BA analysis were used to identify the optimal force platform and fLEX sensor cutoff frequencies to achieve the highest level of system agreement. During data processing, force platform and fLEX events were manually selected with a cutoff frequency of 200 Hz. Once an event (maximum or minimum value) was identified and saved (magnitude, $\mathrm{Event}_{200\mathrm{Hz}}$, and location, $\mathrm{ELOC}_{200\mathrm{HZ}}$), the raw signals were re-filtered at the subsequent cutoff frequencies ($\mathrm{Freq}_{\mathrm{n}}$). The newly filtered signal was then cropped to within ±1 % of $\mathrm{ELOC}_{200\mathrm{HZ}}$. The cropped signals were used to identify $\mathrm{Event}_{\mathrm{Freq}_{\mathrm{n}}}$, this loop was completed for each cutoff frequency (see Figure 61). BA analyses were performed on each paired filtering frequency and results were then entered into two 10 x 10 paired filtering matrices. The matrices were populated with either relative mean bias (Figure 62) and relative standard deviation (Figure 64). Matrix values for mean bias and standard deviation were then ranked from lowest to highest (Figure 63 and Figure 65). The mean of those two matrices was then placed into a ranked mean matrix (Figure 66), then reranked. The five lowest reranked values were used to identify the top force platform and fLEX pairs. Once identified, raw data was reprocessed, and force platform and fLEX data were plotted on the same axis and visually inspected for abnormalities with in the two signals.

Practical Force Platform Filtering Observations

* It must be noted that fLEX is a metal instrument that aimed to reproduce human forces. However, filtering requirements for fLEX may be significantly different from the requirements for human subject research.

During the dynamic translation tests in this study, it was observed that higher force platform cutoff frequencies resulted in improved shear force measurement agreement between the two systems. However, this was not the case for vertical force system agreement. This could indicate that filtering all force platform measurements with the same cutoff frequency might result in underestimation of medial-lateral and anterior-posterior forces. Additionally, when processing peak torque and shear force, the identified cutoff frequencies resulted in the medium load condition being closest to the mean bias line. High and low loading conditions were observed to be inversely positioned about the cumulative load mean bias line. This offset could mean the vertical load influence the required cutoff frequency for identification of applied shear force and free moment measurement. Potentially subject-specific filtering frequencies might be an more advantageous approach filtering shear force and free moment force platform data, or reexamining filtering within the frequency domain vs common time domain methods.

The addition of the synthetic turf atop the force platform found shear force and free moment measurements required higher cutoff frequencies for force platform signals compared to the control condition. Increased force platform cutoff frequency could be due to the synthetic turf

dampening high frequency noise measurements between the force platform and fLEX sensors, thus increasing the force distribution across a higher frequency range. Therefore, during future human studies examining the cleat-turf interface, a high-frequency analysis might be a more appropriate approach to examine force platform data. Previous studies utilizing this high- cutoff frequency approach with a cutoff frequency of 100 Hz (Wannop and Stefanyshyn, 2016) and a cutoff frequency of 200 Hz (Müller et al., 2010) identified significant increases in anterior-posterior force platform measurements during higher traction conditions. Studies using lower cutoff frequencies (Gdovin et al. (2018) used 15 Hz, and Brock et al. (2014) using 50 Hz) were unable to identify the potential differences in force platform measurements. Brock et al. (2014) found court shoes increased medial lateral GRF during a 180º change in direction movement compared to cleated footwear. In additional to filtering frequency, the taping method was found to have high agreement court shoe conditions, but poor agreement during cleated condition. Brock et al. (2014) supports the conclusion that the taping method is effect for low traction shoes (court shoes), but an ineffective method for cleated footwear.

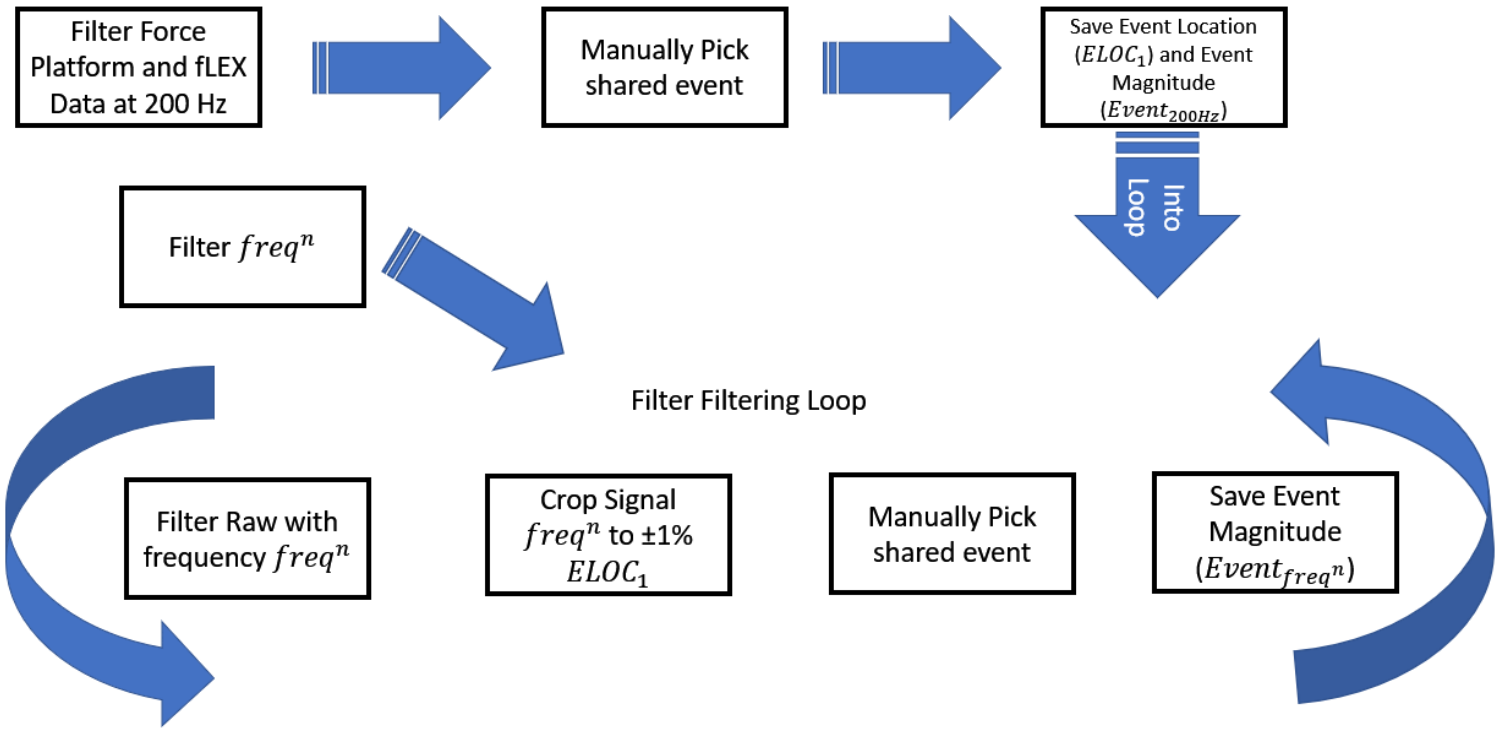


Figure 61. Filtering and Event Picking Loop

	1 ForcePlateFilter_200	2 ForcePlateFilter_100	3 ForcePlateFilter_90	4 ForcePlateFilter_80	5 ForcePlateFilter_70	6 ForcePlateFilter_60	7 ForcePlateFilter_50	8 ForcePlateFilter_40	9 ForcePlateFilter_30	10 ForcePlateFilter_20
1 FlexFilter_200	0.0221	0.0436	0.0443	0.0453	0.0465	0.0477	0.0503	0.0544	0.0567	0.0614
2 FlexFilter_100	-0.0219	-0.0021	-0.0015	-5.6337e-04	4.8273e-04	0.0016	0.0040	0.0078	0.0101	0.0139
3 FlexFilter_90	-0.0247	-0.0050	-0.0043	-0.0034	-0.0024	-0.0013	0.0011	0.0049	0.0071	0.0110
4 FlexFilter_80	-0.0268	-0.0072	-0.0066	-0.0057	-0.0046	-0.0035	-0.0011	0.0027	0.0049	0.0087
5 FlexFilter_70	-0.0284	-0.0088	-0.0081	-0.0073	-0.0062	-0.0051	-0.0028	0.0011	0.0033	0.0071
6 FlexFilter_60	-0.0294	-0.0098	-0.0091	-0.0082	-0.0072	-0.0061	-0.0037	7.3777e-05	0.0023	0.0061
7 FlexFilter_50	-0.0298	-0.0102	-0.0096	-0.0087	-0.0076	-0.0066	-0.0042	-3.6172e-04	0.0018	0.0057
8 FlexFilter_40	-0.0304	-0.0109	-0.0102	-0.0093	-0.0083	-0.0072	-0.0048	-9.6884e-04	0.0012	0.0051
9 FlexFilter_30	-0.0351	-0.0157	-0.0150	-0.0142	-0.0131	-0.0120	-0.0097	-0.0058	-0.0036	3.6612e-04
10 FlexFilter_20	-0.0469	-0.0278	-0.0271	-0.0263	-0.0253	-0.0242	-0.0219	-0.0181	-0.0159	-0.0123

Figure 62. Mean Bias Filtering Matrix

	1 ForcePlateFilter_200	2 ForcePlateFilter_100	3 ForcePlateFilter_90	4 ForcePlateFilter_80	5 ForcePlateFilter_70	6 ForcePlateFilter_60	7 ForcePlateFilter_50	8 ForcePlateFilter_40	9 ForcePlateFilter_30	10 ForcePlateFilter_20
1 FlexFilter_200	78	91	92	93	94	96	97	98	99	100
2 FlexFilter_100	77	15	12	5	4	13	25	50	62	70
3 FlexFilter_90	80	32	27	21	17	11	8	31	44	66
4 FlexFilter_80	83	47	41	36	28	22	9	18	30	55
5 FlexFilter_70	86	56	51	48	40	34	19	7	20	43
6 FlexFilter_60	87	61	57	52	46	39	24	1	16	38
7 FlexFilter_50	88	64	59	54	49	42	26	2	14	35
8 FlexFilter_40	89	65	63	58	53	45	29	6	10	33
9 FlexFilter_30	90	73	72	71	69	67	60	37	23	3
10 FlexFilter_20	95	85	84	82	81	79	76	75	74	68

Figure 63. Mean Bias Ranked Matrix

	1 ForcePlateFilter_200	2 ForcePlateFilter_100	3 ForcePlateFilter_90	4 ForcePlateFilter_80	5 ForcePlateFilter_70	6 ForcePlateFilter_60	7 ForcePlateFilter_50	8 ForcePlateFilter_40	9 ForcePlateFilter_30	10 ForcePlateFilter_20
1 FlexFilter_200	0.0775	0.0886	0.0895	0.0904	0.0914	0.0919	0.0927	0.0940	0.0941	0.1103
2 FlexFilter_100	0.0227	0.0165	0.0168	0.0172	0.0175	0.0169	0.0148	0.0120	0.0162	0.0438
3 FlexFilter_90	0.0246	0.0170	0.0172	0.0174	0.0175	0.0167	0.0144	0.0110	0.0155	0.0428
4 FlexFilter_80	0.0257	0.0177	0.0178	0.0179	0.0179	0.0171	0.0147	0.0110	0.0155	0.0424
5 FlexFilter_70	0.0260	0.0181	0.0181	0.0183	0.0182	0.0174	0.0150	0.0113	0.0154	0.0422
6 FlexFilter_60	0.0256	0.0181	0.0182	0.0184	0.0184	0.0176	0.0152	0.0116	0.0154	0.0424
7 FlexFilter_50	0.0249	0.0180	0.0182	0.0184	0.0184	0.0177	0.0155	0.0122	0.0159	0.0433
8 FlexFilter_40	0.0241	0.0173	0.0174	0.0176	0.0177	0.0170	0.0149	0.0124	0.0175	0.0455
9 FlexFilter_30	0.0241	0.0157	0.0156	0.0155	0.0154	0.0147	0.0128	0.0114	0.0199	0.0484
10 FlexFilter_20	0.0298	0.0196	0.0194	0.0192	0.0190	0.0180	0.0154	0.0112	0.0164	0.0407

Figure 64. Standard Deviation Filtering Matrix

	1 ForcePlateFilter_200	2 ForcePlateFilter_100	3 ForcePlateFilter_90	4 ForcePlateFilter_80	5 ForcePlateFilter_70	6 ForcePlateFilter_60	7 ForcePlateFilter_50	8 ForcePlateFilter_40	9 ForcePlateFilter_30	10 ForcePlateFilter_20
1 FlexFilter_200	91	92	93	94	95	96	97	98	99	100
2 FlexFilter_100	73	31	33	39	46	34	14	7	29	88
3 FlexFilter_90	76	36	38	41	44	32	11	1	25	86
4 FlexFilter_80	79	51	52	54	53	37	12	2	23	84
5 FlexFilter_70	80	57	59	63	62	42	16	4	21	83
6 FlexFilter_60	78	58	61	65	66	48	17	6	19	85
7 FlexFilter_50	77	56	60	64	67	50	22	8	28	87
8 FlexFilter_40	74	40	43	47	49	35	15	9	45	89
9 FlexFilter_30	75	27	26	24	20	13	10	5	72	90
10 FlexFilter_20	81	71	70	69	68	55	18	3	30	82

Figure 65. Stand Deviation Ranking Matrix

	1 ForcePlateFilter_200	2 ForcePlateFilter_100	3 ForcePlateFilter_90	4 ForcePlateFilter_80	5 ForcePlateFilter_70	6 ForcePlateFilter_60	7 ForcePlateFilter_50	8 ForcePlateFilter_40	9 ForcePlateFilter_30	10 ForcePlateFilter_20
1 FlexFilter_200	84.5000	91.5000	92.5000	93.5000	94.5000	96	97	98	99	100
2 FlexFilter_100	75	23	22.5000	22	25	23.5000	19.5000	28.5000	45.5000	79
3 FlexFilter_90	78	34	32.5000	31	30.5000	21.5000	9.5000	16	34.5000	76
4 FlexFilter_80	81	49	46.5000	45	40.5000	29.5000	10.5000	10	26.5000	69.5000
5 FlexFilter_70	83	56.5000	55	55.5000	51	38	17.5000	5.5000	20.5000	63
6 FlexFilter_60	82.5000	59.5000	59	58.5000	56	43.5000	20.5000	3.5000	17.5000	61.5000
7 FlexFilter_50	82.5000	60	59.5000	59	58	46	24	5	21	61
8 FlexFilter_40	81.5000	52.5000	53	52.5000	51	40	22	7.5000	27.5000	61
9 FlexFilter_30	82.5000	50	49	47.5000	44.5000	40	35	21	47.5000	46.5000
10 FlexFilter_20	88	78	77	75.5000	74.5000	67	47	39	52	75

Figure 66. Mean Ranked Matrix

	1 ForcePlateFilter_200	2 ForcePlateFilter_100	3 ForcePlateFilter_90	4 ForcePlateFilter_80	5 ForcePlateFilter_70	6 ForcePlateFilter_60	7 ForcePlateFilter_50	8 ForcePlateFilter_40	9 ForcePlateFilter_30	10 ForcePlateFilter_20
1 FlexFilter_200	90	92	93	94	95	96	97	98	99	100
2 FlexFilter_100	76	20	19	17	23	21	11	26	42	83
3 FlexFilter_90	81	31	30	29	28	16	5	8	32	79
4 FlexFilter_80	84	49	44	41	38	27	7	6	24	74
5 FlexFilter_70	89	61	58	59	52	34	9	3	13	72
6 FlexFilter_60	86	66	64	63	60	39	12	1	10	71
7 FlexFilter_50	87	68	67	65	62	43	22	2	15	69
8 FlexFilter_40	85	55	57	56	53	36	18	4	25	70
9 FlexFilter_30	88	51	50	47	40	37	33	14	48	45
10 FlexFilter_20	91	82	80	78	75	73	46	35	54	77

Figure 67. Reranked Matrix for Control Dynamic Peak

Table 7. Filtering Table Lowpass Cutoff Frequency (Hz)

	Static Peak Torque		Dynamic Peak Torque		Static Shear Force		Dynamic Shear Force		Dynamic Vertical Force	
	fLEX	Force platform	fLEX	Force platform	fLEX	Force platform	fLEX	Force platform	fLEX	Force platform
Interface 1 (Control)	30	40	100	70	40	40	100	50	20	50
Interface 2 (Tape-Court)	50	70	100	70	20	40	100	50	100	50
Interface 3 (Tape-Cleat)	50	100	100	60	100	100	40	20	100	50
Interface 4 (Glued 1-Court)	50	100	40	100	20	100	100	100	100	50
Interface 5 (Glued 1-Cleat)	80	200	100	90	80	100	100	100	100	30
Interface 6 (Glued 2-Court)	40	200	80	200	100	200	200	200	100	20
Interface 7 (Glued 2-Cleat)	20	200	20	200	20	200	20	200	80	100

Appendix E: Sensor Calibration Curves and Other Sensors

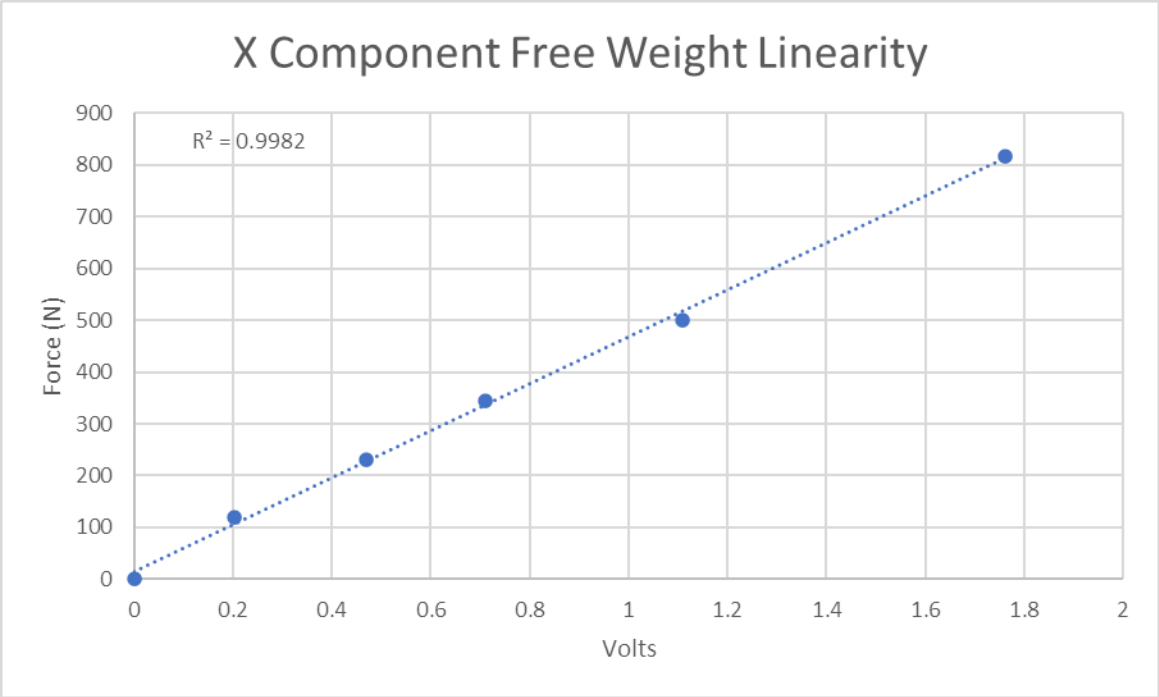


Figure 68. PCB X Free Weight Calibration

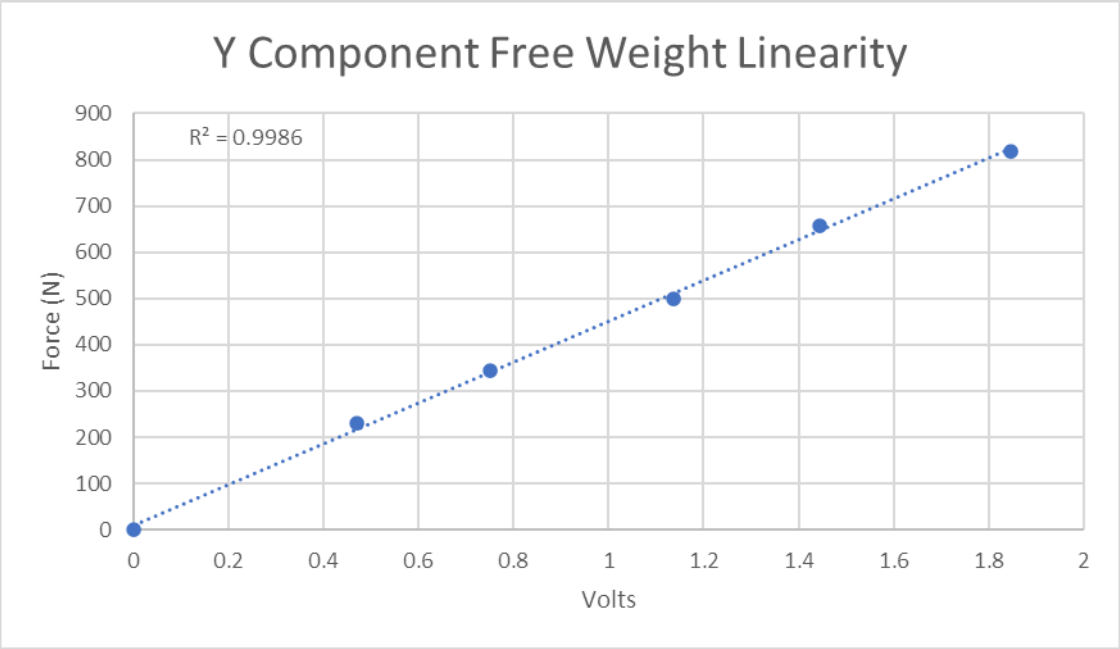


Figure 69. PCB Y Free Weight Calibration

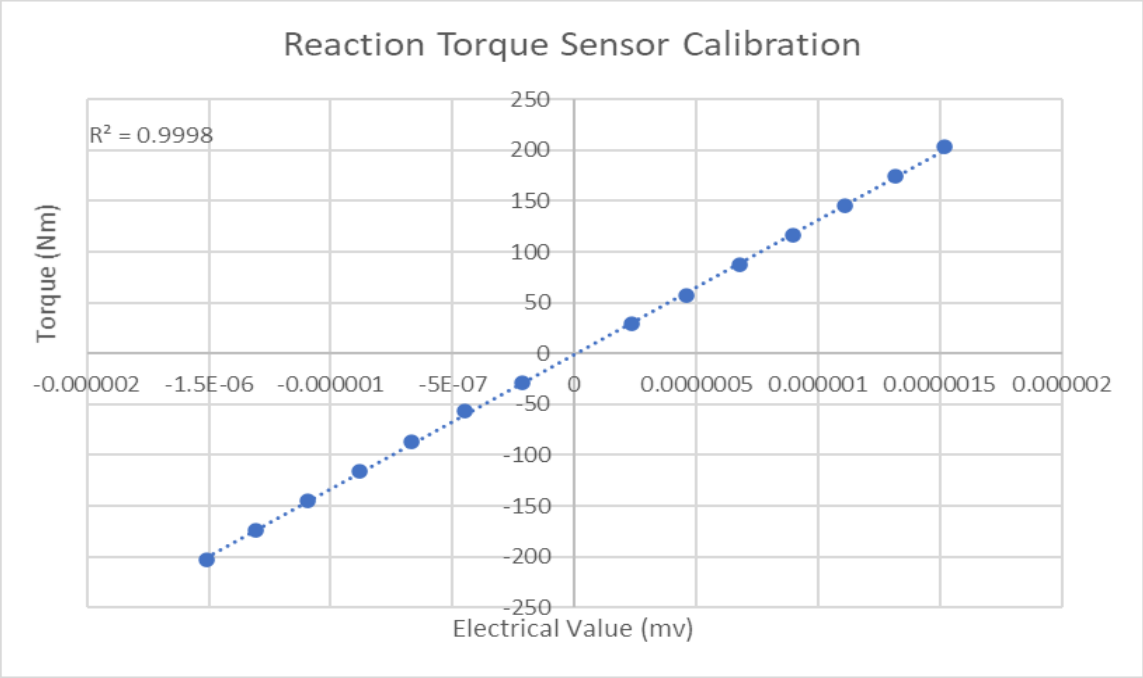


Figure 70. Reaction Torque Sensor Calibration

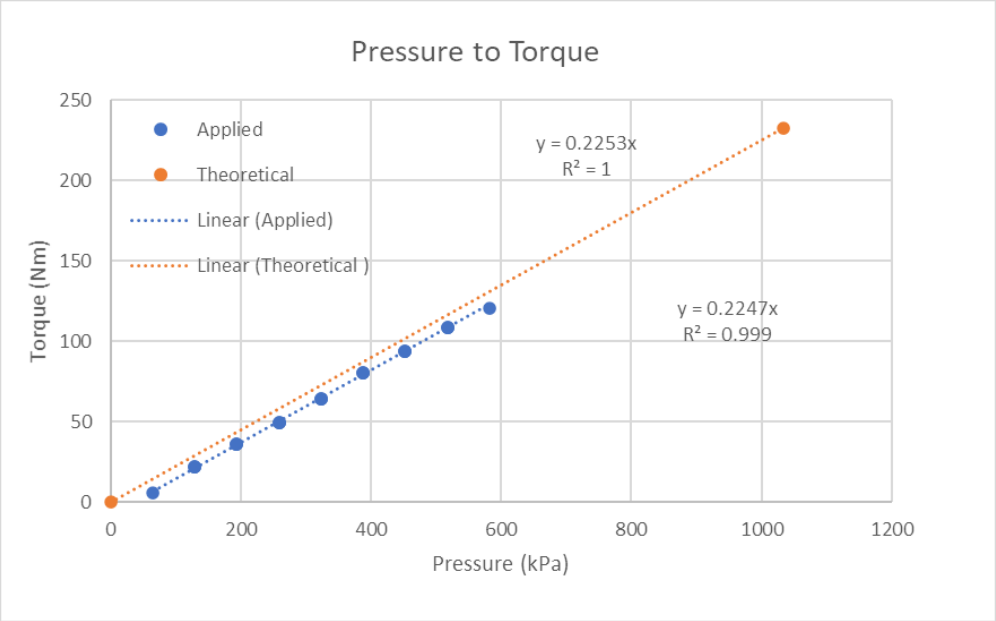


Figure 71. Rotary Actuator Pressure Calibration Linearity

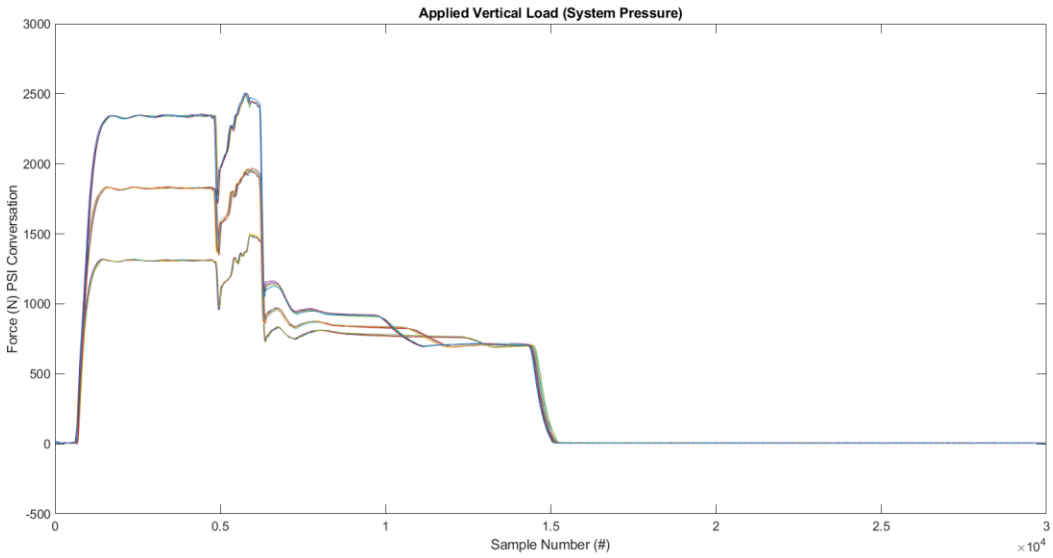


Figure 72. Vertical System Pressure

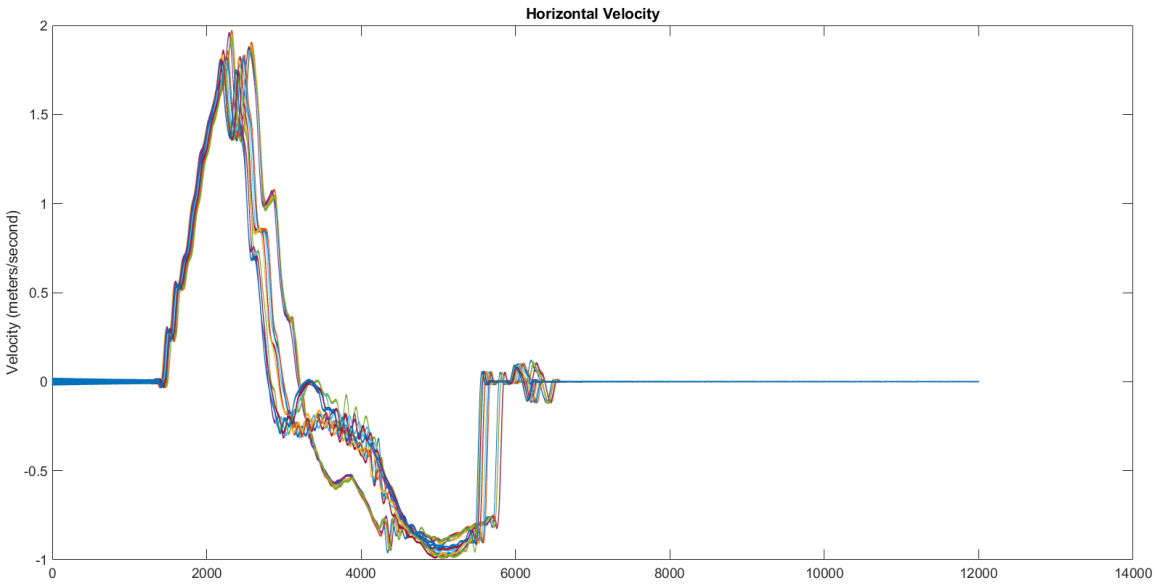


Figure 73. Horizontal Velocity

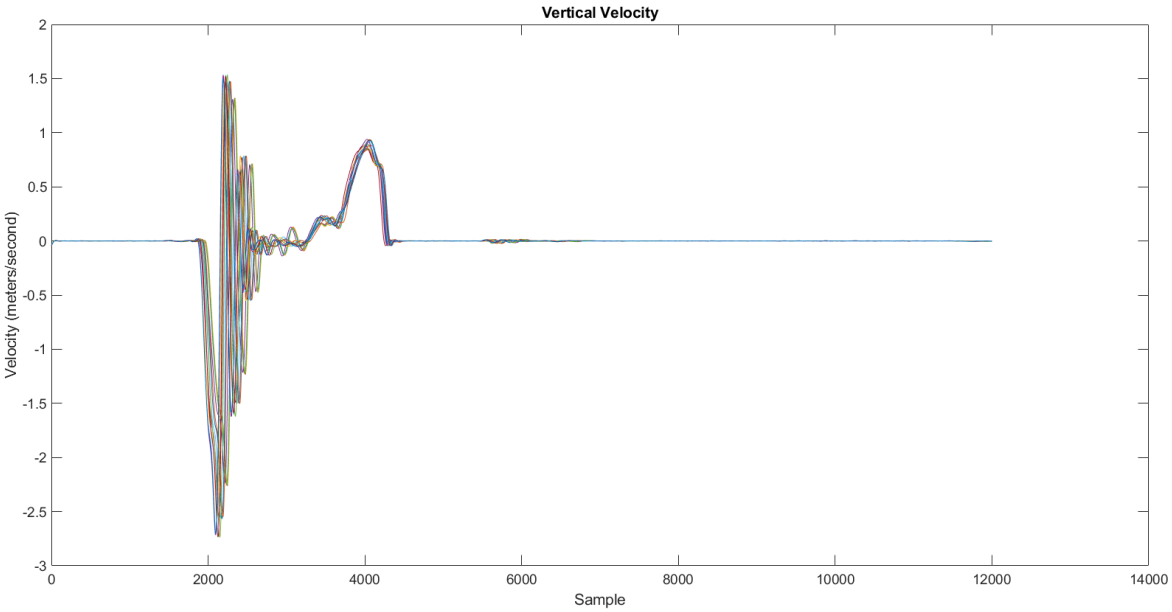


Figure 74. Vertical *Velocity*

VITA

Sean Quisenberry was born in Van Nuys, CA, in 1985 to Byron Quisenberry and Clara Huff. He is the youngest of two children. He graduated from Westlake High School in 2003. Sean graduated from Texas Tech University with a degree in Exercise Science in 2011. Sean then attended Texas State University – San Marcos for a Master of Science in Exercise Sports Science, then began his PhD at the University of Southern Mississippi then moved the University of Tennessee Knoxville where he finished in 2020.